Designing of Novel ADAM17 Inhibitors through Classification-dependent Molecular Modelling Approaches and Subsequent Synthesis of Aryl-sulfonamide Derivatives as Probable ADAM17 Inhibitors

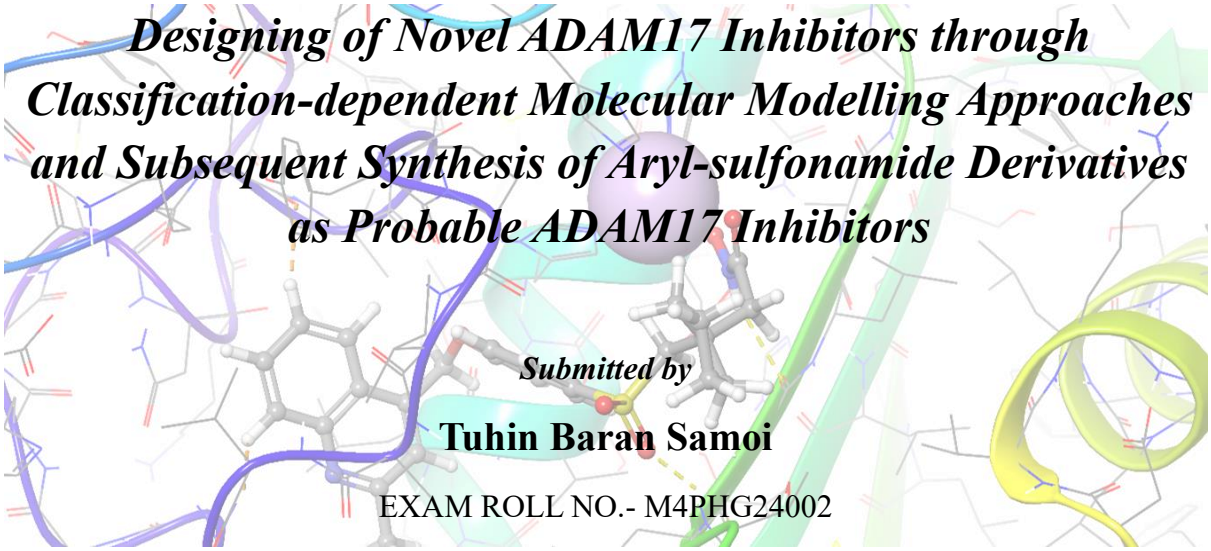

Submitted by

Tuhin Baran Samoi

EXAM ROLL NO.- M4PHG24002

CLASS ROLL NO.- 002211402023

REG. NO.- **163666** of **2022-2023**

Department of Pharmaceutical Technology

Jadavpur University

Session: ***2022-2024***

Under The Guidance

of

Dr. Nilanjan Adhikari

Natural Science Laboratory

Department of Pharmaceutical Technology

Jadavpur University, Kolkata-700032

Thesis submitted in partial fulfilment of the requirements

for the Degree of Master of Pharmacy

Department of Pharmaceutical Technology

Faculty of Engineering and Technology

Jadavpur University, Kolkata

2024

Jadavpur University

Jadavpur, Kolkata-700032

CERTIFICATE OF APPROVAL

This is to certify that Tuhin Baran Samoi (Exam Roll No.- **M4PHG24002**, Reg. No.- **163666** of **2022-23**) has sincerely carried out the research work on the subject entitled ***"Designing of novel ADAM17 inhibitors through classification-dependent molecular modelling approaches and subsequent synthesis of Aryl-sulfonamide derivatives as probable ADAM17 inhibitors"*** under the supervision of Dr. Nilanjan Adhikari, Assistant Professor, Natural Science Laboratory, Department of Pharmaceutical Technology of Jadavpur University. He has incorporated his findings in this thesis submitted by him in partial fulfilment of the requirements for the degree of Master of Pharmacy (Pharmaceutical Technology) of Jadavpur University. He has carried out the research work independently and sincerely with proper care and attention to our entire satisfaction.

27/8/24

Head of the Department

Department of Pharmaceutical Technology

Jadavpur University

Kolkata-700032

Head
Dept. of Pharmaceutical Technology
Jadavpur University
Kolkata - 700 032, W.B. India

Adhikari 27/08/2024

Dr. Nilanjan Adhikari

Natural Science Laboratory

Department of Pharmaceutical Technology

Jadavpur University

Kolkata-700032

DR. NILANJAN ADHIKARI
Assistant Professor
Dept. of Pharm. Tech.
Jadavpur University
Kolkata - 700 032

Dipak Laha 27.8.24

Dean

Faculty of Engineering and Technology

Jadavpur University

Kolkata-700032

DEAN
Faculty of Engineering & Technology
JADAVPUR UNIVERSITY
KOLKATA-700 032

ii

Acknowledgement

The successful completion of this dissertation relied heavily on the guidance and support of many individuals. I feel very fortunate to have had their help throughout the process. Everything I've accomplished is thanks to their contributions, and I am deeply grateful for their assistance.

I am deeply grateful and wish to express my sincere thanks to my esteemed mentor, **Dr. Nilanjan Adhikari** from the Department of Pharmaceutical Technology, Jadavpur University, Kolkata. His exceptional and unwavering guidance, constant encouragement, and generous support were invaluable throughout the dissertation process. I am profoundly indebted to him for his motivation, insightful suggestions, and inspiration, which were crucial to the successful completion of my work.

I extend my heartfelt respect to **Prof. Amalesh Samanta**, the Head of the Department of Pharmaceutical Technology, Jadavpur University, Kolkata, for his invaluable assistance and encouragement. I am also grateful to **Prof. Sanmoy Karmakar**, the former Head of the Department, for his ongoing support and motivation. Additionally, I appreciate the help and support provided by all the esteemed teachers and non-teaching staff in the Department of Pharmaceutical Technology, Jadavpur University.

I am deeply grateful to **Prof. Tarun Jha**, **Mr. Sandip Kr. Baidya** and **Mr. Suvankar Banerjee** for their invaluable guidance and support, which were crucial in helping me understand various aspects of this work.

I would also like to extend my thanks to my senior colleagues in the lab, **Ms. Subha Mandal**, **Mr. Jigme Sangay Dorjay Tamang**, **Mr. Rahul Jana**, and **Mr. Chayanta Sen**, as well as to my fellow colleague **Mr. Sandeep Jana,** my friends, and the Natural Science Laboratory at the Department of Pharmaceutical Technology, Jadavpur University, Kolkata.

I would like to thank **Dr. Balaram Ghosh** from BITS-Pilani, Hyderabad, India, for his ongoing encouragement, essential assistance, and support throughout my work.

I extend my sincere gratitude to **AICTE** and Jadavpur University for their financial and equipment support during my M. Pharm. course.

Finally, I wish to express my profound respect to my father **Baneswar Samoi**, my mother **Alaka Samoi**, and my elder sisters **Jayashri Roy** and **Tanusree Samoi**, for their unwavering help, love, encouragement, and moral support throughout the duration of my work.

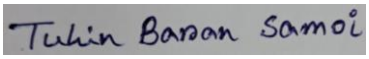

Tuhin Baran Samoi

Date: 27/08/2024

Place: Department of Pharmaceutical Technology

Jadavpur University, Kolkata-700032

Declaration of Originality and Compliance of Academic Ethics

I hereby declare that this thesis includes both a literature survey and original research conducted by me, ***Tuhin Baran Samoi***, as part of my Master of Pharmacy studies. All information in this document has been collected and presented in compliance with academic standards and ethical guidelines.

I also declare that, in accordance with these rules and ethical guidelines, I have properly cited and referenced all materials and results that are not original to this work.

Name: *Tuhin Baran Samoi*

Exam Roll Number: *M4PHG24002*

Class Roll Number: *002211402023*

Registration Number: *163666 of 2022-23*

Thesis Title: "***Designing of novel ADAM17 inhibitors through classification-dependent molecular modelling approaches and subsequent synthesis of Aryl-sulfonamide derivatives as probable ADAM17 inhibitors***"

Signature:  ***[Tuhin Baran Samoi]***

Date: 27/08/2024

Dedicated to

My Parents, Elder Sisters and Teachers

Preface

The dissertation elucidates the deed that done over a span of more than six months (3rd & 4th semester) for the purpose of development of some probable anti-cancer candidates. Investigating cellular mechanisms and molecular interactions is crucial for deepening our knowledge of human biology and disease. ADAM17, also referred to as Tumour Necrosis Factor Alpha Converting Enzyme (TACE), is particularly notable among the many proteins that control these processes. The creation of targeted therapies marks a groundbreaking shift in modern medicine, offering a new level of precision in treating complex diseases. A key aspect of this progress is the search for inhibitors that can specifically target the crucial molecular factors driving disease processes. Among these, ADAM17 has become a key target because of its significant role in various diseases, such as cancer, inflammatory disorders, and neurodegenerative conditions.

A couple of QSAR studies have been done for designing small molecule that might be beneficial for the development of newer ADAM17 inhibitors as anti-neoplastic agents. For this purpose, four new molecules have been designed as probable ADAM17 inhibitors. And, as glutamic acid played a significant role in the biochemical processes in cellular levels thus some glutamate analogues have been synthesized in the laboratory for evaluating their anti-tumour activity.

In conclusion, I hope this thesis will advance the growing knowledge of ADAM17 inhibitors and encourage further research to uncover new insights into ADAM17's role in health and disease.

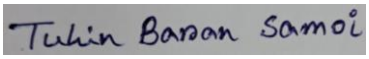

Tuhin Baran Samoi

Contents

Chapter 1: Introduction

1.1. Introduction

Throughout human history, disease has consistently intertwined with the fabric of existence, influencing societies, challenging medical science, and prompting humanity's quest for solutions, the narrative of disease unfolds with both profound difficulties alongside transformative opportunities.

Cancer is one of the most complex and intimidating disease in the modern world. In fact, cancer is not a singular disease but rather a spectrum of over 200 distinct diseases stemming from various cellular abnormalities that's why a treatment that is effective in controlling one type of cancer may be ineffective on another [1]. Generally, cancer is defined as a group of diseases characterized by the uncontrolled growth and spread of abnormal cells. After heart disease, cancer is the largest cause of death globally (**Figure 1.1**), accounting for an estimated 9.7 million deaths, in 2022, according to World Health Organization [2]. About 1 in 5 people develop cancer in their lifetime, approximately 1 in 9 men and 1 in 12 women die from the disease. According to WHO, in 2022, over 275,000 children and adolescents (aged 0–19 years) were diagnosed with cancer globally, and more than 105,000 children died from the disease.

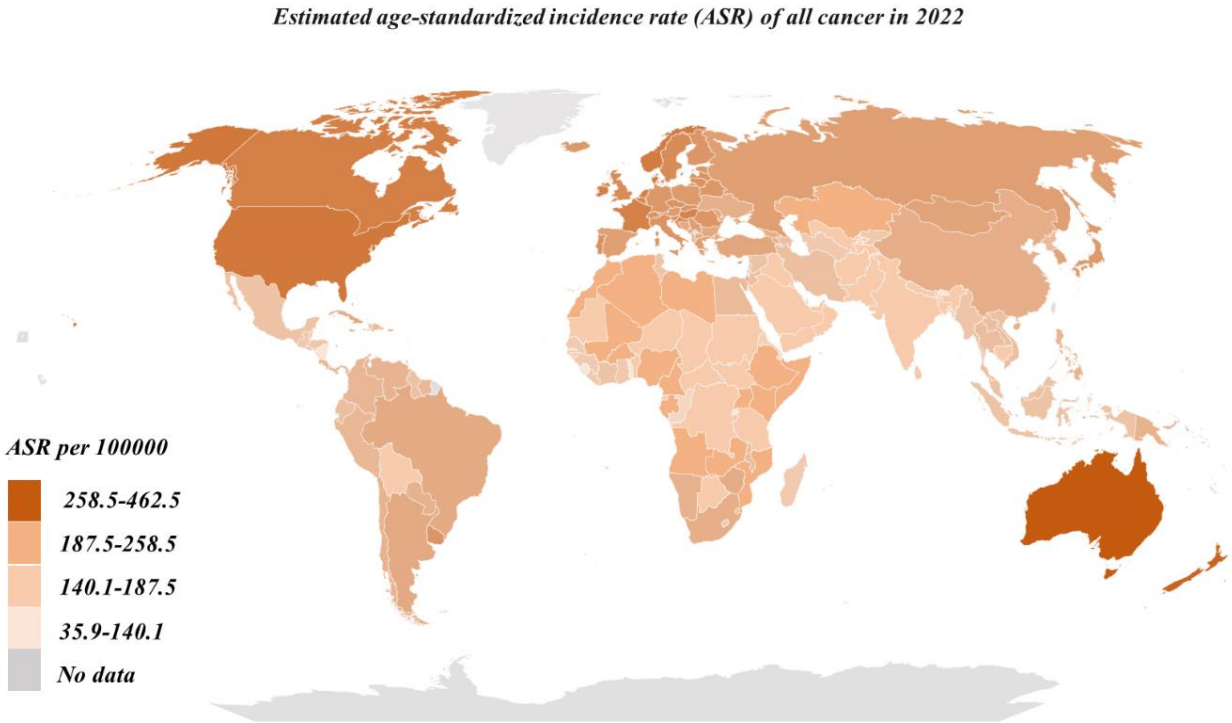

Figure 1.1. Global footprint of cancer in 2022

Cancer cells develop when normal cells lose their typical regulatory mechanisms that govern growth and multiplication. They transform into rogue cells, frequently losing the specialized

traits that differentiate one cell type from another (for example a brain cell from a liver cell) and this phenomenon is referred to as loss of differentiation. This often leads to the formation of neoplasms, which refers to new abnormal growths [3]. Cancer can affect various parts of the body and is named accordingly based on its location or type of tissue it originates from. Examples of cancers that affect specific parts of the body include breast cancer, stomach cancer, lung cancer, prostate cancer, skin cancer, and colorectal cancer, among others (**Figure 1.2**) [4].

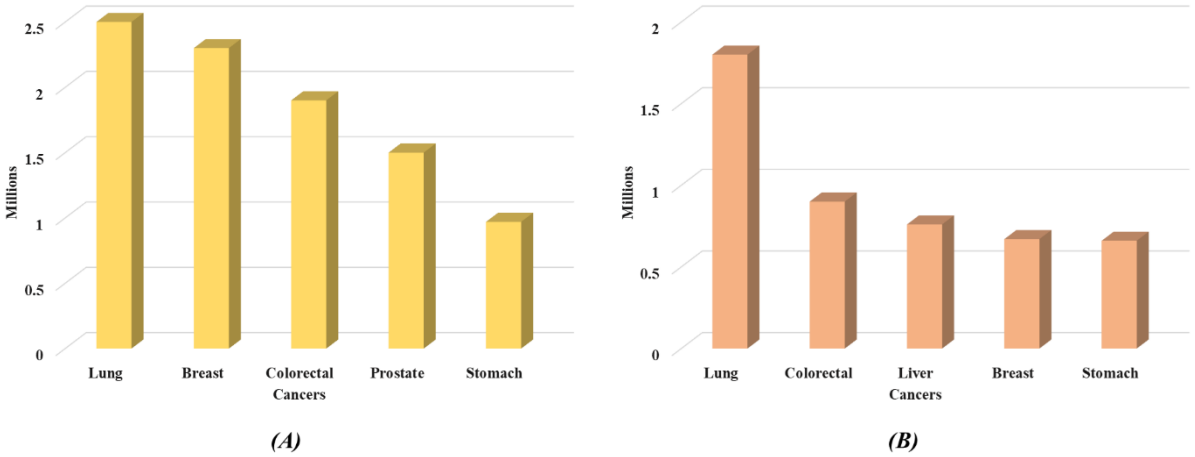

Figure 1.2. ***(A)*** The most common types of cancers in 2020 ***(B)*** The most common causes of cancer death in 2022

1.2. Types of cancer

Cancer can be categorized into various types as follows:

(i) Based on characteristics of neoplasm

(a) *Benign neoplasm or tumour*: Non-invasive localized cancer.

(b) *Malignant neoplasm or tumour*: Tumours have the capability to invade nearby tissues and organs, and they can spread to other parts of the body through the bloodstream or lymphatic system. This process is known as metastasis [5].

(ii) Based on the tissue of origin

(a) *Carcinoma*: This type of cancer originates from epithelial cells, which are found in the skin and the lining of organs and tissues. E.g. Adenocarcinoma, Squamous cell carcinoma etc.

(b) *Sarcoma*: Sarcomas develop from connective tissues, such as bones, muscles, fat, and cartilage. For example, Osteosarcoma, Liposarcoma etc.

(c) *Leukaemia*: Leukaemia originates in blood-forming tissues, such as the bone marrow, and results in the production of abnormal white blood cells. Examples include: Acute lymphocytic leukaemia (ALL), Chronic lymphocytic leukaemia (CLL), Acute myeloid leukaemia (AML) [6].

(d) *Lymphoma*: Lymphomas develop in the lymphatic system, which is part of the body's immune system. For example, Hodgkin lymphoma, non-Hodgkin lymphoma.

(e) *Melanoma*: it originates in melanocytes, which are pigment-producing cells in the skin. It is the most serious type of skin cancer.

(f) *Glioma*: Arise from glial cells, which support nerve cells in the brain and spinal cord.

(g) *Meningioma*: Develop in the meninges, the layers of tissue covering the brain and spinal cord.

1.3. Etiology of cancer

The etiology of cancer encompasses the factors or causes that contribute to its development and progression. Cancer is a complex disease influenced by a combination of genetic predisposition, environmental factors, and lifestyle choices [7]. Here are the primary etiological factors associated with the development of cancer:

1.3.1. Genetic Factors

- *Inherited mutations:* Some individuals have a higher predisposition to certain cancers because they inherit genetic mutations from their parents. For instance, mutations in the BRCA1 and BRCA2 genes are linked to increased susceptibility to breast and ovarian cancers.
- *Somatic mutations:* Mutations acquired in specific genes during a person's lifetime can also contribute to the development of cancer. Genetic abnormalities such as the activation of proto-oncogenes and the inactivation of tumour suppressor genes (e.g., p53) are known to contribute to the development of cancer. These mutations can arise due to exposure to carcinogens (substances that cause cancer), radiation, or errors that occur during DNA replication.

1.3.2. Environmental Exposures

- *Carcinogens:* Certain substances in the environment can indeed elevate the risk of developing cancer. Examples include tobacco smoke, which is linked to lung cancer; asbestos, associated with mesothelioma; and various industrial chemicals, which can lead to different types of cancer depending on the extent and duration of exposure.

- *Radiation:* Ionizing radiation, such as X-rays and UV radiation from the sun, can damage DNA and elevate the risk of cancer, including skin cancer like melanoma and leukaemia.
- *Pollution:* Air, water, and soil pollutants often contain carcinogens that have the potential to contribute to the development of cancer over time.

1.3.3. Lifestyle Factors

- *Usage of tobacco:* Possibly as many as 30% of cancers are caused by smoking and other forms of tobacco use are significant risk factors for various types of cancer, including lung, throat, and bladder cancers.
- *Dietary factors:* A diet high in processed foods, red and processed meats, and low in fruits and vegetables may increase the risk of certain cancers. In contrast, diets that are rich in fruits, vegetables, and whole grains are associated with a lower risk of cancer. Alcohol consumption is classified as a human carcinogen and is known to produce reactive oxygen species, impair the body's nutrient breakdown, and elevate oestrogen levels in the blood. It is significantly linked to an increased risk of liver cancer, oesophageal squamous cell carcinoma, and stomach cancer.
- *Obesity:* Being overweight or obese is associated with an elevated risk of several types of cancer, including breast, colon, and pancreatic cancers. And Lack of regular physical activity is linked to a higher risk of certain cancers.

1.3.4. Infectious agents

- *Viruses:* Viruses have been identified as contributors to at least six types of human cancers and are responsible for approximately 15% of cancer-related deaths worldwide. For instance, the Epstein-Barr virus is known to cause Burkitt's lymphoma and nasopharyngeal carcinoma. Human papillomaviruses, which are sexually transmitted, can lead to cervical cancer. Hepatitis B virus is responsible for approximately 80% of liver cancers, and HIV infection can lead to Kaposi's sarcoma and lymphoma.
- *Bacteria:* The bacterium Helicobacter pylori is known to cause many stomach ulcers and is also associated with an increased risk of stomach cancer.

1.3.5. Chronic inflammation

- *Inflammatory conditions:* Chronic inflammation in tissues or organs can heighten the risk of DNA damage and cell mutations, which may contribute to the development of cancer. For instance, inflammatory bowel disease (IBD) is linked to an increased risk of colorectal cancer.

1.3.6. Hormonal factors

- *Imbalances of hormones:* Excessive hormone exposure, whether from natural sources like oestrogen in postmenopausal women or from medications such as hormone replacement therapy, can raise the likelihood of developing specific cancers like breast and uterine cancers.

Occasionally, the treatments utilized to fight cancer, such as radiotherapy and chemotherapy, can lead to the development of a different cancer in patients who survive. For instance, approximately 5% of patients cured of Hodgkin's disease later develop acute leukaemia. However, the risk of developing a second cancer is typically outweighed by the benefit of successfully treating the original cancer. Understanding these intricate interactions is crucial for devising strategies aimed at cancer prevention, early detection, and personalized treatment approaches. Ongoing research efforts are continuously revealing new insights into the causes of cancer, thereby enhancing our ability to tackle this complex and formidable disease.

1.4. Pathogenesis of cancer

Cancer development involves a sophisticated interaction among genetic, environmental, and lifestyle factors that collectively influence the growth and advancement of abnormal cells [8] (**Figure 1.3**).

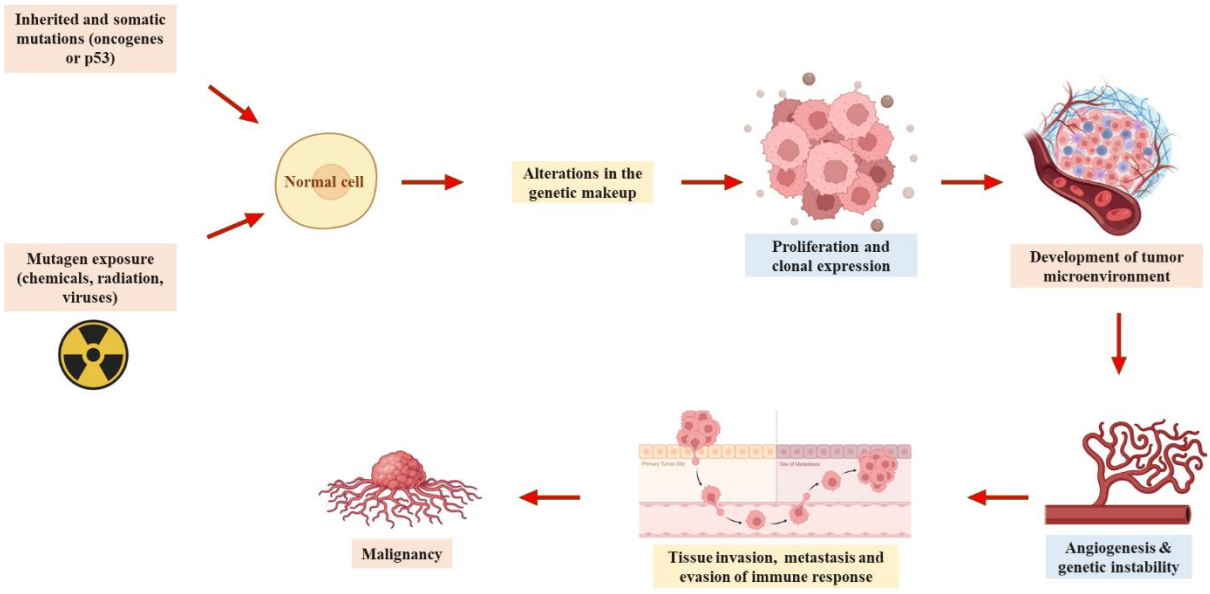

Figure 1.3. Schematic representation of the development of cancer

1.5. Conventional treatment of cancer

Treating cancer requires employing diverse strategies to eradicate cancerous cells, manage their growth, and preventing their recurrence. A significant challenge in cancer treatment arises from

the fact that it is not a single disease but rather a collection of numerous cellular abnormalities. There are three conventional methods for treating cancer: surgery, radiotherapy, and chemotherapy [9]. Chemotherapy is typically used alongside surgery and radiotherapy. Furthermore, combining multiple therapies often proves more effective than using a single drug. This approach offers advantages such as enhanced treatment efficacy, reduced toxicity, and avoidance of drug resistance. Because cancer cells originate from normal cells, identifying targets that are exclusively present in cancer cells is challenging. Consequently, most traditional anticancer medications target structures found in both types of cells. Therefore, the effectiveness and specificity of these drugs rely on their ability to accumulate more in cancer cells than in normal cells. Many traditional anticancer drugs operate by disrupting DNA function and are categorized as cytotoxic. Some directly target DNA, while others indirectly interfere by inhibiting enzymes crucial for DNA synthesis.

Surgery stands as the oldest therapeutic method for treating many types of cancer. Solid tumours like those found in breast, head, and neck cancers are often managed through surgical removal. The goal of this approach is to completely eliminate localized cancer by excising the tumour and surrounding tissues.

Radiation therapy, also called radiotherapy, is a prevalent cancer treatment method. It utilizes high-energy radiation to reduce tumour size and eliminate cancer cells, aiming to either destroy the cancer cells or halt their growth while minimizing harm to nearby healthy tissue. The dosage of radiation employed in cancer radiation therapy varies based on several factors such as the type of cancer, its location, its stage, and the treatment objective (whether curative or palliative). Radiation therapy is often employed in the treatment of common cancers such as breast, prostate, lung, cervix, and rectal cancer.

Chemotherapy involves the administration of drugs, known as chemotherapeutic agents, to combat cancer. These drugs target and eliminate rapidly dividing cancer cells, a hallmark of most cancer types. Chemotherapy is employed with curative intent to aim for a cure or long-term remission in cancer treatment. Alternatively, it can be used palliatively to reduce tumour size, alleviate symptoms, particularly in cases of advanced or metastatic cancers. Chemotherapeutic agents encompass cytotoxic drugs like methotrexate, cisplatin, topotecan, cytarabine, paclitaxel, and etoposide, among others [10].

1.6. Modern approaches to treat cancer

Contemporary methods for treating cancer involve various approaches designed to enhance results while reducing adverse effects. This strategy incorporates targeted therapy, immunotherapy, hormone therapy, personalized combination therapies, bone marrow transplantation, and other advanced treatments.

Targeted therapy introduced to targets specific molecules involved in cancer growth or survival. It involves monoclonal antibodies, small molecule inhibitors, and other agents targeted at specific molecules. For example, drugs that target HER2 (such as trastuzumab for breast cancer) and EGFR inhibitors (like cetuximab for colorectal cancer) and rituximab, a chimeric antibody targeting CD20 receptor for the treatment of lymphoma.

Immunotherapy enhances the body's immune system to identify and eliminate cancer cells. Immunotherapy has revolutionized cancer treatment by aiming to enhance immune responses against tumours with fewer off-target effects compared to direct cancer cell-killing agents like chemotherapy. These therapies activate the immune system or amplify its activation to target cancer cells through natural mechanisms, which cancer often evades. Consequently, immunotherapy is acknowledged as a promising approach for treating and potentially curing certain types of cancer. This involves checkpoint inhibitors, adoptive cell transfer (e.g., CAR-T cell therapy), and cancer vaccines.

Hormone-based therapies are employed for hormone-dependent cancers. If a cancer cell relies on a specific hormone, an opposing hormone can be administered to counteract its effects. Alternatively, hormone antagonists can be used to block the action of the necessary hormone. For instance, selective aromatase inhibitors like anastrozole and letrozole are utilized in the treatment of breast cancer.

Nanotechnology holds significant promise for revolutionizing cancer treatment by utilizing the distinctive properties of nanoparticles. Nanoparticles (NPs) including polymeric types like nanogels, nanofibers, and liposomes, as well as metallic ones such as gold nanoparticles (GNPs), silver nanoparticles (AgNPs), calcium nanoparticles (CaNPs), quantum dots (QDs), and carbon nanotubes (CNTs) have transformed cancer diagnostics and treatments. By functionalizing these nanoparticles with various biological molecules, such as antibodies, they can more effectively target and deliver treatments and enable early detection of cancer cells, leveraging their plasmon resonance properties [11]. Nanotechnology-boosted photodynamic therapy (PDT) and immunotherapy are emerging as promising cancer treatments, offering substantial potential to enhance patient outcomes. Combining these approaches has led to

synergistic effects in preclinical studies, resulting in improved immune responses against cancer and the ability to overcome the immunosuppressive tumour refer microenvironment [12].

In some cases, bone marrow transplantation with healthy stem cells is required following high-dose chemotherapy or radiation therapy. Occasionally, a combination of treatments tailored to the specific cancer type, stage, and genetic profile of the individual patient is used to achieve improved outcomes. In conclusion, cancer treatment incorporates a multifaceted approach that integrates surgery, radiation, chemotherapy, targeted therapies, immunotherapy, and supportive care. Ongoing advancements in tumour biology and treatment strategies contribute to enhancing outcomes and the quality of life for individuals with cancer. In this study, we aimed at a unique enzyme called A Disintegrin and Metalloproteinase 17 to create new small molecules for treating cancer and other diseases.

1.7. ADAMs

Over the past few decades, there has been a growing recognition of proteases as pivotal targets in the pathophysiology of human diseases, particularly cancers. Numerous studies have shown that alterations in protease activity play a significant role in various pathological conditions, including cancer, chronic degenerative diseases, and inflammatory disorders. In the context of cancer, proteases can accelerate tumour progression by facilitating invasion, metastasis, and angiogenesis. Metalloproteases constitute a distinct class of proteases that rely on a metal ion cofactor, commonly zinc, to facilitate their catalytic activity. The metal ion is bound within the active site of metalloproteases, playing a critical role in the hydrolysis of peptide bonds. A disintegrin and metalloproteinases (ADAMs) [13] are one such prominent family of metalloproteinases belonging to the metzincin superfamily. Dysregulation of ADAMs has been associated with a range of diseases, such as cancer, inflammatory disorders, cardiovascular diseases, and neurological conditions. ADAMs are closely related to other metalloenzymes such as ADAM-TSs (ADAMs with thrombospondin domains) & matrix metalloproteinases (MMPs) [14]. For instance, ADAM17 (also known as TACE) plays a role in the shedding of TNF-alpha and other cytokines, which contributes to inflammation and the progression of cancer.

The ADAMs, a family of proteins known as a disintegrin and metalloproteinases, play crucial roles in cell biology by influencing cell adhesion, migration, proteolysis, and signalling [15]. Mammalian genomes contain 40 ADAMs, with humans having 21 identified ADAM proteins

[16]. Among these, 13 (ADAM8, 9, 10, 12, 15, 17, 19, 20, 21, 28, 30, 33, and DEC1) are known or predicted to be catalytically active, while 8 (ADAM2, 7, 11, 18, 22, 23, 29, and 32) are considered catalytically inactive [17]. Despite their lack of catalytic activity, these inactive ADAMs contribute to intracellular communication primarily through their adhesive properties rather than by cleaving or "shedding" cell surface molecules. ADAMs exhibit dual functions in cellular adhesion and the proteolytic cleavage of various cell surface molecules. Consequently, ADAMs play significant roles in mediating cell signalling events that determine cellular fate (including apoptosis), proliferation, and growth. Given their diverse functions, ADAMs are pivotal in both physiological and pathophysiological processes and may serve as potential therapeutic targets for various diseases [15].

1.8. General structure of ADAMs

A disintegrin and metalloproteases (ADAMs) are multi-domain proteins. Pro-domain is one of them; it renders ADAMs inactive, and furin and other protein convertases cleave this pro-domain in the Golgi apparatus to activate ADAM17. An essential domain for catalysis and ligand shedding is the metalloprotease domain. The disintegrin domain helps to preserve the extracellular region's structure by interacting with integrins and promoting adhesion [15].

The activity of substrate binding and shedding is regulated by the membrane proximal domain. The membrane proximal domains of ADAM10, ADAM17, and other ADAMs, along with EGF-like repeats, control the activity of substrate binding and shedding. Signaling molecules interact with the cytoplasmic tail of ADAMs. The phosphorylation of the cytoplasmic tail controls the trafficking, subcellular location, and activation of ADAMs [18].

1.9. Comprehensive structure of ADAM17

A disintegrin and metalloprotease17 (ADAM17) a cell surface protease of the metzincin family was discovered in 1997 as the protein responsible for the extracellular cleavage or shedding of tumour necrosis factor-α (TNF-α) and was originally named TNF-α converting enzyme (TACE) [12]. ADAM17 is synthesized as an inactive precursor containing an N-terminal pro-domain that constrains the enzyme activity through a cysteine switch mechanism which is common to the majority of metzincins [19].

ADAM17 comprises the following domains; a pro-domain, a catalytic/metalloproteinase domain, a disintegrin domain, a membrane proximal domain, a transmembrane domain, a Conserved Adam seventeeN Dynamic Interaction Sequence (CANDIS) region and a cytoplasmic tail (**Figure 1.4**) [20].

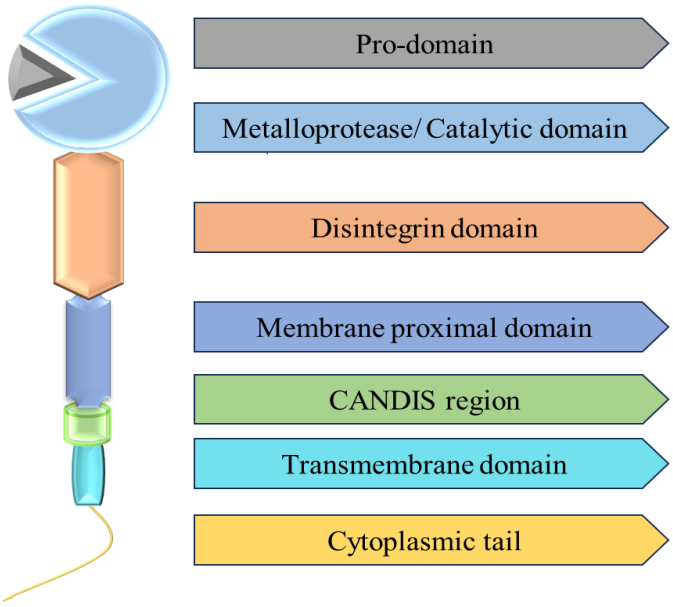

Figure 1.4. The structure of Generalised domains of ADAM17

1.9.1. Pro-domain

By obstructing the metalloproteinase catalytic site, the pro-domain maintains ADAM17's inactive state. Recent research has demonstrated that the precursor of ADAM17 can remain inactive without the help of the so-called "cysteine switch" mechanism, which functions in many matrix metalloproteinases (MMPs) and ADAMs and involves the coordination of the zinc ion by a cysteine found in the pro-domain [21]. The pro-domain of ADAM17 was the initial inhibitor of the enzyme, and the proteolytic cleavage of its pro-domain was necessary for the activation of ADAM17. The pro-domain may be not necessary for the transportation to cell surface, but it might play important role in the extracellular system [22]. In addition to its inhibitory function, the pro-domain also acts as a chaperone and protect the enzyme from degradation during transport through the secretory pathway [21].

1.9.2. Catalytic/metalloproteinase domain

The catalytic domain or metalloproteinase domain of ADAM17 contains a conserved catalytic site sequence with three histidine residues (HEXXHXXGXXH) and one glutamic residue, which are responsible for Zn^{2+}-binding and the cleavage of peptide bonds. There are two highly Conserved and adjacent cysteine sulfhydryl motifs (cysteine-X-X-cysteine, CXXC), and the motifs were the targets for the exchange of protein's thiol-disulfide [23]. The processing of various membrane bound proteins is heavily dependent on the catalytic domain [24].

1.9.3. Disintegrin domain

Integrins are adhesion receptors mediate the interaction of cell-cell and cell-extracellular matrix (ECM), and participate in many cell progressions including cell adhesion, cell migration & proliferation. Integrin is a prognostic indicator and up-regulated in many types of cancers [25]. Disintegrins are a family of small cysteine-rich peptides that could bind to integrins. The disintegrin domain of ADAM17 could competitively inhibit the function of integrin and was first discovered in viper venom [26]. Later, disintegrins was confirmed in not only platelets but endothelial cells also. The disintegrin domain of ADAM17 enabled cancer cells to interact with fibroblast and microenvironment, while soluble disintigrin impair this interaction and increased the proteolysis activity of ADAM17 [27].

1.9.4. Membrane proximal domain

The Membrane proximal domain is also known as stalk region. It is also an important domain as it regulates the substrate binding & shedding activity [18]. A short segment called Conserved Adam seventeeN Dynamic Interaction Sequence (CANDIS) is present between membrane proximal domain and the transmembrane helix. This small region plays pivotal role in substrate recognition and interaction between enzyme and substrate.

1.9.5. Transmembrane domain

Predominantly subcellular localization is the function of transmembrane domain. Function experiments using truncating mutation of ADAM17 suggested that transmembrane domain was necessary for the cleaving of TNF-α [28].

1.9.6. Cytoplasmic domain

The 130 amino acid long cytoplasmic domain binds to a variety of intracellular signalling molecules including protein kinase C (PKC), extracellular signal-regulated kinase (ERK) and mitotic arrest deficient 2 (MAD2), but the exact functional role of these interactions is still largely unknown. Although intracellular signals can influence ADAM17 catalytic activity, this seems to be independent from the cytoplasmic domain and is probably mediated through other transmembrane proteins [29]. ADAM17-mediated shedded substrates leading to subsequent

ripping of trans-membrane proteins by the intra-membrane protease γ-secretase, which cleaves single-pass transmembrane proteins within the transmembrane domain (**Figure 1.5**).

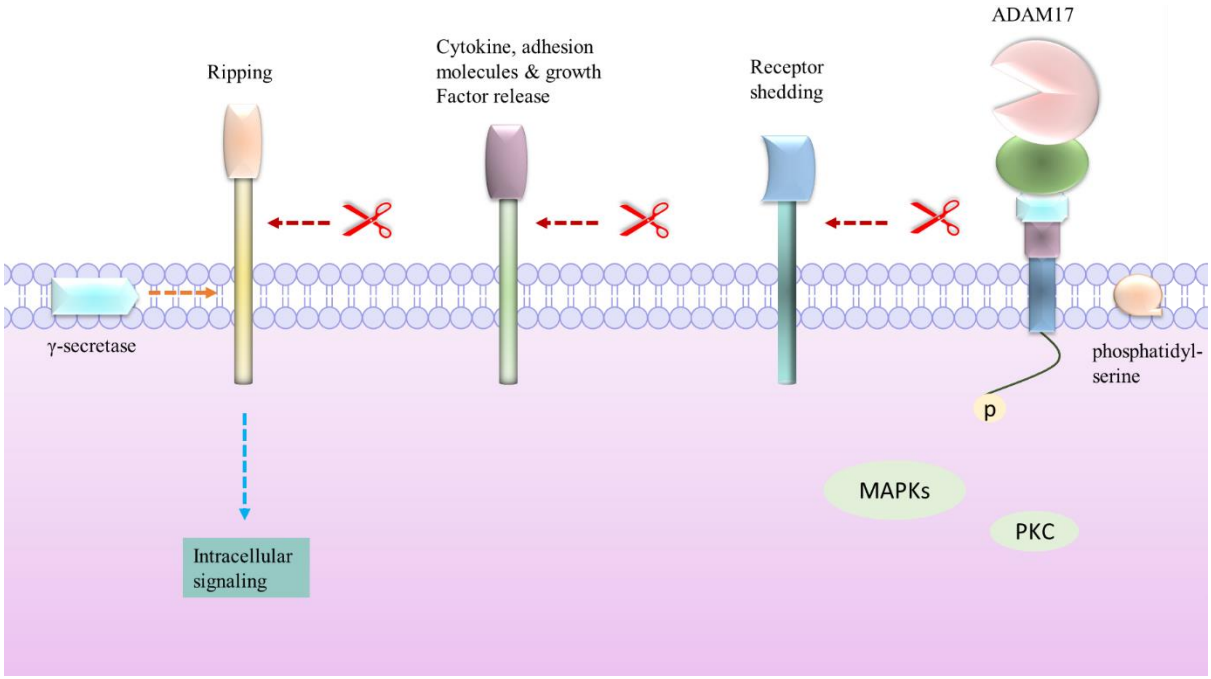

Figure 1.5. Schematic overview of ADAM17 mediated signalling

The cytoplasmic domain is critical for the activation of integrin-disintegrin binding-mediated magnification cascade of signalling pathways & other signalling like focal adhesion kinase (FAK), extracellular regulated kinase (ERK1/2) and protein kinase B (AKT/PKB) pathways. However, most of the activation of these signalling contributes to the progression and drug resistance of cancer treatment [30].

1.10. Molecular insight into the catalytic domain of ADAM17

To inhibit the biochemical pathways of the ADAM17 enzyme, inhibitors must bind to its active site properly. The catalytic domain of ADAM17 is shaped like an oblate ellipsoid, with a notch on its flat side creating a relatively small active-site cleft. This cleft separates a smaller lower sub-domain from the larger upper main molecular body. In the center, there is a highly twisted five-stranded β-pleated sheet (strands sI-sV), flanked on one side by α-helices hB and hB2 and on the other side by helices hA and hC. β-strands sII and sIII are connected by a large "multiple turn loop", along with a "long intermediate" α-helix (hB) and a nearby short α-helix (hB2), all positioned above the β-pleated sheet, effectively shielding its central part from bulk water. This multiple-turn loop bulges out at points, forming a "spur-like" and "acidic" protuberance (see fig.11).

The linker between sIII and sIV ends in a short bulge before connecting to the edge strand sIV, an antiparallel β-strand, and the segment linking sIV to sV, which is divided into two surface loops. The first loop attaches to the main molecular body, while the second forms a long β-hairpin loop (sIVa-sIVb) protruding from the molecular surface (see fig.11). Additionally, a bulging loop connects sV with the active site helix hC, centrally located within the molecule [31].

Adjacent to the catalytic zinc ion on the right side is the hydrophobic, medium-sized S1' specificity pocket. Furthermore, on the right side, a polar entrance leads to a second hydrophobic S3' pocket, which is contiguous within the molecule with the S1' pocket. However, the catalytic domain of ADAM17 differs from other ADAMs in several respects: it consists of 259 residues, making its chain considerably longer, and most of ADAM17's ancillary residues are clustered, creating two surface protrusions from the multiple-turn loop of the sIV-sV linker and a more pronounced sV-hC connector. Like other mammalian ADAMs, ADAM17 lacks a calcium binding site but features a deep S3' pocket in addition to its broader S1' pocket. (**Figure 1.6**) [32].

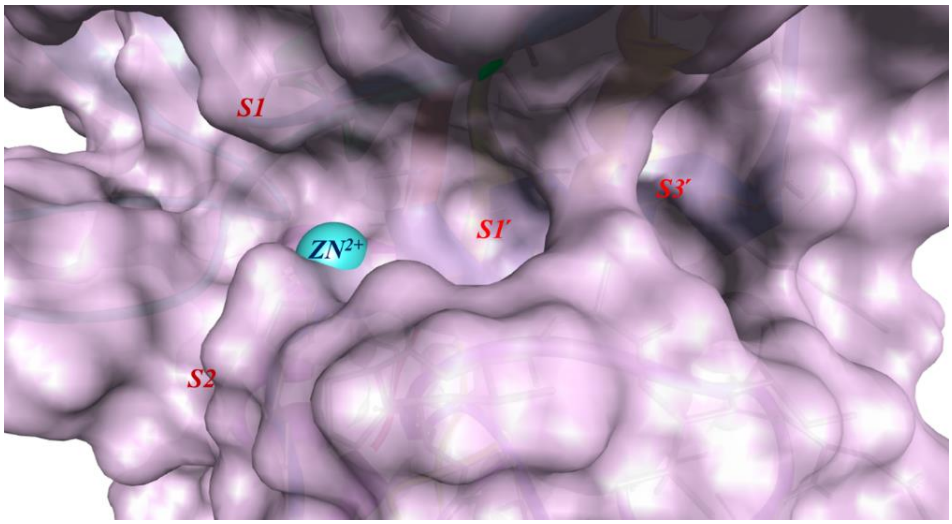

Figure 1.6. Catalytic site of ADAM17 enzyme (PDB ID: 2FV5)

1.11. Functional importance of ADAM17

ADAM17 was the first “sheddase" to the characterized. It mediates ectodomain shedding of different proteins, spanning from signalling molecules, such as cytokines, growth factors and their receptors, to adhesion molecules and endocytic receptors [33].

1.11.1. Development of embryo

ADAM17 plays a crucial role in embryonic development. Several research indicates that embryos lacking ADAM17 in mice exhibit abnormalities in various tissues including mammary epithelium, vascular system, lung, eye, hair, heart, and skin. This often results in early death during pregnancy or shortly after birth. The surviving mice deficient in ADAM17 show lower numbers of lymphocytes, impaired development of T and B cells, and reduced body weight. [16].

1.11.2. Adipocyte differentiation

ADAM17 can be seen as having both positive and negative effects on the differentiation of adipocytes (lipocytes & fat cells). While numerous studies highlight the harmful impact of ADAM17 shedding on adiposity, one of its substrates, pre-adipocyte factor (pref-1), appears to have potential benefits, particularly in inhibiting adipocyte differentiation [34]

1.11.3. Hepatic health

ADAM17 influences liver health in a manner that is debated, exhibiting dual roles similar to 'Jekyll and Hyde'. It can have both advantageous and harmful effects on liver biology. Research focusing on increasing the activity of this metalloproteinase has underscored its significant involvement in hepatic steatosis and inflammation, thereby influencing the onset of metabolic syndrome [35]. However, research also suggests that ADAM17 is involved in safeguarding hepatocytes against apoptosis during drug-induced liver failure. Furthermore, adenoviral introduction of ADAM17 prevented acetaminophen-induced liver failure in a relevant model of severe hepatitis dependent on Fas activation. [36]. Although there are marked detrimental consequences of having excess amounts ADAM17 activity, yet there is also need of ADAM17 for the important roles that it plays.

1.12. Functions of ADAM17 in cellular level

Being a multifunctional metalloproteinase enzyme, ADAM17 plays crucial role in various cellular processes. At the cellular level, ADAM17 is involved in:

1.12.1. Protein ectodomain shedding

The primary role of catalytically active ADAMs, such as ADAM17, is to cleave the ectodomains of various transmembrane proteins, typically near the membrane. This process, known as ectodomain shedding, affects proteins with diverse functions including EGFR

ligands, pro-inflammatory cytokines like TNF-α and its receptor TNFRI, adhesion molecules, and the amyloid precursor protein (APP) [37]. Ectodomain shedding by ADAM proteinases is crucial for various modes of signal transduction, such as paracrine, autocrine, and juxtracrine signalling. It allows released ligands to diffuse and interact with receptors on the same cell (autocrine signalling) or neighbouring cells (paracrine signalling). Additionally, proteolytic processing can activate membrane-bound ligands, influencing cell behaviour through juxtracrine or autocrine mechanisms [38]. The cleavage of proteins by ADAM17, for example, can activate EGFR through HB-EGF, leading to cell proliferation. Conversely, shedding may also terminate signalling initiated by ligands by removing receptors from the cell surface [39].

1.12.2. Regulated intramembrane proteolysis (RIP)

Regulated intramembrane proteolysis (RIP) is a step-by-step enzymatic process where a transmembrane protein undergoes initial shedding of its ectodomain by a specific enzyme. This is followed by a subsequent cleavage within the membrane itself, resulting in the formation of an intracellular domain fragment that often participates in signal transduction. Notch signalling and the processing of the amyloid precursor protein are well-known examples of this proteolytic mechanism. [40]. Signalling through Notch, a protein involved in cell-fate decisions, involves cleavage of the Notch receptor first on its ectodomain by ADAM10 & ADAM17 at a so called α-position [41], which is followed by a second intramembrane cleavage by multi-protein protease complex γ-secretase, which includes enzymes like presenilin. The intracellular domain of Notch is transferred to the nucleus where it regulates transcription of various genes. Another example is the processing of the amyloid precursor protein, which is responsible for amyloid plaque formation in Alzheimer's disease [42]. APP is cleaved first by ADAM17 or ADAM10 and similar to Notch, the remaining molecule is processed by presenilin [43]. The intracellular fragment induces intracellular Ca^{2+}signalling [44]. This process results in a soluble extracellular fragment that does not contribute to amyloid plaque formation [45]. Apart from events triggered by soluble factors, reverse signalling could offer cellular feedback and facilitate the transport of additional factors to the cell surface. Further investigation is needed to understand the implications of this phenomenon known as "Backwards Signalling." It would also be intriguing to determine whether all transmembrane proteins, whose ectodomains are processed, undergo transmembrane proteolysis [46].

1.12.3. Inter-receptor crosstalk "Triple Membrane Passing Signalling"

Ectodomain shedding plays a crucial role in intercellular communication involving various types of cell surface receptors. The interaction between G protein-coupled receptors (GPCRs) and receptor tyrosine kinases (RTKs) was initially documented in 1999. This mechanism involves GPCR-induced activation of a matrix metalloenzyme, leading to the shedding of the EGFR ligand heparin-binding EGF (HB-EGF), which exemplifies "triple membrane passing signalling" [47]. The exact intracellular connections between GPCR and ADAM activation remain unclear, but the involvement of the cytoplasmic domain of ADAM appears both plausible and effective. This aspect was investigated by Grandis et al., who explored the activation of EGFR signalling following cell stimulation with gastrin-releasing peptide [48].

1.13. Known substrates of ADAM17

Research conducted in recent years has shown that ADAM17 has over 90 substrates with specific functions (**Table 1.1**). These substrates are involved in a range of cellular processes, including cell adhesion, migration, development, inflammation, immune response, tumorigenesis, and signal transduction.

Table 1.1. List of known substrates of ADAM17

Receptors	***Cytokines***	***Adhesion molecules***	***Growth factors***	***Others***
ACE2 (49), *APP* (50)	*TNFα* (77)	*ICAM1* (86)	*AREG* (96)	*Pref1* (103)
c-MET (51), *Integrin b1* (52)	*TNFβ* (78)	*L1-CAM* (87)	*Epigen* (97)	*Klotho* (104)
IL-6R (53), *IL-11R* (54)	*MICA* (79)	*NCAM* (88)	*Epiregulin* (98)	*EGFRL* (105)
IL-1RII (55)	*MICB* (80)	*VCAM1* (89)	*TGFα* (99)	*Glycocalyx* (106)
CD30, *CD40* (56)	*INFγ* (81)	*EpCAM* (90)	*NRG1* (100)	*SEMA4D* (107)
CD147/EMMPRIN (57)	*CSF1* (82)	*CD44*	*HB-EGF* (101)	*Vasorin/VASN* (108)
CD163, *CA IX* (58)	*CX3CL1* (83)	*CD166/ ALCAM* (91)	*Tomoegulin2/TMEFF2/HPP1* (102)	
CD89/FcaR (59)	*Jagged1*	*E-cadherin* (92)		
EPCR (60), *ErbB4*	*FLT-3L*	*L-selectin/ CD62L* (93)		
GPV, *GPVI* (61)	*Kit-ligand l & 2* (84)	*Collagen XVII* (94)		

IGFR1, GHR (62)	*LAG-3* (85)	*Desmoglein2* (95)
GPIbα (63), *IGF2R*	*RANKL*	*Nectin4*
NPR, Notch1 (64)		*PTP-LAR*
TGFβR1 (65), *TIM-3*		
TIL4, TNFR1 (66)		
Trop2 (67), *KIM1*		
VEGFR2 (68), *VPS10P*		
sVLDLR (69)		
Syndecan-1 and -4		
LOX1, LRP1 (70)		
LeptinR (71)		
JAM-A/FIIR (72)		
MEGF10 (73), *MerTK* (74)		
p55TNFαR1		
P75, p75 TNFR (75)		
PTPα/PTPRA (76)		

1.14. ADAM17 as therapeutic target in diverse disease conditions

1.14.1. Cancer

Cancer is the second leading cause of death worldwide, so it became a serious issue for the human beings. According to the World Health Organization (WHO), it affects one in three people and accounts for a quarter of all deaths in the developed world. Due to the shedding activity, ADAM17 releases several factors (TNF-α, TGF-α, EGFR, HB-EGF), recent researches have confirmed that these relevant factors released by ADAM17 promote carcinogenesis [109]. ADAM17 is closely related to the genesis & development of distinct cancer types including lung cancer, breast cancer, gastric cancer, ovarian cancer, cervical cancer, bladder cancer etc.

1.14.1.1. Lung cancer

Lung cancer is the leading cause of cancer-related death. According to histological pattern, lung cancers are classified as non-small-cell lung cancer (NSCLC), squamous-cell carcinoma & adenocarcinoma [110]. Usually, ADAM17 is an oncogene & its upregulation is correlated with the progression of lung cancer. In case of adenocarcinoma KRAS (Kristen rat sarcoma

viral oncogene) mutation contributes to the phosphorylation of ADAM17 threonine via p^{38} MAPK pathway, as a result ADAM17 promote its substrate IL-6R shedding, leading to progression of Cancer [111]. In addition, co-factor of adam17, iRhom2, further promotes KRAS-induced tumor cell growth by regulating the release of ERBB ligands, further promotes cancerous cell growth. In NSCLC patients the EGFR pathway is over-activated due to overexpression of ADAM17 [112]. An inhibitor of the tyrosine kinase of the EGFR namely, gefitinib has shown efficacy in clinical trial for NSCLC, but woefully, due to resistance to the drug overall response was much lower than expectation. To overcome the issue an ADAM17 inhibitor, INCB3619 uses along with gefitinib to treat lung cancers [113].

1.14.1.2. Breast cancer

Breast cancer is the most common malignancy in women worldwide. According to WHO, in 2022, there were 2.3 million women diagnosed with breast cancer and 670 000 deaths globally (WHO report, march 2024). Despite advanced treatments including chemotherapy, radiotherapy & surgical resection breast cancer remain a serious health problem [114]. As ADAM17 can shed several ligands including TGF-α, EGF, AREG, further stimulate epidermal growth factor receptor, which frequently over-expressed and dysregulated in different tumor tissues, this EGFR ligand binding leads to auto-phosphorylation & subsequent stimulation of p13K/AKT and MAPK pathways which further causes breast cell proliferation & invasion (**Figure 1.7**) [115]. Interestingly, ADAM17 releases MCSF and mediates the secretion of CCL2 from breast tumor cells, and thereafter MCSF and CCL2 participate in the interaction with macrophages and activate the central transcription factor (NF-κB) in macrophages then, VEGF is activated through stimulating the NF-κB signaling pathway and subsequent macrophage secretions, which promotes endothelial cell tube formation and causes tumor angiogenesis [116]. So, inhibition of ADAM17 prevents the shedding of EGFR ligands in cells derived from breast tumors, indicating that ADAM17 inhibitors can be beneficial to target EGFR pathway to treat breast cancer [117].

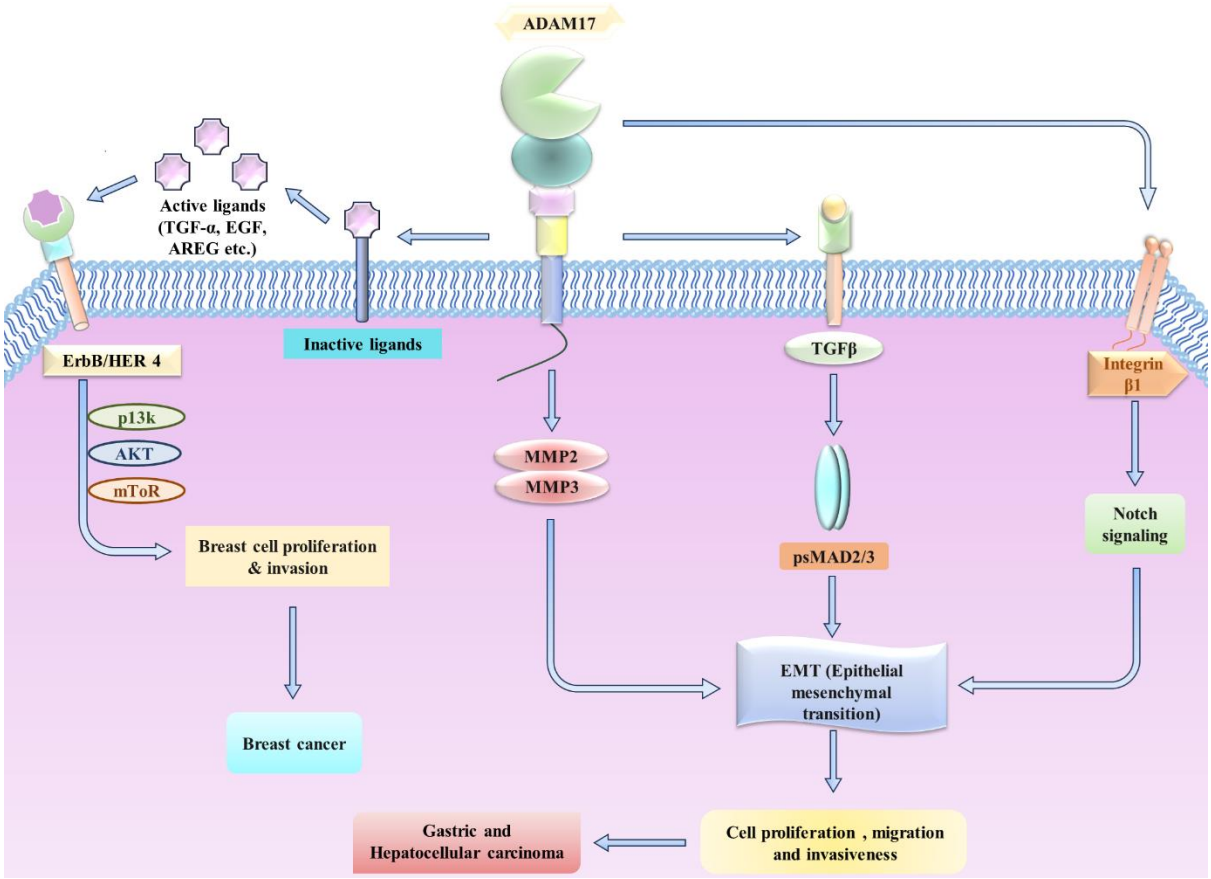

Figure 1.7. Schematic diagram illustrating the role of ADAM17 enzyme in diverse cancers

1.14.1.3. Gastric cancer

This type of cancer forms in the tissue lining of stomach thus, it is also called stomach cancer, is a relatively common form of cancer and can affect any part of the stomach. The precise cause of gastric cancer is not completely understood, but several factors are known to increase the risk. These include infection with Helicobacter pylori bacteria, chronic stomach inflammation over an extended period, smoking or specific genetic mutations. ADAM17 is also associated with the pathogenesis of gastric cancer. A recent meta-analysis associated with gastric cancer indicated that ADAM17 might be a tumor marker for prognosis in gastric cancer [118]. ADAM17 promotes gastric cancer through the activation of Notch signaling pathway leads to a transformation of cell morphology called Epithelial Mesenchymal Transition (**Figure 1.7**) which finally promotes cell proliferation that leads to gastric cancer [119].

1.14.1.4. Other types of cancer

Apart from the above discussed cancers, ADAM17 is also expressed in many other types of cancers such as ovarian cancer, liver, cancer, bladder cancer, colorectal cancer etc. Ovarian

cancer is the fifth most common cause of cancer-related deaths in women and often goes undetected until it has spread within the pelvis and abdomen. Fabbi et al. discovered that in ovarian cancer patients ADAM17 remarkably up-regulated & high concentration of ADAM17 in blood serum and ascitic fluid of patients may be used as hematologic tumor marker for the detection of ovarian cancer [120]. Actually, ADAM17 promotes malignancy of ovarian cancer & causes chemo-resistance by shedding of TNF-α, TGF-α, HB-EGF, AREG and activating the EGFR pathway [121]. ADAM17 cleaves notch receptor and activate notch signaling pathway & thereby it contributes to hepatocellular carcinoma [122] (**Figure 1.7**). In these cancers the overexpression of ADAM17 mostly, correlate with the activation of the EGFR pathway. Thus, ADAM17 inhibitors should block EGFR signaling and it could be therapeutically useful alone or in combination with any other anti-EGFR drugs [123].

1.14.2. Inflammatory disorders

1.14.2.1. Rheumatoid Arthritis

Rheumatoid arthritis is a widespread autoimmune condition marked by persistent inflammation of the synovial membranes, resulting in joint damage and bone erosion. It affects around 1% of the global population and is primarily recognized for its ongoing systemic inflammation [124].

Rheumatoid joints contain inflammatory infiltrates that spread from the synovia. Eventually, this synovitis leads to the degradation of the joint surface, resulting in loss of function [125].

TNF levels are increased in most common inflammatory diseases, supporting the involvement of ADAM17 in their progression, including rheumatoid arthritis. The TNF-α signalling pathway is over-activated in the inflammatory infiltrates and induces the production of the degrading enzymes that contribute to the erosion of cartilage and bone [126]. Human RA cartilage displays upregulated ADAM17 mRNA expression, indicating that the metalloproteinase is responsible, at least in part, for the over-activation of the TNF-α pathway [127]. Neutralization of the TNF-α signalling pathway, by blocking the interaction of the cytokine with its cognate receptors, has been demonstrated as a feasible approach for treating RA. BMS-561392, a selective ADAM17 inhibitor may useful to treat rheumatoid arthritis [128].

1.14.2.2. Osteoarthritis

Osteoarthritis (OA) is the most common joint disorder, is associated with an increasing socioeconomic impact owing to the ageing population and mainly affects the diarthrodial joints. It is characterized by the loss of cartilage, remodelling of subchondral bone, and the development of osteophytes. These changes lead to restricted movement, stiffness, and joint pain. Major risk factors include aging, obesity, and joint injury. [129]. High levels of sol-TNF are associated with OA, implying enhanced activity of ADAM17 in this disease [130]. This in turn, suppresses the synthesis of the major cartilage components & promotes the release of the cartilage degrading proteases MMP-1, MMP-3, MMP-13 [131]. Despite a clear involvement of tumour necrosis factor-α converting enzyme in the pathophysiology of OA, clinical trials of ADAM17 inhibitors have not yield conclusive results & thus these inhibitors are generally believed to not be beneficial in osteoarthritis [132].

1.14.2.3. Atherosclerosis

Atherosclerosis is a chronic inflammatory disease of the arteries and is the underlying cause of about 50% of all deaths in westernized society, it is actually a lipid-driven process initiated by accumulation of low-density lipoprotein or remnant lipoprotein in the arteries [133]. Atherosclerosis is closely related to ADAM17 & increased ADAM17 expression and activity are positively correlated with the cardiovascular events [134]. The inflammatory process of atherosclerosis is closely related to Ecs and monocytes/macrophages, the inflammatory mediators (IL-6, IL-8) happen to be substrate of ADAM17 [135]. Reducing ADAM17 activity will significantly reduce circulating levels of endothelial cell adhesion molecules (ECAM), therefore a large extent ADAM17 may be a key step in triggering the initial inflammation of the endothelium. In the initial stages of atherosclerosis, inhibition of ADAM17 is expected to control deterioration [136].

In atherosclerosis, ADAM17 facilitates inflammation through several pathways. Specifically, in endothelial cells, ADAM17 induces the shedding of endomucin (EMCN) from the cell surface (**Figure 1.8**). This shedding process promotes leukocyte adhesion and contributes to inflammation within the affected tissues. In vascular smooth muscle cells, ADAM17 induces the production of inflammatory factors through the epidermal growth factor (EGRF)-extracellular signal regulated kinase (ERK1/2) pathway. In macrophages, ADAM17 leads to an increase of tumour necrosis factor (TNF)-α and interleukin (IL)-6 [135]. Therefore, by inhibiting the ADAM17 mediated inflammation by inhibitors should be preferable to treat atherosclerosis.

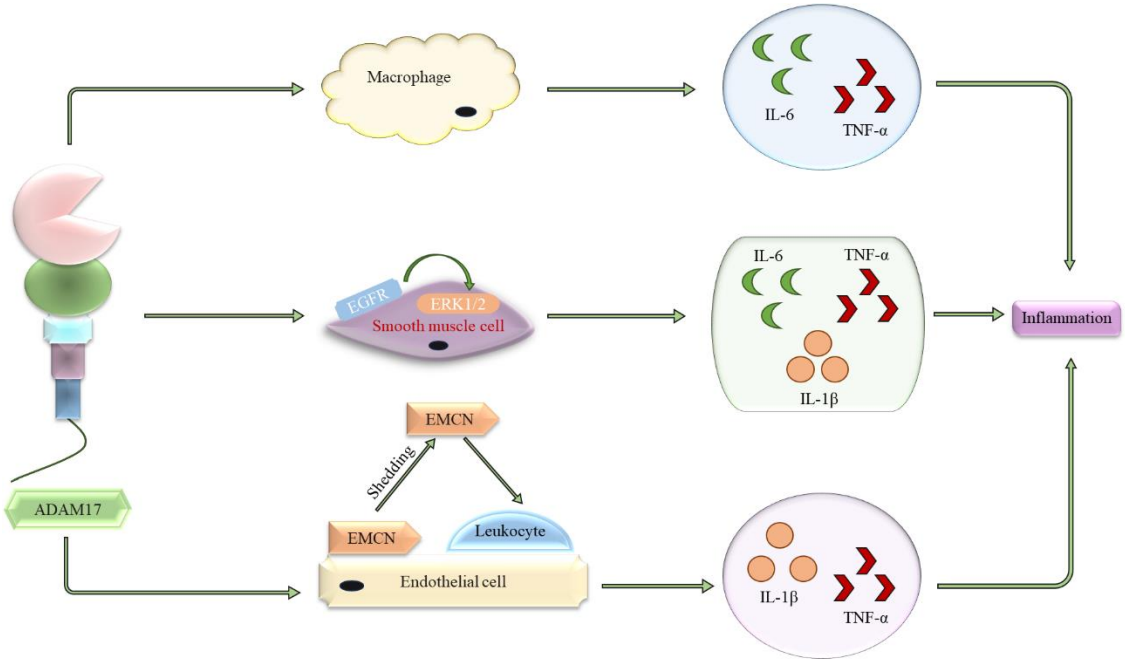

Figure 1.8. The role of ADAM17 in inflammation

1.14.2.4. Inflammatory bowel disease

Inflammatory bowel disease (IBD) is basically a chronic & life-threatening inflammatory disease of gastrointestinal tract characterized by occurrences of abdominal pain, diarrhoea bloody stools, etc. Ulcerative colitis & Crohn's disease collectively known as inflammatory bowel disease, become major cause of lifetime morbidity [137].
Basically, ADAM17 expressed in colonic mucosa of human being, increase in inflammatory bowel disease and its expression is upregulated by TNF-α in the endothelial cells [138]. In IBD worsen mucosal inflammatory response caused by over-activation of TNF-α signalling, this increased TNF-α signalling promotes up-regulation of inducible nitric oxide synthase (iNOS) which also plays major role in IBD [139]. In IBD ADAM17 also activates IL-6 trans-signalling pathway and this IL-6 leads to inflammation in colonic mucosa. An experiment showed that the colitis induced in rats by trinitrobenzene sulphonic acid (TNBS) is characterized by an increase in the levels of soluble TNF-α, ADAM17 and iNOS, an ADAM17 inhibitor BB1101 inhibits TNBS induced increase in ADAM17 activity, TNF-αrelease and iNOS expression [140]. Thus, ADAM17 inhibitors should be useful as therapeutic agent in the treatment of IBD.

1.14.3. Neurodegenerative disease

1.14.3.1. Alzheimer's disease

Alzheimer's disease (AD) is a progressive neurodegenerative disorder that is predominantly the leading cause of dementia in the elderly [141]. Pathologically, it is characterized by two

key hallmarks: extracellular beta-amyloid (Aβ) plaques and intracellular neurofibrillary tangles (NFTs) [142].

These beta amyloid (Aβ) plaques are generated from a transmembrane protein called amyloid precursor protein (APP) which is processed by α, β & γ-secretase (**Figure 1.9**) to illuminate the cellular pathway of amyloid beta peptides production [143]. This APP is processed in two definite ways which are respectively, amyloidogenic pathway & non-amyloidogenic pathway. In amyloidogenic pathway APP is cleaved by β & γ secretase to generate the neurotoxic amyloid beta peptides, which promotes neuro-degeneration [144]. Firstly, the ectodomain shedding by β-secretase leads to release of soluble APPβ fragment (sAPPβ) then the 99 amino acid containing transmembrane part cleaved by γ-secretase to release Aβ peptides & APP intracellular cytoplasmic domain (AICD) [145]. In non-amyloidogenic pathway APP is cleaved by α-secretase inside the Aβ domain, in this case, the cleavage can attenuate Aβ peptides production &this cleavage result to the generation of sAPPα and C83 [146]. As ADAM17is endowed with α-secretaseactivity thus, it can regulate the production amyloid beta peptides more specifically attenuate Aβ peptides production [147].

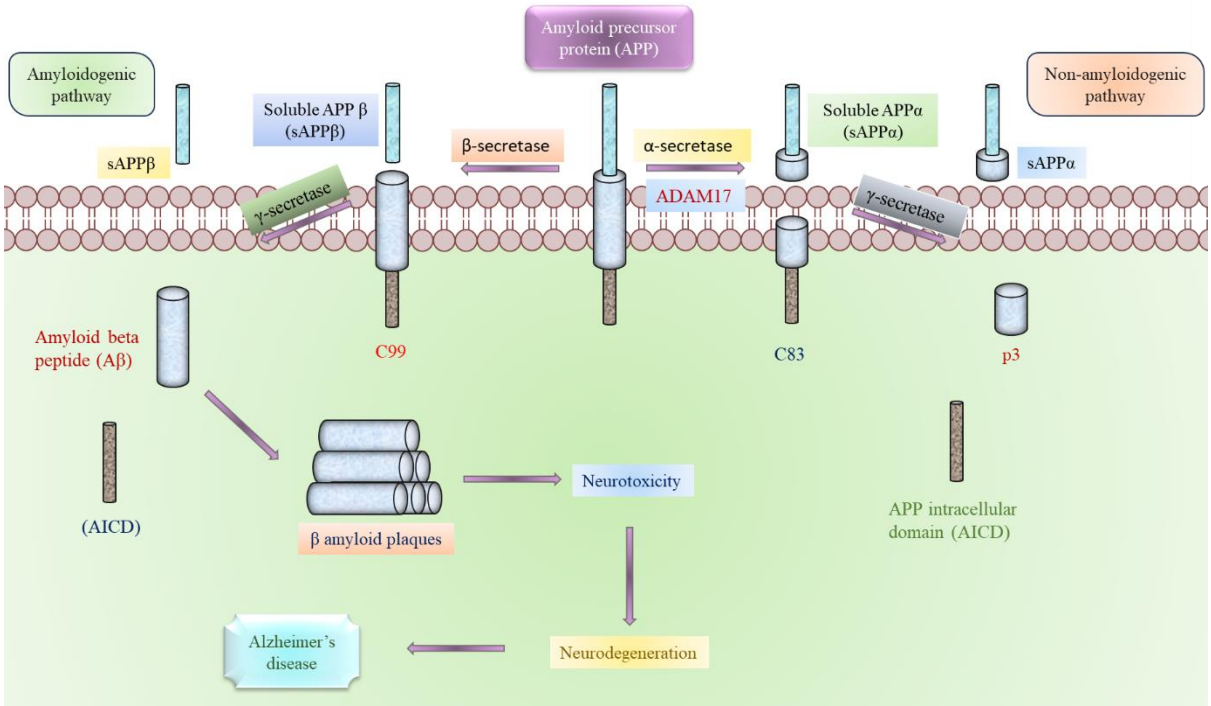

Figure 1.9. Proteolytic pathway of amyloid precursor protein (APP) in Alzheimer's disease

Actually, ADAM-17 plays dual role in the pathogenesis of alzheimer's disease. In one hand, it attenuates neurotoxic Aβ peptides production through the APPα shedding and neuroprotective APPα generation [146]. On the other hand, ADAM17 cleaves various Pro-inflammatory

mediators in activated microglia, these cytokines or inflammatory factors aggravate the neuronal dystrophy leads to neuro-degeneration [148].
In spite of contradictory role of ADAM17 in AD the potential treatment should be applied by activating ADAM17 with caution.

1.14.4. Respiratory diseases

ADAM17 plays a significant role in respiratory tract diseases such as emphysema and asthma. Emphysema is a progressive condition affecting the distal airways and lung parenchyma, characterized by permanent enlargement of distal air spaces, irreversible destruction of alveolar tissue, reduced gas exchange area, and ultimately leading to shortness of breath [149]. Asthma is a chronic airway disease distinguished by airway inflammation and airway hyper-responsiveness (AHR) [150]. Expression of ADAM17 is up-regulated in emphysema including other lung diseases such as asthma &chronic obstructive pulmonary disease (COPD) [151]. Here, ADAM17 plays a major role in the activated shedding of EGFR ligands {transforming growth factor-α (TGF-α), epiregulin, amphiregulin, heparin binding epidermal growth factor (HB-EGF)} and cleaves TNF-α, tumor necrosis factor receptor (TNF-R), interleukin 6 receptor (IL6R), L-selectin, intracellular adhesion molecule 1(ICAM-1) etc. [152]. Additionally, ADAM17 can activate membrane responses depending on its phosphorylation status. Cigarette smoking generates reactive oxygen species (ROS) that result in the activation of sarcoma (SRC) kinases (**Figure 1.10**), PKCε promotes phosphorylation of ADAM17 at threonine/serine residues, with consequent EGFR activation & hyper-proliferation of lung cells [153]. In asthma ADAM17 also plays vital role, such as EGFR mediated increased fibrocyte proliferation & transformation in asthma patients [154]. Thus, inhibition of ADAM17 seems to be a beneficial therapeutic approach to treat respiratory diseases.

1.14.5. Cardiovascular diseases

Cardiovascular diseases (CVD) refer to a group of disorders that affect the heart and blood vessels which is the largest cause of worldwide. ADAM17 has significant role in different heart diseases. Certain animal models suggest a role of ADAM17 in the development of heart, regulating valvulogenesis but some other studies suggest that ADAM17 contributes to various cardiac diseases such as hypertrophic obstructive cardiomyopathy, dilated cardiomyopathy, myocarditis, abdominal aortic aneurysm, etc. [155].

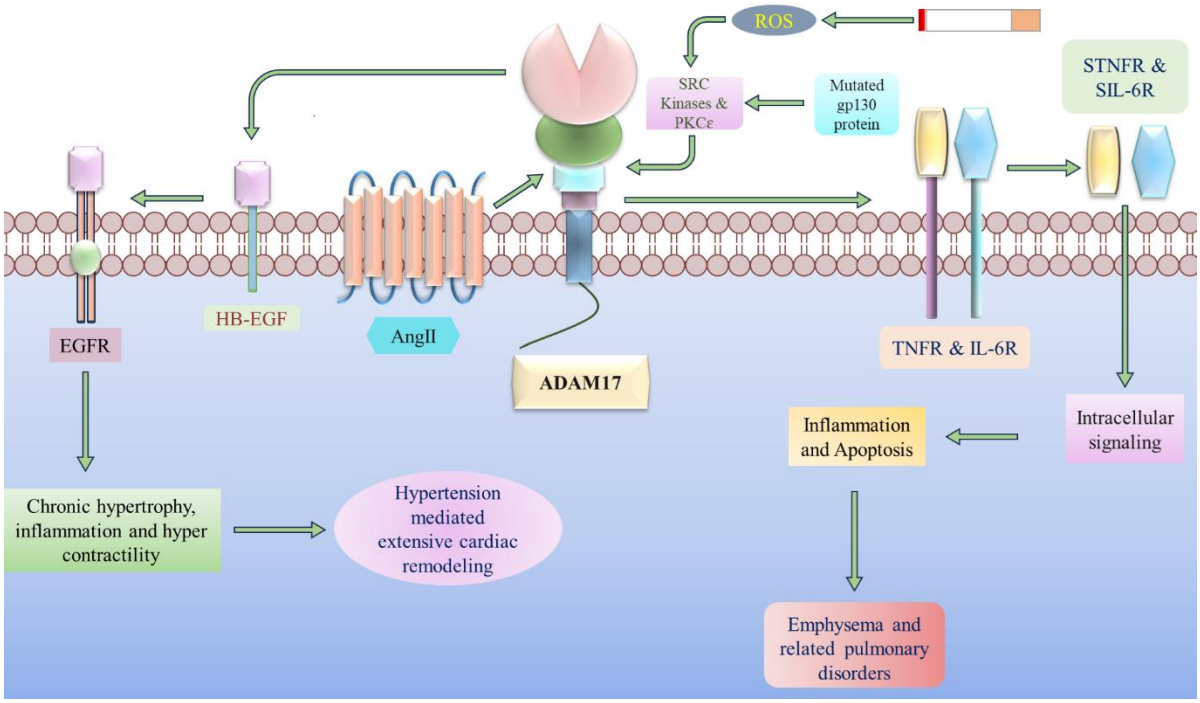

Figure 1.10. Schematic diagram demonstrating the role of ADM17 signalling in emphysema and hypertension

High expression of ADAM17 had been noted in peripheral blood mononuclear cells (PBMC) of patients with congestive heart failure, myocardial infarction& ventricular arrhythmia [156]. As ADAM17 mediates angiotensin II induced EGFR trans-activation in vascular smooth muscle cells (VSMCs) causing growth promoting signal transduction thus, inhibition of EGFR also mitigated hypertensive vascular remodeling in mice infused with angiotensin II [157]. Therefore, in a mouse model of angiotensin II induced hypertension with smooth muscle ADAM17 deletion or pharmacological inhibition of ADAM17 vascular hypertrophy and perivascular fibrosis is attenuated [158]. Angiotensin II readily activates ADAM17 via its Tyr702 phosphorylation through the GPCR, this leads to pro HB-EGF shedding and subsequent EGFR trans-activation which further leads to hypertensive vascular remodeling (**Figure 1.10**). Besides ADAM17 is identified as central gene correlated with angiotensin II induced abdominal aortic aneurysm (AAA) [159]. ADAM17 expression is increased in experimental models of AAA, and temporal or systemic deletion of ADAM17 averts development of AAA [160]. These findings firmly suggest that inhibiting ADAM17 activity could be beneficial for preventing complications of abdominal aortic aneurysms and chronic vascular remodeling in hypertension.

1.14.6. Renal diseases

Renal diseases, also referred to as kidney diseases, cover a broad spectrum of conditions affecting the kidneys, which are vital organs responsible for filtering waste products from the blood, regulating electrolyte balance, and maintaining fluid balance in the body. ADAM17 signaling is fundamental for modulating cellular processes during kidney development, whereas upregulation and activation of ADAM17 is involved in kidney diseases. ADAM17/EGFR signaling is not only involved in the initiation of AKI and its progression to CKD, but also is of importance in other kidney diseases such as polycystic kidney disease and diabetic kidney disease. Chronic kidney disease (CKD) that is characterized by extracellular matrix deposition and fibrotic transformation of kidney tissue can develop from renal diseases of different origins [161]. Some data suggest that enhanced EGFR activation can contribute to the fibrosis process and it was shown that the GPCR agonist angiotensin II induces EGFR trans-activation by ADAM17 activation and TGF-α shedding. Chemical inhibition of ADAM17 diminished chronic angiotensin II induced glomerular fibrosis suggesting that ADAM17 inhibition could be important therapeutic target to treat fibrotic kidney disease [162].

1.14.7. Other diseases

Apart from the above-mentioned diseases ADAM17 plays crucial role in metabolic disorders, psoriasis, multiple sclerosis etc. ADAM17 seems to be involved in diet related disease, obesity caused by a high fat diet (HFD) in mice leads to enhancement of the expression of ADAM17 [163]. Expression of ADAM17 is significantly increased in the liver & adipose tissue of mice that have been fed HFD and that is positively involved with the development of insulin resistance. Therefore, by inhibiting ADAM17 activity via several therapeutic strategies may increase insulin sensitivity and finally have a beneficial effect on obesity [164]. The advantageous effect of ADAM17 inhibitor for treating psoriasis was shown in phorbol ester-induced epidermal hyperplasia, a murine model of the disease [165]. In case of multiple sclerosis ADAM17 increased significantly in peripheral blood mononuclear cells. Additionally, ADAM17 was observed together with TNFR2 and T-lymphocytes in multiple sclerosis patients [166]. Furthermore, immunohistochemical analysis of nerve biopsies from leprosy patients displayed an over-expression of ADAM17 compared with normal tissues [167]. Ultimately, it can be said that ADAM17 might be a promising & beneficial therapeutic target for the above discussed diseases or disorders.

Chapter 2: Literature Review

2.1. Introduction

In all living organisms, including humans, various enzymes are involved in regulating specific biological reactions. One such group is proteases, which facilitate the proteolytic hydrolysis of peptide bonds and thereby regulate numerous cellular processes. Nowadays proteases have become a major focus of interest due to their critical role in various cellular processes essential for proper cell function. Disruption in the activity of these proteases can lead to the development of numerous diseases. Among these, ADAMs (a disintegrin and metalloproteinases) are Zn2+-dependent, modular cell surface proteins belonging to the adamalysin protease family. They play a role in cellular adhesion and the proteolytic cleavage of various molecules on the cell surface. ADAMs are closely related to other metalloenzymes like ADAM-TSs (which have thrombospondin domains) and matrix metalloproteinases (MMPs). ADAM17 and several other members of the ADAM family are primarily known for processing single-spanning membrane proteins, including cytokines, growth factors, receptors, chemokines, and regulators involved in neurological processes and diseases.

Recent studies discover the overexpression of ADAM17 in several pathophysiological conditions includes cancers, inflammatory disorders, neurodegenerative diseases, respiratory diseases, and cardiovascular diseases. This has led to growing speculation that targeting ADAM17 could be a viable strategy for treating various diseases. Despite the significant role of the multifunctional protease ADAM17 in the development of several conditions, there has been little progress in developing small molecules that serve as effective therapeutic inhibitors of ADAM17.

2.2. A summary of the reported inhibitors of ADAM17

Given ADAM17's role in various diseases and conditions, there has been a continual interest in creating selective inhibitors that target ADAM17 to address different pathological issues. Several pharma companies have attempted to develop ADAM17 inhibitors, but their efforts have largely been unsuccessful due to issues with toxicity and adverse effects encountered during development of the molecules. Pharmaceutical companies are actively seeking new ADAM17 inhibitors with enhanced selectivity, efficacy, and safety. Additionally, research is focused on understanding the wider effects of ADAM17 inhibition across different diseases and refining therapeutic strategies.

INCB7839, also known as Aderbasib, is a small-molecule, selective ADAM17 inhibitor (**Figure 2.1**) developed by Incyte Corporation. It has been tested in clinical trials for its potential use in cancer treatment, especially targeting tumours with elevated levels of TNF-α. The drug functions by blocking ADAM17's activity in shedding cytokines and growth factors that promote tumour growth. Another small molecule, INCB3619, has also been developed by the same company as an ADAM17 inhibitor.

Bristol-Myers Squibb developed BMS-561392 (DPC-333) that targets ADAM17. This compound has been investigated for its potential to decrease inflammation and inhibit cancer growth by targeting the enzyme's activity. Its development aimed to capitalize on its capacity to influence immune responses and impact the progression of diseases. This selective inhibitor (**Figure 2.1**) reported in the literature for the treatment of inflammatory diseases namely rheumatoid arthritis.

GI254023X a selective, reversible small molecule inhibitor (**Figure 2.1**) of ADAM17 developed by GlaxoSmithKline (GSK). It has mainly been investigated in preclinical studies to assess its effectiveness in reducing inflammation and controlling cytokine shedding. Research has demonstrated that this compound can prevent the migration and invasion of breast cancer cells in laboratory cultures. However, clinical trials encountered issues due to the inhibitor’s lack of selectivity, affecting additional targets. Additionally, because hydroxamates can cause liver toxicity, the trials were halted during phase I/II.

AZD8931 is a dual inhibitor of ADAM17 and the Epidermal Growth Factor Receptor (EGFR), developed by AstraZeneca. This compound has been assessed for its potential in treating cancers with abnormal EGFR signalling by combining ADAM17 inhibition with EGFR targeting to manage tumour growth and progression.

WAY-281418 was developed by Wyeth Research (now part of Pfizer). It is a small molecule (**Figure 2.1**) designed to selectively inhibit ADAM17 activity. The compound shows promise for treating diseases where ADAM17 is crucial, especially in inflammatory and autoimmune conditions.

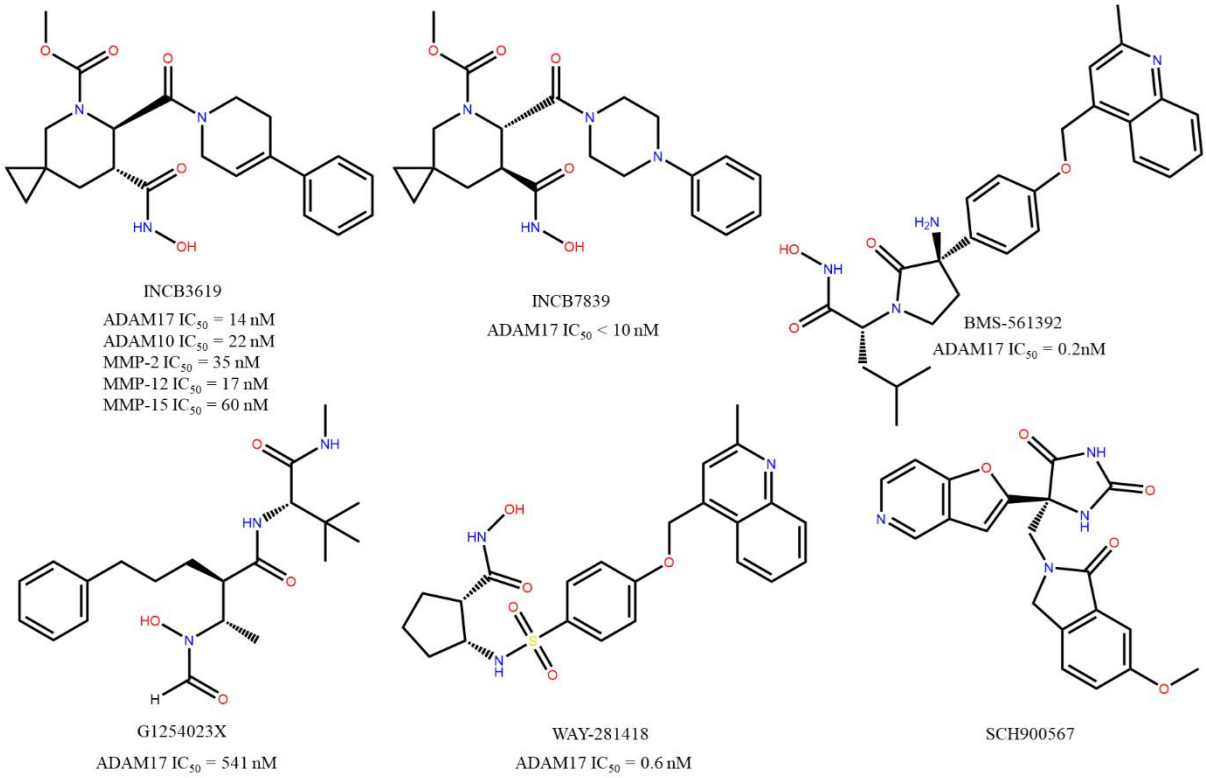

Figure 2.1. Some potent ADAM17 inhibitors

SCH 900567 is a compound developed by Schering-Plough, which is now part of Merck & Co., Inc. This ADAM17 inhibitor (**Figure 2.1**) was being investigated as a potential treatment for rheumatoid arthritis.

Nuti et al., reported arylsulfonamido-based hydroxamic acid derivative as selective ADAM17 inhibitor, namely, JG26 (**Figure 2.2**). In fact, JG26 displayed a 126-fold selectivity for ADAM-17 over MMP-2, an 860-foldselectivity over MMP-9, a 10000-fold selectivity over MMP-14, and no measurable inhibitory activity toward MMP-1 (IC_{50} > 500 μM). Reported it as probable ADAM17 inhibitor for treatment of ovarian cancer but further investigation is also needed to access the effect of the improved ADAM17 selectivity in other cancers [168].

In continuation of the above research Cuffaro et al., reported 3 dimer derivatives (**Figure 2.2**) of JG26 as possible selective ADAM17 inhibitors (compounds 1-3). Additionally, these compounds showed a high selectivity over ADAM10 and most of the tested MMPs. They undisclosed that these derivatives showed activity in inhibiting the invasiveness of MDA-MB-231 breast cancer cells [169].

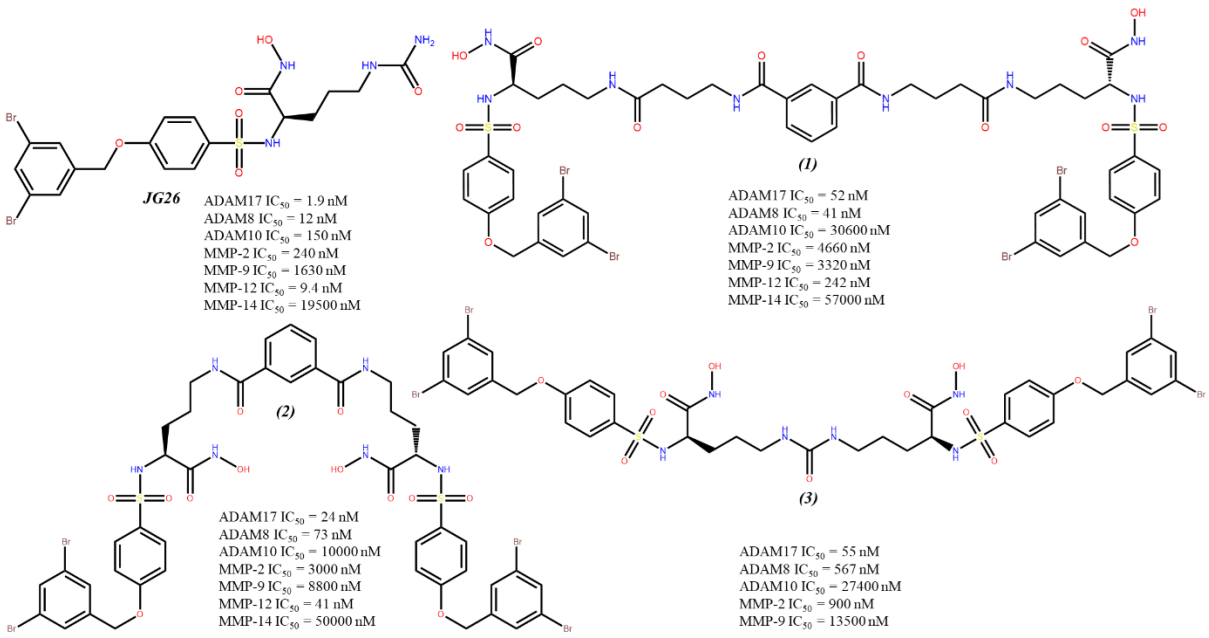

Figure 2.2. Few ADAM17 inhibitors

Rosner et al., reported tartrate based small molecules (compounds 4-7) as ADAM17 inhibitors [170]. Besides, ADAM17 The molecules demonstrated strong selectivity for the MMP panel and showed equal potency against ADAM10 (**Figure 2.3**). They reported finding the first tartrate scaffold that employs tridentate coordination to bind to the active site zinc of ADAM17. This series of tartrates is especially noteworthy as it effectively substitutes hydroxamate-based TACE inhibitors. Its distinctive binding mode provides access to both the prime and non-prime binding pockets.

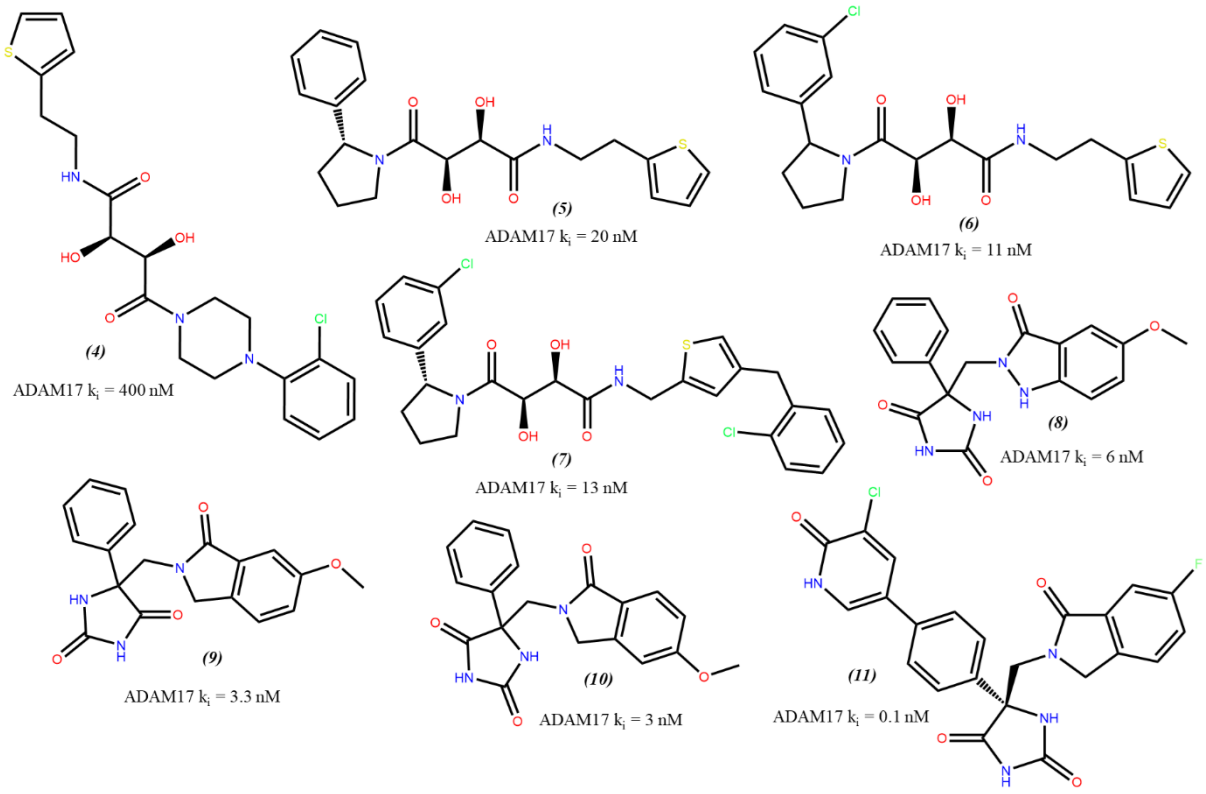

Figure 2.3. Some molecules that showed ADAM17 inhibitory activity

Yu et al., reported a series of selective and potent ADAM17 inhibitors (compounds 8-10) (**Figure 2.3**) using the hydantoin moiety as a zinc-binding ligand and revealed the first X-ray structures of inhibitors with a hydantoin zinc ligand bound to ADAM17 [171]. In continuation of the above study Yu et al., reported A series of biaryl hydantoin ADAM inhibitors (**Figure 2.3**) demonstrated sub-nanomolar activity. Many of these inhibitors also showed favorable pharmacokinetics in rats and good selectivity against MMP-1, -3, -7, -9, -13, and ADAM10. Additionally, the activity of these ADAM17 inhibitors in human whole blood is enhanced compared to their earlier hydantoin ADAM17 leads [172].

Pu et al., reported new quinazoline derivatives as ADAM17 inhibitors [173] with strong anti-inflammatory effects. According to the authors, this was the first study to show that quinazoline derivatives (compound 12) inhibited TACE-mediated production of TNF-α in the treatment of rheumatoid arthritis (RA). The compound showed excellent anti-inflammatory activity by inhibiting TNF-α production and exhibited an IC_{50} value of 8.86 μM in RAW264.7 cells (**Figure 2.4**).

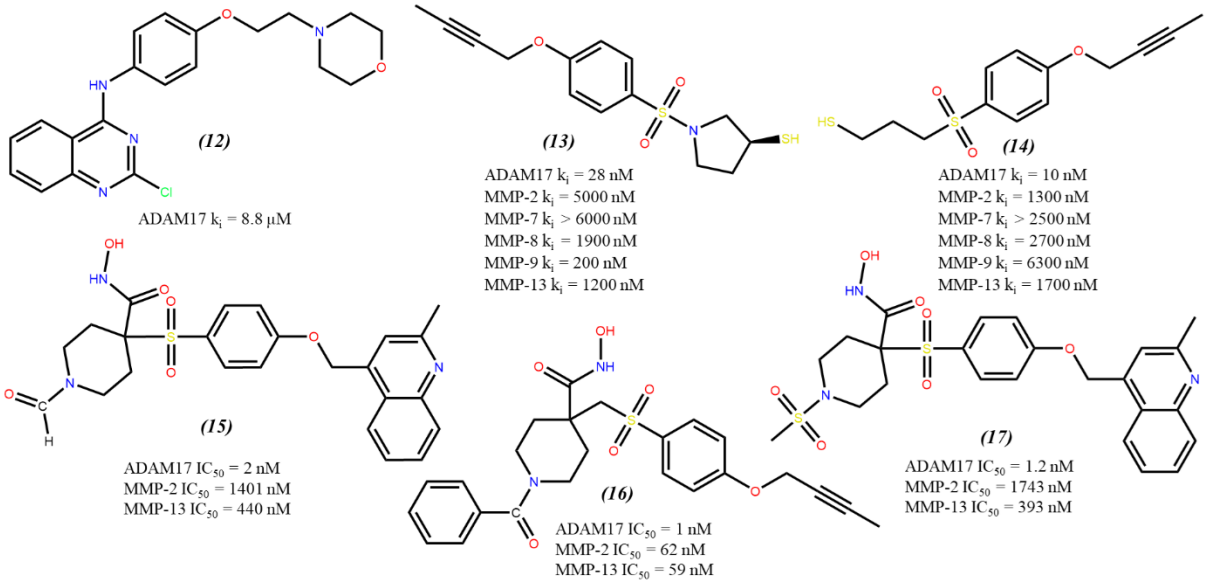

Figure 2.4. Few ADAM17 inhibitors

Bandarage et al., have designed and synthesized a new series of thiol-containing aryl sulfones (**Figure 2.4**) as TACE inhibitors. Most of these compounds exhibit highly potent inhibition in enzyme assays using the isolated enzyme and also showed good selectivity over MMP-2, -7, -8, -9, and -13 enzymes [174].

Zhang et al., reported a series of a-sulfone piperidine hydroxamate ADAM17 inhibitors (compound 16 & 17) bearing a quinolinyl methyl group (**Figure 2.4**). These compounds have been demonstrated to be highly effective inhibitors of the ADAM17 enzyme and, depending on the substituent on the piperidine nitrogen, can offer excellent selectivity against MMP-2 and MMP-13 [175].

Nelson et al., reported a novel series of benzodiazepine inhibitors (**Figure 2.5**) of the MMPs and ADAM17, and author claims that all the compounds exhibited selectivity for MMP-9 and MMP-13 over MMP-1 and ADAM17 [176]. Zask et al., synthesized several small molecules featuring 1,4-diazepine and 1,4-thiazepine ring systems (**Figure 2.5**) as the main scaffolds. They reported that these compounds are potent inhibitors of ADAM17, as well as MMP-1 and MMP-13 [177].

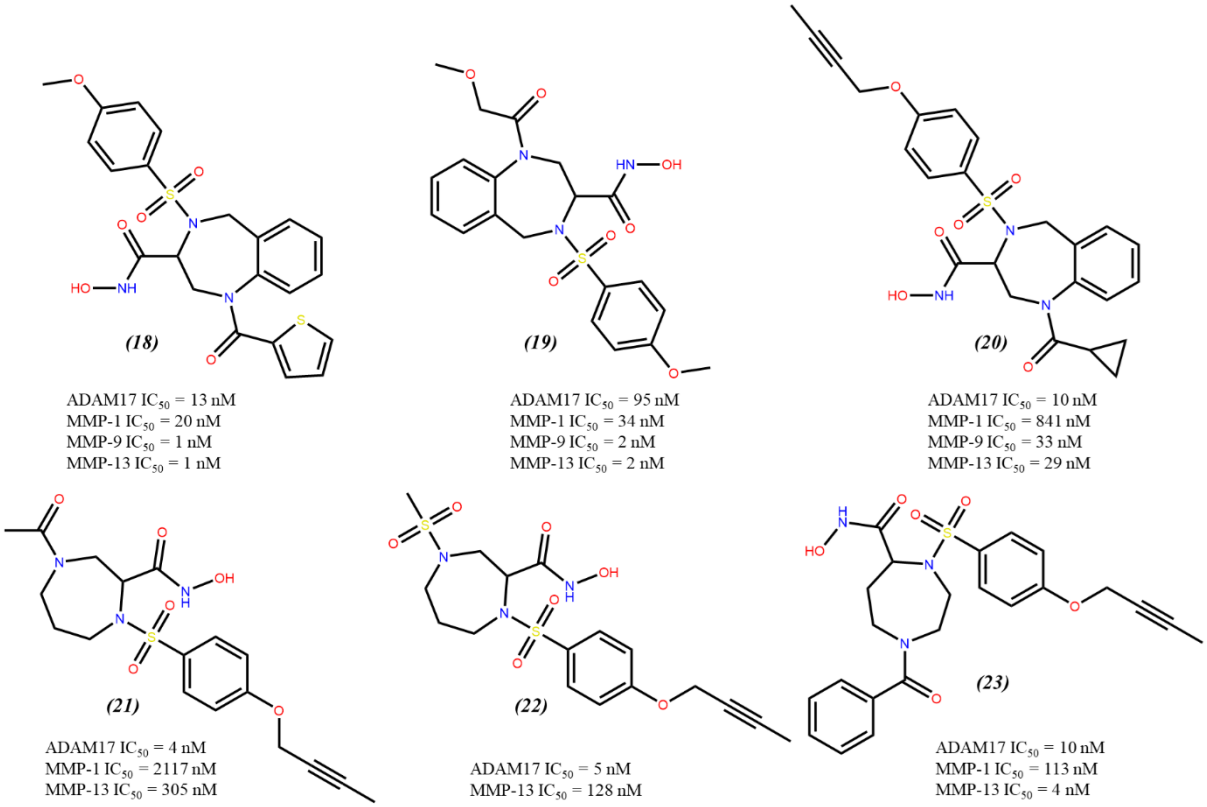

Figure 2.5. Some examples of ADAM17 inhibitors

Lombart et al., designed and synthesized a series of β-sulfone 3,3-piperidine hydroxamate (compounds 24-27) ADAM17 inhibitors (**Figure 2.6**). All of these analogs demonstrated excellent enzyme activity with low nanomolar IC50 values in a FRET assay and showed significant selectivity over MMPs, with up to 1100-fold selectivity [178].

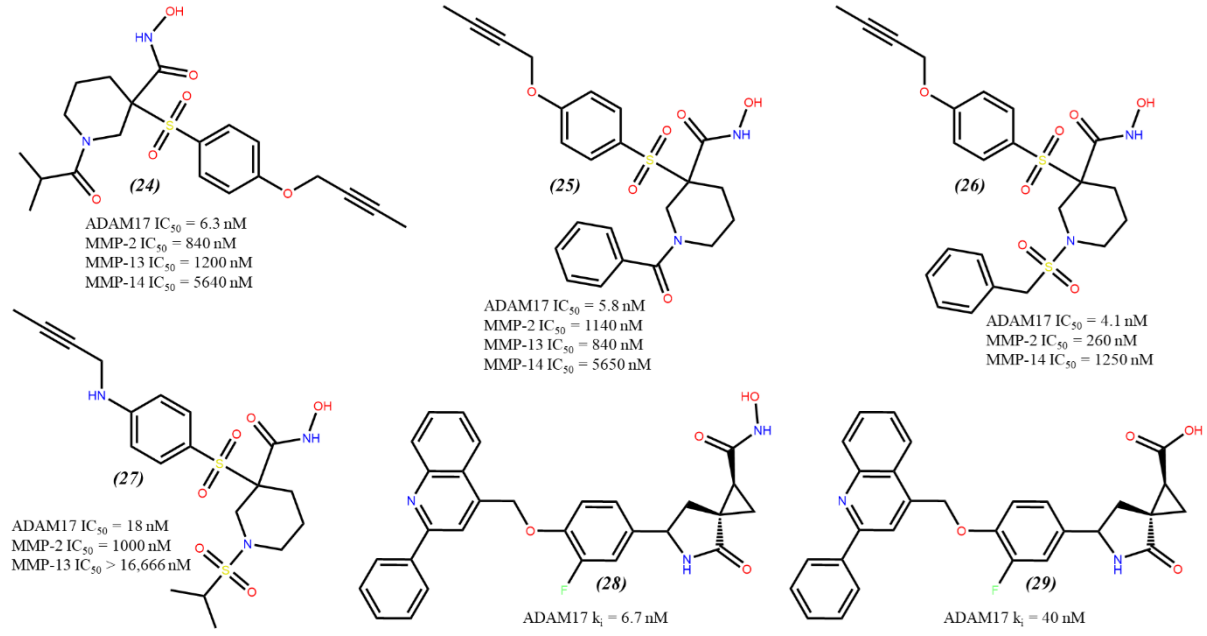

Figure 2.6. Some ADAM17 inhibitors

Guo et al., synthesized novel spirocyclopropyl hydroxamate and carboxylate compounds as inhibitors of ADAM17 (compounds 28 & 29). They have introduced a novel scaffold that enables potent ADAM17 inhibition for both hydroxamate and carboxylate compounds (**Figure 2.6**). Carboxylate ADAM17 inhibitors are especially noteworthy due to their chemical stability and potentially advantageous pharmacokinetics. While there have been reports of carboxylate inhibitors binding to MMPs, there is limited information on their binding to ADAM17 [179].

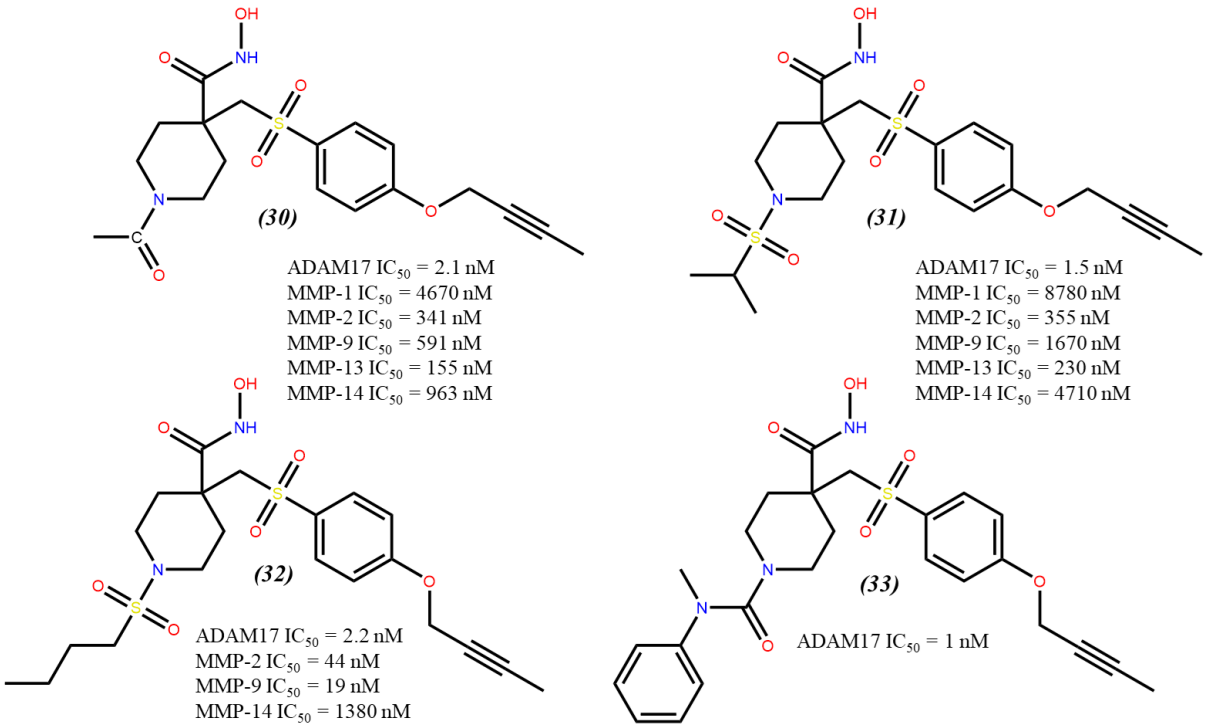

Figure 2.7. Few ADAM17 inhibitors

Park et al., reported a series of butynyloxyphenyl b-sulfone piperidine hydroxamic acid ADAM17 inhibitors (**Figure 2.7**). According to author, all of the compounds (compounds 30-33) were found to be highly effective inhibitors of ADAM17 in isolated enzyme assays, and several also showed strong performance in cell-based assays using Raw cells and human whole blood (HWB) [180].

2.3. Patented ADAM17 inhibitors

In recent years, several ADAM17 inhibitors (**Table 2.1**) have been patented, highlighting the increasing interest in this field and the potential of these compounds to meet important medical needs. These patented inhibitors are crafted to specifically target ADAM17's enzymatic activity, with the goal of modifying its function to benefit patients affected by conditions associated with its dysregulation.

Table 2.1. Few Patented ADAM17 inhibitors

Cpd. No.	*Structure of compounds*	*ADAM17 inhibitory activity*	*Developer*	*References*
1	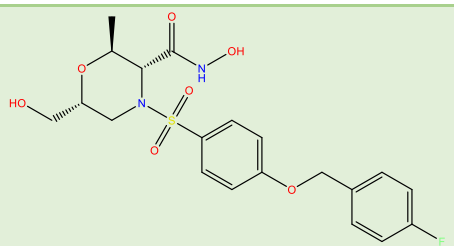	*IC_{50} = 4.5 nM*	*Pfizer*	*181*
2	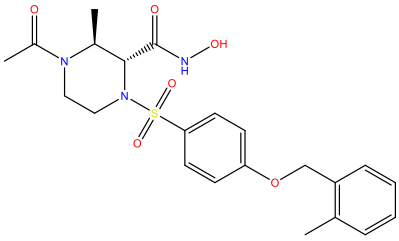	*IC_{50} = 6.2 nM*	*Pfizer*	*181*
3	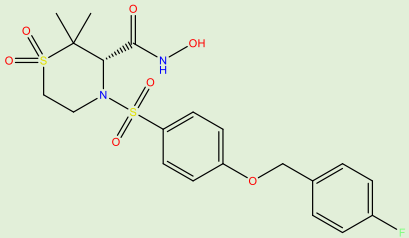	*IC_{50} = 7.2 nM*	*Pfizer*	*181*
4	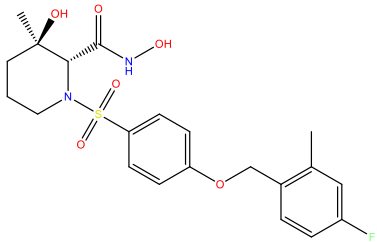	*IC_{50} < 10 nM*	*Pfizer*	*182*
5	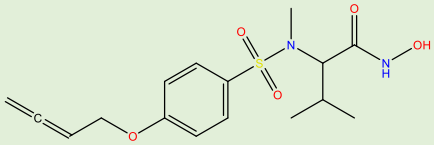	*IC_{50} = 36 nM*	*Wyeth*	*183*
6	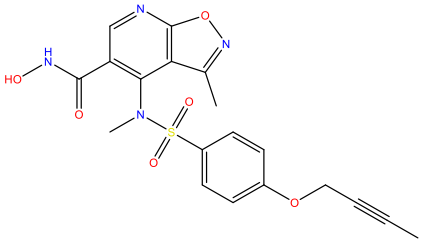	*IC_{50} = 5.9 nM*	*Wyeth*	*184*
7	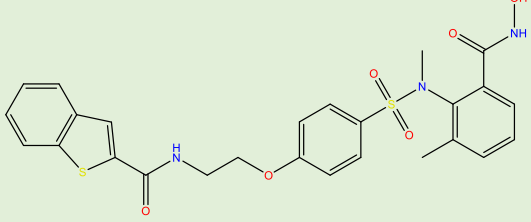	*IC_{50} = 15.2 nM*	*Wyeth*	*185*

8	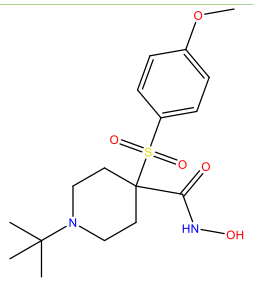	*IC_{50} = 9.7 nM*	*Wyeth*	*186*
9	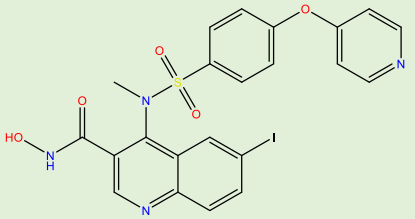	*IC_{50} = 24 nM*	*Wyeth*	*187*
10	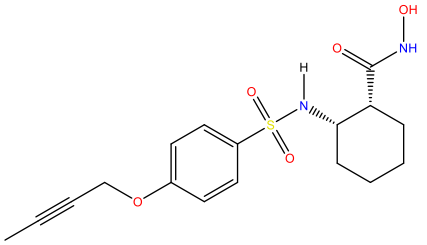	*IC_{50} = 15 nM*	*Wyeth*	*188*
11	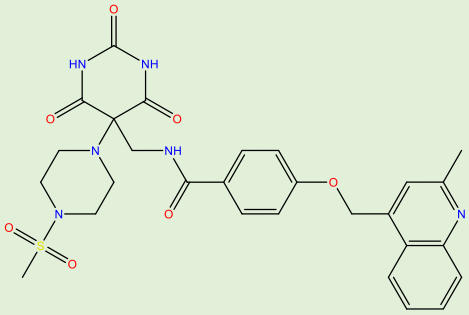	*IC_{50} = 2 nM*	*Bristol-Myers Squibb co.*	*189, 190*
12	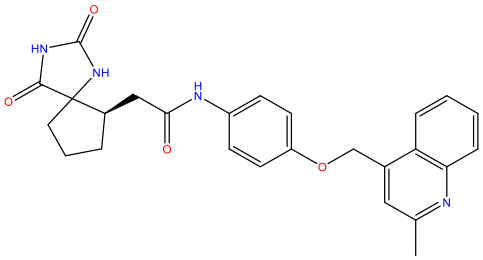	*IC_{50} = 11 nM*	*Bristol-Myers Squibb co.*	*191, 192*
13	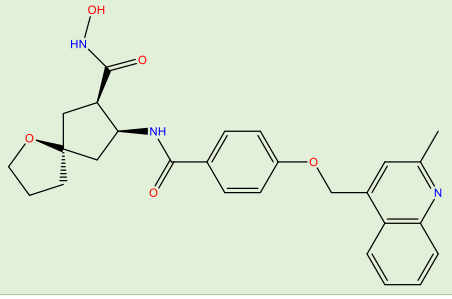	*IC_{50} = 1 nM*	*Bristol-Myers Squibb co.*	*193*

14	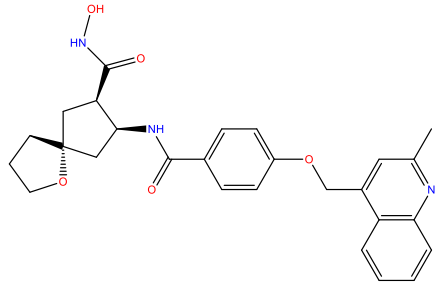	*IC_{50} = 1 nM*	*Bristol-Myers Squibb co.*	*193*
15	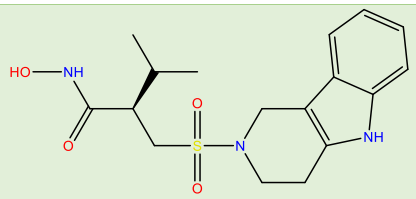	*Not known*	*Darwin Discovery Ltd.*	*194*
16	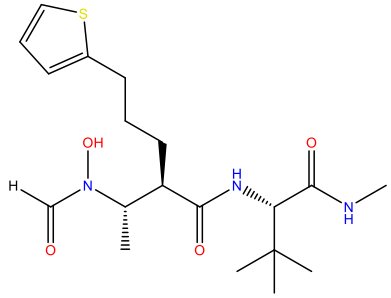	*K_i = 50-500 nM*	*Glaxo Wellcome*	*195, 196*
17	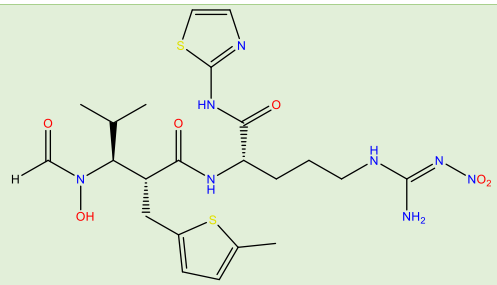	*K_i < 50 nM*	*Glaxo Wellcome*	*195, 196*
18	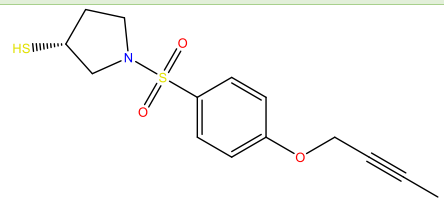	*K_i = 28 nM*	*Vertex Pharmaceuticals*	*174, 197*
19	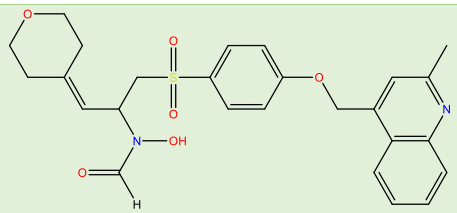	*IC_{50} = 1.9 nM*	*Kaken Pharmaceuticals*	*198*
20	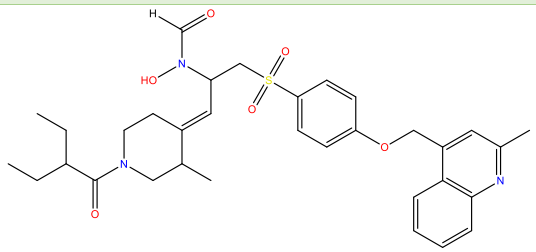	*IC_{50} = 2 nM*	*Kaken Pharmaceuticals*	*198*

2.4. Examining the QSAR studies conducted on ADAM-17 inhibitors

Yang et al., reported the design and synthesis of α-alkoxyaryl alkyl group substituted coumarin based ADAM17 inhibitors, focusing on optimizing modifications to the *S1′* pocket. It included a QSAR study employing the Genetic Function Approximation (GFA) technique (**Table 2.2**). Additionally, they have docked α-substituted chromen-based analogues into the ADAM17 enzyme to gain a clearer understanding of the structure–activity relationship for this series of compounds. They conducted a docking study to verify that α-substituents with long and bulky groups on the coumarin core of ADAM17 inhibitors penetrate the *S1′* and *S3′* pockets, forming van der Waals interactions that enhance inhibitory activity [199].

Table 2.2. data related to GFA conducted by Yang et al.

No.	*Equation*	r^2	r^2 *(adj)*	r^2 *(pred)*	*RMS residual error*	*S.O.R. p-value*	*Friedman L.O.F.*
1	*pIC50 = -120.91 + 12.369 (Balaban_index_JX) - 736.95 (FNSA3) - 0.85767 (Log D) + 1.5867 (Num_Atoms) + 1.0541 (Num_Chains) + 0.070294 (WNSA2)*	0.912	0.879	0.798	0.269	0.105	$1.79\ E^{-05}$

Bahia et al., conducted docking-based CoMFA and CoMSIA analyses on a series of potent anthranilic acid derivative (ANTs) ADAM17 inhibitors to elucidate key interactions between ADAM17 and ANTs, as well as to identify the features most influencing the inhibitory activity of these compounds. In this study, they reported the importance of bulky steric chain at the 4th position of benzene sulfonyl group to occupy the pocket of enzyme deep inside and the importance of H-bond donor and acceptor groups and the presence of their respective positions also [200].

2.5. Clinical studies conducted on ADAM17 inhibitors

Clinical studies on ADAM17 inhibitors are crucial for translating preclinical discoveries into effective treatments. These trials assess the safety, efficacy, and pharmacokinetics of ADAM17 inhibitors in humans, focusing on their potential to treat diseases linked to ADAM17 dysregulation. As research advances, these studies will offer valuable insights into the inhibitors' effectiveness and safety, potentially paving the way for new treatment options for patients. Currently occurring clinical trials of ADAM17 inhibitors are listed in **Table 2.3.** [201].

Table 2.3. Recently occurring clinical trials of ADAM17 inhibitors for treating different pathophysiological conditions

Trial ID	*Diseases*	*ADAM17 inhibitors*	*Phase*	*Last update posted*	*Status*
NCT00820560	Solid Tumors and Hematologic Malignancy	INCB7839	Phase I	17-01-2018	Completed
NCT00864175	Breast cancer	INCB7839 + Transtuzumab + Docetaxel	Phase I & II	18-01-2018	Terminated
NCT04295759	Anaplastic Astrocytoma, Anaplastic Oligodendroglioma and Malignant Glioma	INCB7839	Phase I	15-05-2023	Active but not Recruiting
NCT00312780	Diabetic Nephropathy	XL784	Phase II	23-02-2010	Completed
NCT02141451	Diffuse Large B Cell Non-Hodgkin Lymphoma	INCB7839 + Rituximab	Phase I & II	19-02-2022	Completed
NCT04557228	Type 2 Diabetes mellitus	Dietary supplement: Phosphatidylserine	NA	06-04-2023	Recruiting
NCT01254136	Breast cancer	INCB7839	Phase I & II	25-01-2012	Terminated

Chapter 3: Rationale Behind the Study

Proteases are currently receiving significant attention because of their roles in crucial cellular processes that are essential for proper cell function. When the activities of these proteases are impaired, it can contribute to the onset of various diseases. Given their responsibility for breaking down proteins involved in numerous pathological conditions, proteases have become a promising target for therapeutic interventions [202]. A Disintegrin and Metalloproteinases (ADAMs), which are zinc-dependent transmembrane glycoproteins belonging to the adamalysin protease family, catalyze proteolytic cleavage of peptide bonds. This enzymatic action results in either protein degradation or the release of active peptides [203]. In addition to ADAMs, matrix metalloproteinases (MMPs) and ADAMTS (ADAM with thrombospondin motifs) are also metalloproteinase enzymes that require a Zn2+ ion as a cofactor for their catalytic activity [204]. ADAMs are involved in a wide array of cellular processes, encompassing cell proliferation, differentiation, morphogenesis, tissue remodeling, hemostasis, inflammation, angiogenesis, immunity, and ultimately, cell death [205].

In 1997, A Disintegrin and Metalloproteinase 17 (ADAM17) was originally discovered as the enzyme responsible for the extracellular cleavage or shedding of tumour necrosis factor-alpha (TNF-α). As a result, it was commonly referred to as TNF-α converting enzyme (TACE). But now It is widely recognized that this protease is responsible not only for the shedding of TNF-α but also for over 90 other substrates, including adhesion molecules, cytokines, chemokines, growth factors, and receptors [206]. As a member of the protease family, ADAM17 performs cleavage of integral proteins involved in a wide range of biological processes, such as cell proliferation, differentiation, neurogenesis, tissue remodelling, inflammation, ovulation, fertilization, and senescence [207].

Structurally, ADAM17 consist of a pro-domain, a catalytic/metalloproteinase domain, a disintegrin domain, a membrane-proximal domain, a transmembrane domain, a Conserved Adam seventeeN Dynamic Interaction Sequence (CANDIS) region and a cytoplasmic tail. Each and every domain plays some specific roles. The catalytic domain, or metalloproteinase domain, of ADAM17 contains a Zn2+ co-factor responsible for cleaving peptide bonds. Following this domain is the disintegrin domain, which competitively inhibits integrin function, while the transmembrane domain anchors the protein to the cell surface [208]. A small helical region known as the Conserved Adam Seventeen Dynamic Interaction Sequence (CANDIS) lies between the membrane-proximal domain and the transmembrane domain, aiding in substrate recognition and enzyme-substrate interactions. The cytoplasmic tail

interacts with signaling molecules, and phosphorylation of this tail regulates the activation, trafficking, and localization of ADAM17 [209].

Abnormal expression of ADAM17 is being observed in numerous diseases eventually, which is further responsible for irreversible shedding of the extracellular domain of membrane-bound proteins as biologically active molecules that play pivotal roles in the bio-chemical pathways related to several pathophysiological conditions. Several studies have revealed that ADAM17 plays dual roles in humans, serving beneficial functions such as aiding in embryonic development and adipocyte differentiation. However, it is also noted that ADAM17 is upregulated in some of the most severe diseases, including cancer, Alzheimer's disease, and various inflammatory conditions (**Figure 3.1**) [210, 211]. Recognizing the importance of ADAM17 in cancer and other pathophysiological states the development of selective ADAM17 inhibitor is now a matter of great concern.

By analyzing the enzyme-ligand interaction study of ADAM17 enzyme, it was observed that zinc binding group (ZBG), hydrogen bond forming group and hydrophobic moiety are important pharmacophoric feature. Thus, a series of hydroxamate (a good ZBG) based sulfonylphenoxy-methylquinoline derivatives of ADAM17 inhibitor have been under taken to identify the salient physicochemical and structural features required for higher ADAM17 inhibitory activity to develop more effective and safer ADAM17 inhibitors [212].

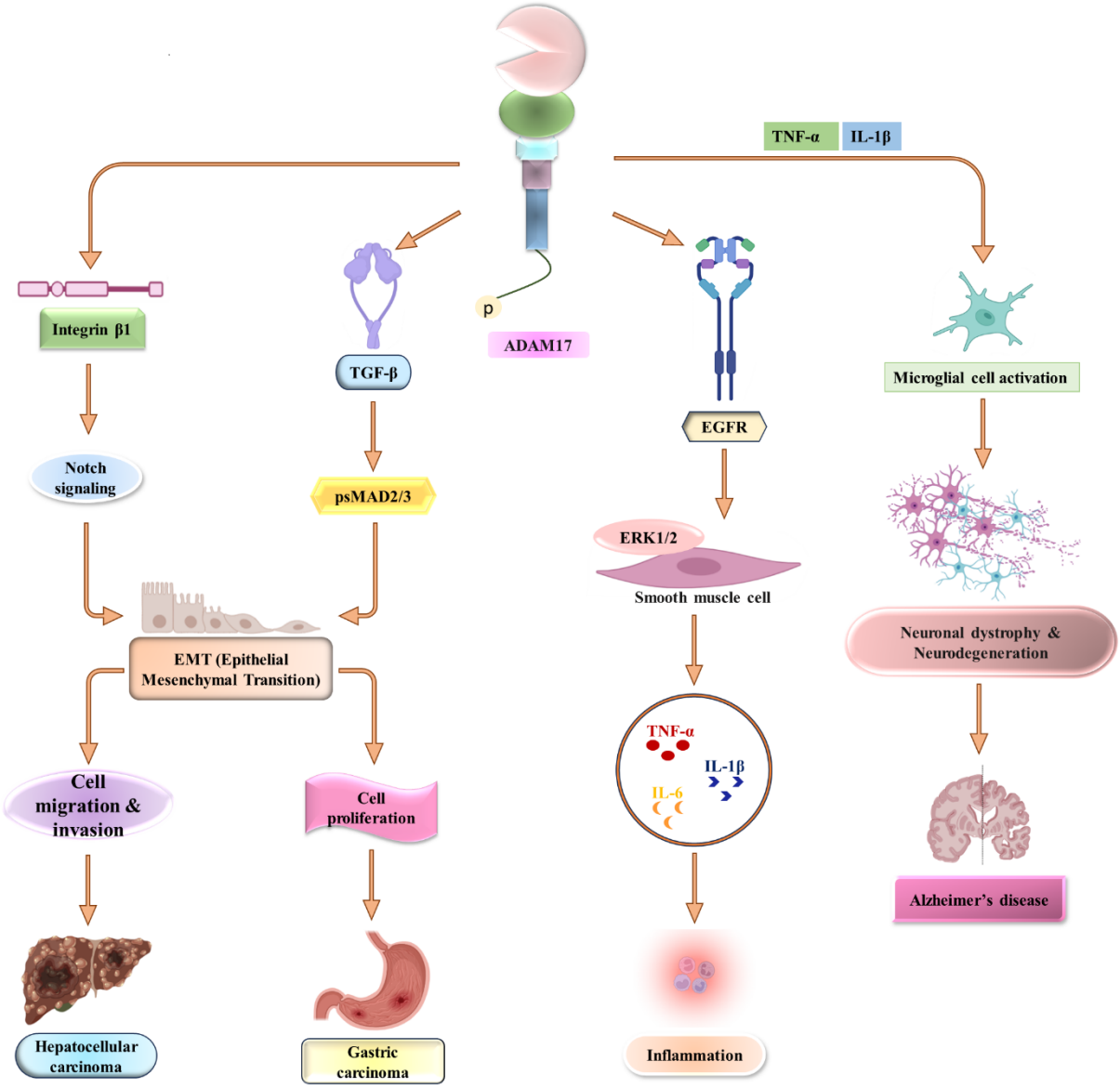

Figure 3.1. Role of ADAM17 in diverse disease conditions

Chapter 4: Materials & Methods

4.1. Dataset preparation

To conduct the study, a total of 94 small ADAM17 inhibitors (**Appendix Table T1**) having a common sulfonyl phenoxy-methyl quinoline scaffold were procured from the literature [213-216]. Initially ChemDraw Ultra 5.0 was used to draw the 2D molecular structures of these compounds [citation for chemdraw]. Before conducting the classification-dependent molecular modelling study, the ADAM17 inhibitory activity (IC_{50} in nM) of these molecules were converted into their corresponding negative logarithmic values (pIC_{50}) for a standard datapoint distribution using ***Eq. 1***.

$$pIC_{50} = -log(IC_{50}/10^9) \qquad (1)$$

A threshold value of pIC_{50} = 8.000 (IC_{50} = 10 nM) was taken into consideration to discriminate the dataset molecules into *actives* ($pIC_{50} \geq 8.000$) and *inactives* ($pIC_{50} < 8.00$). Through this kind of differentiation, 41 molecules were deemed *active* and subsequently assigned a value of 1, while the rest 53 compounds were classified as *inactive* and assigned a value of 0. Compound **93** (IC_{50} = 0.8 nM) and compound **9** (IC_{50} = 3,600 nM) were the most active and least active molecules, respectively, out of the 94 total compounds.

4.2. Calculation of descriptors

Molecular descriptors of the dataset molecules were calculated using the *PaDEL-Descriptor* software [217]. Initially, all these descriptors, i.e., 1,444 1D, and 2D PaDEL descriptors were calculated. Subsequently, dataset preprocessing was carried out using the DTC laboratory tool [218]. During this procedure, a variance cut-off of 0.001 and a correlation coefficient cut-off of 0.99 were employed to eliminate the highly correlated descriptors, after completion of the pretreatment process, a total of 743 descriptors remained. Additionally, various molecular characteristics of these molecules—including molecular weight (MW), lipophilicity (AlogP), number of hydrogen bond donors and acceptors (nHBD and nHBA, respectively), molecular polar surface area (MPSA), as well as counts of aromatic and aliphatic groups were computed using Discovery Studio 3.0 (DS 3.0) software [219]. Topological fingerprint descriptors were also generated during this analysis.

4.3. Division of dataset

The dataset division process is a crucial step in QSAR studies. For this study, the DTC laboratory tool [218] was employed to partition the dataset compounds into two separate sets:

a training set and a test set. This partitioning was based on the Kennard-Stone method, where 30% of the dataset molecules were allocated to the test set (N_{Test} = 29), and the remaining 70% were assigned to the training set (N_{Train} = 65). The training set compounds were used to build the model, while the test set compounds served for model validation purposes.

4.4. Classification based 2D-QSAR studies

4.4.1. Linear discriminant analysis (LDA) study

LDA aims to find a linear combination of features that best separates two or more classes or clusters of data. In QSAR Linear discriminant analysis (LDA) is a QSAR modeling method that categorizes dataset compounds into distinct classes based on groups (typically binary). The generalized equation for LDA is as follows:

$$\boldsymbol{DF = X_0 + X_1Y_1 + X_2Y_2 + \ldots\ldots + X_nY_n} \qquad (2)$$

Where, *DF* denotes the discriminant function, Y_1, Y_2……Y_n indicates the *n* numbers of independent parameters, and X_1, X_2, ……., X_n are the discriminant coefficients of the respective variables and X_0 is a constant.

The LDA model was built using STATISTICA 7 software [220], employing a forward stepwise approach with specific criteria: $F_{inclusion}$ = 4.00, $F_{exclusion}$ = 3.90, and tolerance = 0.001. Following the completion of the forward stepwise method, the model with the fewest descriptors and the lowest Wilk's lambda (λ) value was chosen as the optimal LDA model for subsequent analysis.

4.4.2. Bayesian classification study

Bayesian classification study is one of the efficient and easy statistical method used for classification tasks. Here it is used to identify the good and bad fingerprint feature that are accountable for regulating the biological activity. It's based on Bayes' theorem [221], which describes the probability of an event, based on prior knowledge of conditions that might be related to the event. Bayes' theorem is expressed as:

$$P(S|T) = \frac{P(T|S)P(S)}{P(T)} \qquad (3)$$

Where $P(T) \neq 0$, S denotes model/hypothesis, T indicates observed data, $P(S)$ stands for prior belief and $P(T)$ represents the evidenced data; $P(S|T)$ indicates posterior probability and $P(T|S)$ denotes the likelihood.

In this study, various fundamental molecular characteristics of these molecules were computed, including:

- Lipophilicity (***AlogP***)
- Molecular weight ***(MW***)
- Molecular fractional polar surface area (***MFPSA***)
- Number of hydrogen bond acceptors (***nHBA***) and donors (***nHBD***)
- Number of rings (***nR***)
- Number of aromatic rings (***nAR***)
- Number of rotatable bonds (***nRB***)

Additionally, extended connectivity fingerprints of diameter 6 (***ECFP_6***) were also calculated. These descriptors were utilized to construct a Bayesian classification model using the 'Create Bayesian Model' protocol integrated into DS 3.0 software [219].

4.4.3. Recursive Partitioning (RP) study

Recursive partitioning (RP) analysis is a straightforward and widely employed statistical method that effectively uncovers relationships within large and complex datasets. This method is typically utilized to classify dataset molecules into distinct clusters based on various molecular features (independent variables). It operates by employing a recursive algorithm to generate decision trees, thereby facilitating the exploration of relationships and patterns within the data [222].

The tree-like structures generated by recursive partitioning analysis can be converted into a series of predictive rules using Boolean logic. These rules provide a clear and interpretable framework for predicting outcomes or classifications based on the values of the independent variables within the dataset. Classification trees are structured with nodes that are hierarchically linked. Each node represents a decision point based on specific features or variables. When a node does not have any further child nodes branching from it, it is termed a leaf node [223]. The final decision or classification outcome is determined by the activity class associated with the leaf node of the decision tree. The RP model was built using the 'Create Recursive Partitioning' model protocol within Discovery Studio 3.0 software [219]. It utilized a set of

molecular properties that are akin to those employed in the development of the Bayesian Classification model, in addition to the functional class fingerprint of diameter 6 (FCFP_6).

4.4.4. SARpy analysis

SARpy (Structure-Activity Relationships in Python) is a tool introduced by Gini and co-workers [224]. It is designed to extract structural fragments from chemical structures and subsequently generate important structural alerts in SMILES format. This tool is particularly useful for identifying key structural features that may influence the activity or properties of molecules. The structural alerts generated by SARpy are based on their likelihood ratio. This ratio indicates the probability or likelihood that a specific structural fragment or feature is associated with a particular activity or property of interest [225]. The likelihood ratio can be calculated by the following formula:

$$\textbf{Likelihood ratio} = \frac{\textbf{True positive}(TP)}{\textbf{False positive}(FP)} \times \frac{\textbf{Negative}}{\textbf{Positive}} \qquad (4)$$

To identify potential structural alerts or an active ruleset, fragment generation considered a range of 2 to 18 atoms, with a minimum occurrence value of 5. The analysis focused on compounds classified as 'ACTIVE' within the target activity class, using an 'OPTIMAL' single alert precision approach. SARpy analysis was performed on the training set to generate the active ruleset, which was subsequently validated using compounds from the test set [226].

Structural alerts with higher likelihood ratios are considered more predictive and are often used to flag chemical structures that may exhibit certain biological activities or toxicological properties [225].

4.5. Molecular docking study

Molecular docking study was performed to predict binding interactions of the ligand with the bioactive configuration of ADAM17 enzyme. To perform molecular docking of the most active and least active compound respectively 93 and 9 at the active site of ADAM17 enzyme (PDB ID: 2FV5) the Maestro v12.5 [227] software from the Schrodinger suite was utilized. And the binding interactions between the enzyme's catalytic site and these compounds were observed for further analysis.

4.5.1. Protein preparation

The '*Protein Preparation Wizard*' protocol of the Schrodinger Maestro v12.1 software was used to prepare and optimize the protein structure (PDB ID: 2FV5) [228]. In this process, the water molecules were eliminated from the structure along with the addition of hydrogen atoms, and subsequently, missing atoms were included in the side chain during protein preparation. The OPLS_2005 force field was employed in the protein preparation process to perform the restrained minimization of the protein structure [227]

4.5.2. Ligand preparation

The ligands were prepared with the help of the '*LigPrep*' module of the Schrodinger Maestro v12.1 software using the OPLS_2005 forcefield while desalting and retaining all the specified chirality [227].

4.5.3. Receptor grid generation

The receptor grid generation was executed using the '*Receptor Grid Generation*' module of the Schrodinger Maestro v12.1 software. The ligand diameter midpoint box was specified (15 Å × 15 Å × 15 Å) and the other parameters like rotatable groups, and exclude volumes were kept unchanged for receptor grid generation [227].

4.5.4. Ligand docking

Finally, docking was executed with the extra-precision (XP) method using the '*Ligand docking*' protocol of Schrodinger Maestro v12.1 software [227]. Zinc ion was used as constraint during this ligand docking process.

4.6. Statistical validation metrics for evaluation of QSAR models

Statistical validation metrics (**Table 4.1**) are used to assess the performance and reliability of predictive models. To substantiate the reliability and predictive capability of the constructed classification-based QSAR models (LDA, Bayesian classification, SARpy, and RP analysis), evaluating their performance is crucial. Therefore, a receiver operating characteristic (ROC)-based assessment was conducted to validate the robustness and goodness of fit of these models. A summary of the essential statistical validation parameters listed in the following Table.

Table 4.1. Essential statistical parameters for model evaluation

Metrics	Description	
Sensitivity (Se)	$Se = \frac{TP}{TP + FN}$	TP indicates True Positive (active predicted as active)
Specificity (Sp)	$Sp = \frac{TN}{TN + FP}$	TN signifies True Negative (inactive predicted as inactive)
Precision (Pr)	$Pr = \frac{TP}{TP + FP}$	
Accuracy (Acc)	$Acc = \frac{TP + TN}{TP + FP + TN + FN}$	FP represents False Positive (inactive predicted as active)
F-measure	$F - measure = \frac{2 \times sensitivity \times Precision}{Precision + Sensitivity}$	
Matthew's correlation coefficient (MCC)	$MCC = \frac{TP \times TN - FP \times FN}{\sqrt{(TP + FP)(TP + FN)(TN + FP)(TN + FN)}}$	FN suggests False Negative (active predicted as inactive)
Recursive operating characteristics graph Euclidean distance (ROCED)	$ROCED = (\lvert d_{training} - d_{test} \rvert + 1) \times (d_{training} + d_{test}) \times (d_{test} + 1)$ Here, $d = \sqrt{(1 - Se_r)^2 + (1 - Sp_r)^2}$	
ROCED corrected with fitness function (ROCFIT)	$ROCFIT = \frac{ROCED}{FIT(\lambda)} \quad where, FIT(\lambda) = \frac{(1 - \lambda) \times (n - p - 1)}{(n + p^2) \times \lambda}$ Where, n is number of compounds in training set and p is number of descriptors	
Area under curve-receiver operating characteristics (AUC-ROC)	$AUC - ROC = 1 - \frac{\sum_{i=1}^{n} r_i}{n \times (N - n)} + \frac{n + 1}{2 \times (N - n)}$ Where n is the number of actives, N is the total number of compounds and r_i signifies the rank of the *i*th active compound	

Chapter 5: Result and Discussion

5.1. Linear discriminant analysis (LDA) model

Based on the results obtained from the linear discriminant analysis (LDA) study, the developed LDA model (**Eq. 1**) includes seven descriptors, which are detailed in **Table 5.1**. Additionally, the performance parameters for the LDA model (**Eq. 1**) can be found in **Table 5.2**. These tables collectively provide insights into the specific descriptors used in the model and the corresponding performance metrics that assess its effectiveness in classifying compounds based on the given data.

$$DF = -691.81 + 530.07 \times GATS2m - 212.41 \times MATS6c + 460.83 \times GATS3v - 38.46 \times GATS5i + 0.94 \times AATSC1m + 342.08 \times GATS8v + 153.49 \times GATS3c \quad (1)$$

Here, $N_{Train} = 65$, $N_{Test} = 29$, *Wilk's* $\lambda = 0.175$, $R_C = 0.908$, $D^2_M = 18.756$, $\chi^2 = 103.552$, F (7, 57) = 38.267, $MCC_{Train} = 0.939$, $AUCROC_{Train} = 0.998$, $MCC_{Test} = 0.795$, $AUCROC_{Test} = 0.976$, *ROCED* = 0.259, *ROCFIT* = 0.109.

Table 5.1. Explanation of descriptors used to build the LDA model

Descriptors	***Explanation***	***Contribution***
GATS2m	Geary autocorrelation - lag 2 / weighted by mass	Positive
MATS6c	Moran autocorrelation - lag 6 / weighted by charges	Negative
GATS3v	Geary autocorrelation - lag 3 / weighted by van der Waals volumes	Positive
GATS5i	Geary autocorrelation - lag 5 / weighted by first ionization potential	Negative
AATSC1m	Average centered Broto-Moreau autocorrelation - lag 1 / weighted by mass	Positive
GATS8v	Geary autocorrelation - lag 8 / weighted by van der Waals volumes	Positive
GATS3c	Geary autocorrelation - lag 3 / weighted by charges	Positive

In relation to the developed LDA model, it was observed that seven molecular features from the equation mentioned earlier were utilized to categorize the compounds into active and inactive groups. The discriminant function (DF) of the developed LDA model demonstrated a lower Wilks' lambda ($\lambda = 0.175$), a higher canonical coefficient (RC = 0.908), and a higher chi-square value ($\chi^2 = 103.552$), indicating a clear distinction between active and inactive

molecules. Based on the dataset division, it was observed that out of 65 compounds in the training set, 27 were classified as active while the remaining 38 were deemed inactive. Similarly, among the 29 compounds in the test set, 14 were classified as active and 15 as inactive. According to the LDA model, all 27 active molecules in the training set were correctly identified as truly active (TP). For the inactive class, 36 compounds were accurately classified as truly inactive (TN), while two inactive molecules were incorrectly identified as active (FP). No active compounds were mistakenly classified as inactive (FN) in the training set. From the results of the LDA model, it was observed that out of the 14 active molecules in the test set, 13 were accurately identified as active (TP), while one was incorrectly predicted as inactive (FN). Additionally, of the 15 inactive molecules in the test set, 13 were correctly classified as inactive (TN), while 2 were incorrectly identified as active (FP). Several statistical metrics were assessed to evaluate the fit and predictive performance of the LDA model.

Table 5.2. Values of statistical parameters associated with the classification-based QSAR models

Model	*Dataset*	*ROC*	*TP*	*TN*	*FP*	*FN*	*Se*	*Sp*	*Pr*	*Acc*	F_1	*MCC*
LDA	*Training*	0.998	27	36	2	0	1.000	0.947	0.931	0.969	0.964	0.939
	Test	0.976	13	13	2	1	0.929	0.867	0.867	0.897	0.897	0.795
Bayesian	*Training*	0.885[#]	27	35	3	0	1.000	0.921	0.900	0.954	0.947	0.910
classification	*Test*	0.938	13	13	2	1	0.929	0.867	0.867	0.897	0.896	0.795
RP study	*Training*	0.864	25	29	9	2	0.926	0.763	0.735	0.831	0.819	0.679
	Test	0.819	6	14	1	8	0.429	0.933	0.857	0.690	0.571	0.422
SARpy	*Training*	--	26	29	9	1	0.963	0.763	0.743	0.846	0.839	0.717
analysis	*Test*	--	13	13	2	1	0.929	0.867	0.867	0.897	0.897	0.795

[#]*ROC* value denotes ROC_{5CV}

The LDA model demonstrated 100% sensitivity, 94.70% specificity, and 93.10% precision, with an overall accuracy of 96.90% for the training set. In external validation on the test set, the model achieved a sensitivity of 92.90%, specificity of 86.70%, precision of 86.70%, and an accuracy of 89.70%. Additionally, the higher values of the Matthews Correlation Coefficient (MCC) for both the training set (MCC_{Train} = 0.939) and the test set (MCC_{Test} = 0.795) suggested a strong quality of binary classification. Moreover, the receiver operating characteristic (ROC) curves for the LDA model are shown in **Figure 5.1(A)**, and the

corresponding statistical parameters are detailed in **Table 5.2**. Additional statistical analyses related to the development of the LDA model are provided in **Appendix Table T2 to T7**.

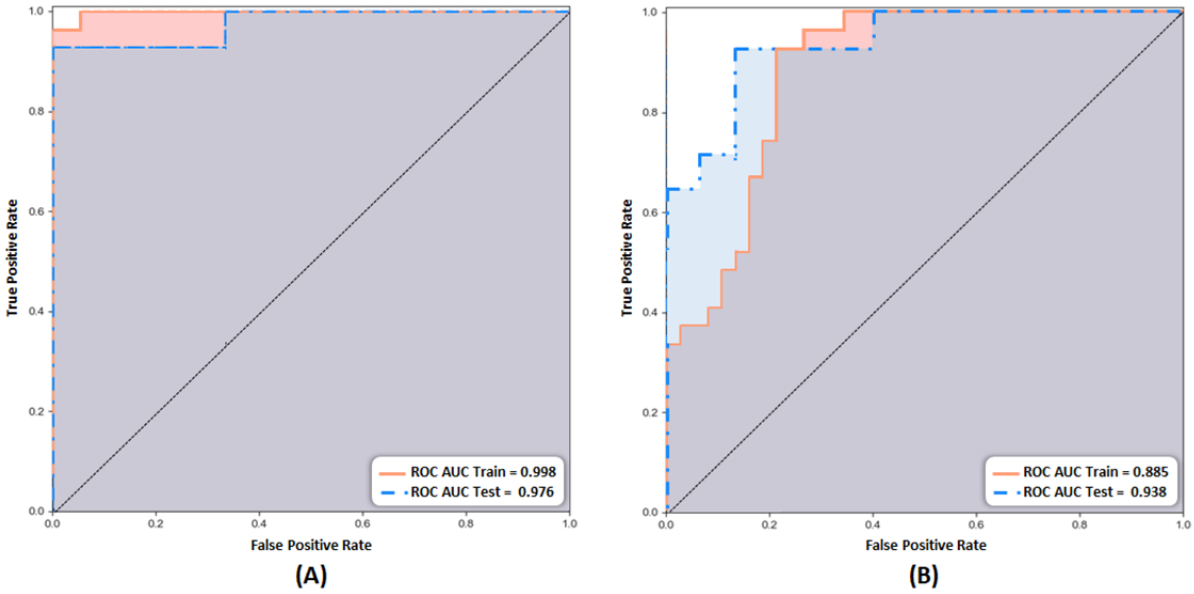

Figure 5.1. ROC plots of (A) LDA model and (B) Bayesian classification model

5.1.1. Mechanistic interpretation of the LDA model

Among the seven molecular descriptors used to develop the LDA model (**Table 5.1**), five descriptors (GATS2m, GATS3v, AATSC1m, GATS8v, GATS3c) had positive contributions, while two descriptors (MATS6c and GATS5i) had negative contributions to ADAM17 inhibitory potency.

GATS2m, an autocorrelation descriptor signifies Geary autocorrelation - lag 2 / weighted by mass [229], can help differentiate between active and inactive compounds. According to Equation (5), GATS2m has a positive impact on ADAM17 inhibition. Compounds with higher GATS2m values (> 0.9) demonstrated stronger ADAM17 inhibition (such as compounds 65-74, 76-78, 80-84, 87-90, and 92-94), while those with lower GATS2m values (compounds 7, 10-12, 17, 29, and 51-53) showed reduced ADAM17 inhibitory activity.

MATS6c, which represents Moran autocorrelation - lag 6 / weighted by charges [229], was found to negatively affect the discrimination function. Compounds with higher MATS6c values (such as compounds 8-15, 22, 25-26, and 40-47) displayed lower ADAM17 inhibition activity. Conversely, compounds with lower or negative MATS6c values (like compounds 33-34, 36-39, 55-60, and 63-65) showed higher ADAM17 inhibition. Additionally, it was noted that these more active compounds typically feature a substituted azetidine or piperidine scaffold.

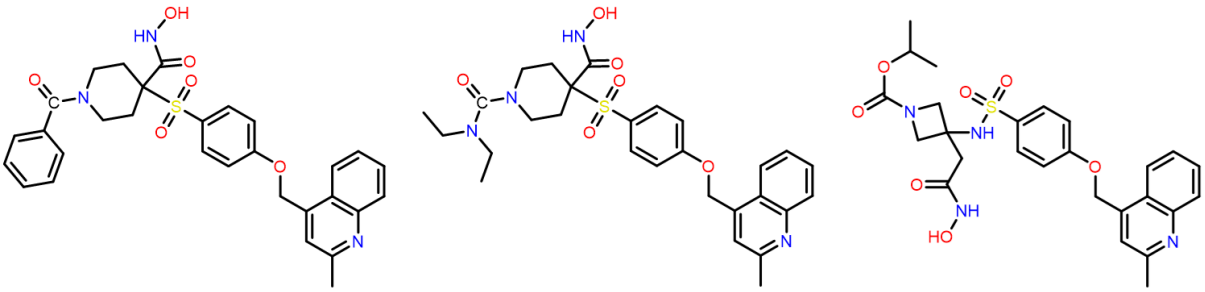

Compound 58
Value of AATSC1m = 6.404
ADAM17 IC_{50} = 1 NM

Compound 60
Value of GATS8v = 0.881
ADAM17 IC_{50} = 3 NM

Compound 37
Value of MATS6c = -0.112
ADAM17 IC_{50} = 6 NM

Figure 5.2. Representative molecules with their respective values and biological activity

GATS3v represents Geary autocorrelation - lag 3 / weighted by van der Waals volumes [229]. This parameter positively impacts the discrimination function. Molecules with higher GATS3v values (such as compounds 33, 79, and 92-94) demonstrated better activity compared to those with relatively lower GATS3v values. GATS5i, which indicates Geary autocorrelation - lag 5 / weighted by first ionization potential, was found to negatively influence the discrimination function [229]. Interestingly, molecules with higher GATS5i values (such as compounds 3, 14-19, 52-53, 76, and 86) showed lower activity. In contrast, compounds with lower GATS5i values (including compounds 36-37, 39, and 81-82) demonstrated better inhibitory activity against ADAM17. AATSC1m is another autocorrelation descriptor that represents Average centered Broto-Moreau autocorrelation - lag 1 / weighted by mass [229], molecules with lower AATSC1m values were observed to be more active compared to those with higher AATSC1m values. For instance, compound 58, which has a lower AATSC1m value of 6.404, demonstrated greater inhibition of the ADAM17 enzyme (**Figure 5.2**). GATS8v and GATS3c are Geary autocorrelation - lag 8 / weighted by van der Waals volumes and Geary autocorrelation - lag 3 / weighted by charges, respectively. Both descriptors were found to positively contribute to the discrimination function. Specifically, certain ranges of GATS8v values were associated with higher or lower activity levels. For instance, compound 60 (**Figure 5.2**), with a relatively low GATS8v value of 0.881, exhibited higher activity. Notably, highly active compounds were also found to contain a substituted piperidine ring. Additionally, the results indicated that higher values of GATS3c were associated with lower inhibitory activity, while lower values of this descriptor were linked to higher activity. For instance, compound 93, which has a comparatively low GATS3c value of 0.865, demonstrated stronger inhibitory activity against ADAM17 (**Figure 5.2**). In summary, the LDA study suggests that compounds featuring

substituted azetidine and substituted piperidine rings in their structures are likely to be more effective at inhibiting ADAM17.

5.2. Bayesian classification study

The use of Bayesian classification modeling in this study is highly advantageous for identifying key molecular fragments that could influence the ADAM17 inhibitory potential of the compounds in the dataset. The Bayesian classification *(BC)* model was applied using molecular properties in conjunction with ECFP_6 descriptors. The Bayesian classification model demonstrated strong performance, achieving a Leave-One-Out cross-validated ROC score (ROC_{LOO}) of 0.893 and a 5-fold cross-validated ROC score (ROC_{5CV}) of 0.885 for the training set. Additionally, it attained a higher ROC score of 0.938 for the test set, reflecting excellent predictive capability. The ROC plots for both the test and training sets are shown in **Figure 5.1(B)**. Additionally, the calculated statistical validation parameters are presented in **Table 3.3.**

5.2.1. Mechanistic interpretation of the BC model

Overall, the Bayesian classification model identified 20 good and 20 bad fragments, revealing both positive and negative influences on ADAM17 inhibitory activity (**Appendix Figure F1 and F2**, respectively). These substructural fragments were organized into different groups to facilitate further investigation. The 20 effective structural fragments were grouped into several clusters for analysis: (a) substituted piperidine rings (G1-G3, G20), (b) substituted tertiary amine groups (G4, G10), (c) branched alkyl groups (G5, G18), (d) substituted hydroxamate moieties (G6, G8, G16), (e) substituted phenylsulfonyl alkyl moieties (G7, G9, G15, G17, G19), (f) substituted cyclohexyl rings (G11, G12, G13), and (g) substituted dimethyl pyrrolidine rings (G14). On the other hand, the ineffective substructural fragments were also organized into distinct clusters: (a) substituted sulfonyl pyrrolidine moieties (B1, B5), (b) N-substituted benzene sulfonamide groups (B2, B4, B18), (c) substituted sulfonamide groups (B3, B17), (d) substituted sulfonyl piperidine rings (B6, B7), (e) substituted pyrrolidine moieties (B8, B9, B13), (f) substituted piperazine rings (B10-B12, B14-B16), and (g) substituted cyclobutyl amide/substituted cyclobutyl sulfonamide moieties (B19, B20).

A detailed analysis of the dataset revealed that molecules containing the substituted piperidine ring (G1-G3, G20) in their structures (compounds 55-62, 66-70, 72-73, 74, 78, 81) displayed enhanced inhibitory activity against the ADAM17 enzyme (**Figure 5.3**). Conversely, the substructural features G4 and G10 highlighted the significance of having a substituted tertiary

amine function in the structures. Consequently, several compounds with this structural feature (compounds 61, 65, 67, 72, 74, 77, 81, 84, and 89) exhibited improved ADAM17 inhibitory activity (**Figure 5.3**). Furthermore, compounds with the branched alkyl moiety (G5 and G18) demonstrated significant ADAM17 inhibitory activity (compounds 65-73, 76-82, and 88-94) (**Figure 5.3**). Notably, these compounds also featured the substituted phenylsulfonyl alkyl moiety (G7, G15, G9, and G19), indicating the importance of this scaffold in achieving effective ADAM17 inhibition for several of these compounds (compounds 65-73, 94).

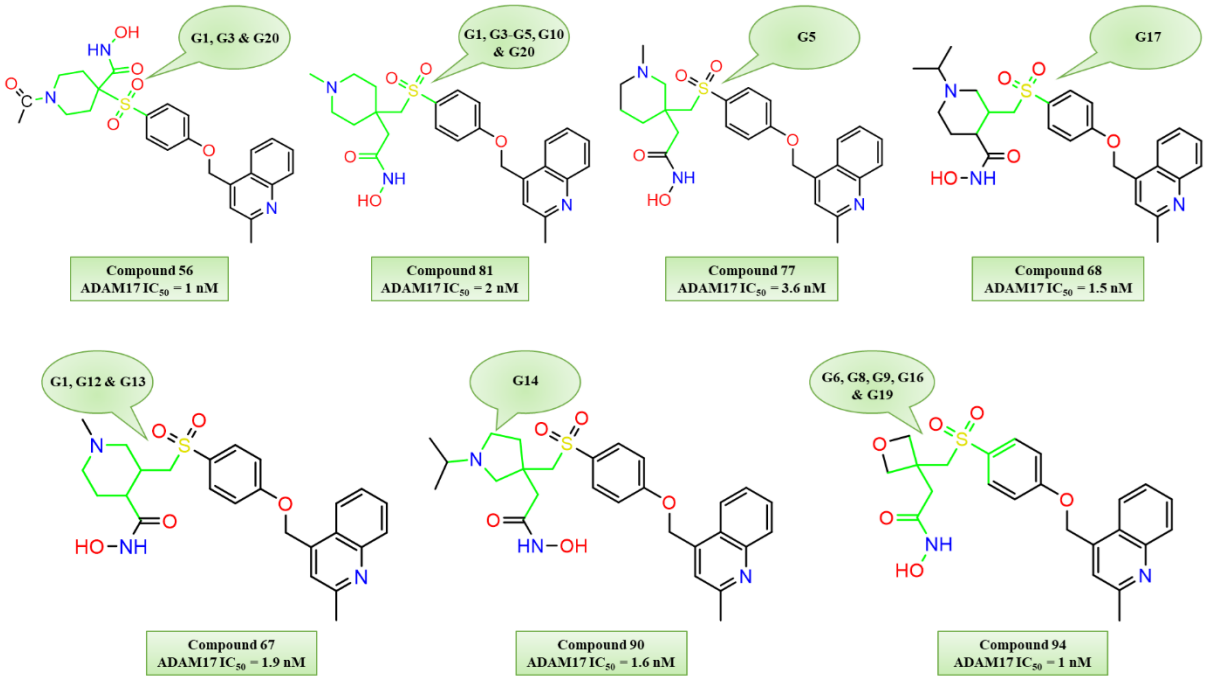

Figure 5.3. Highly active ADAM17 inhibitors, along with their corresponding beneficial Bayesian substructural fragments (highlighted in green), are depicted

Several compounds containing substituted hydroxamate groups (G6, G8, G16) in their structures (compounds 65-73, 93) were found to exhibit improved inhibitory activity. Additionally, the presence of the substituted cyclohexyl ring (features G11-G13) was identified as a favorable trait for ADAM17 inhibition, and this feature was observed in multiple molecules (compounds 66-70, 76-79). Furthermore, the substituted dimethyl pyrrolidine ring (G14) and the substituted ethyl sulfane moiety (G17) were identified as advantageous structural features for enhanced ADAM17 inhibition. As a result, compounds with G14 features (compounds 88-92) and those with G17 attributes (compounds 65-73) demonstrated significant contributions to ADAM17 inhibition (**Figure 5.3**).

Conversely, the Bayesian classification analysis revealed that the substructural features B1 and B5, which include the substituted sulfonyl pyrrolidine moiety, had a negative impact on ADAM17 inhibition. Consequently, molecules with these attributes (B1 and B5) exhibited lower activity (compounds 1, 10-13) (**Figure 5.4**). Additionally, compounds featuring the N-substituted benzene sulfonamide group (B2, B4, B18) (such as compounds 1-4, 18-27, 28, 35, and 40-53) exhibited a negative effect on ADAM17 inhibition (**Figure 5.4**). Moreover, these compounds also contained substituted sulfonamide groups (B3, B17) in their structures (**Figure 5.4**). In addition, compounds with substituted sulfonyl piperidine rings (B6, B7) (such as compounds 2-4 and 14-15) were also less active. Furthermore, substructural fragments B8, B9, and B13 highlighted the negative impact of the substituted pyrrolidine moiety (e.g., compounds 8-9) on ADAM17 inhibition (**Figure 5.4**).

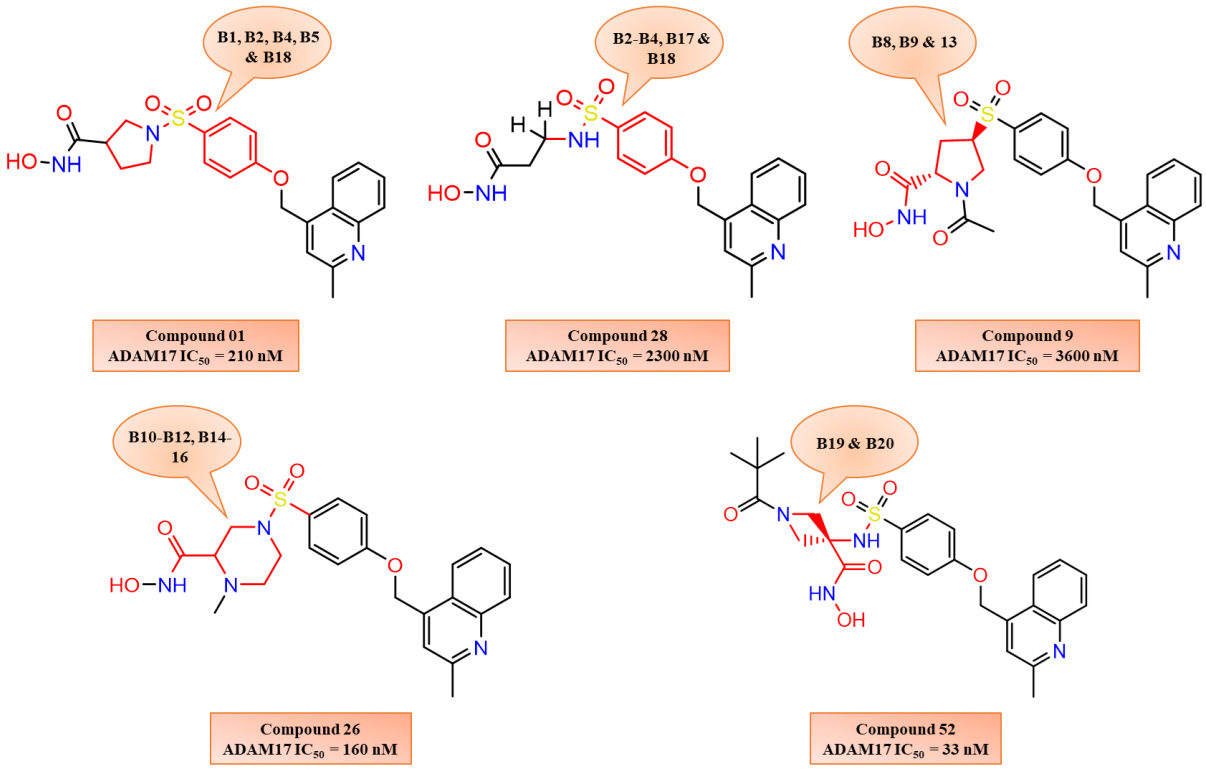

Figure 5.4. Less active ADAM17 inhibitors, along with their associated detrimental Bayesian substructural fragments (highlighted in red), are depicted

Conversely, compounds with substituted piperazine rings (B10-B12, B14-B16) (such as compounds 16-17, 25-27) were also less active. Additionally, substructural features B19 and B20, which indicate the presence of substituted cyclobutyl amide or substituted cyclobutyl sulfonamide moieties, were found in several compounds (compounds 35-36, 43, 47, and 52) that exhibited comparatively lower activity against the ADAM17 enzyme (**Figure 5.4**).

5.3. Recursive partitioning study

In the recursive partitioning study, two decision trees (Tree-1 and Tree-2) were developed using elemental molecular properties similar to those in Bayesian modeling, along with functional class fingerprints of diameter 6 (FCFP_6), to differentiate between highly active molecules and less active ones. In this study, Tree 1 (**Figure 5.5**) was deemed the most effective decision tree, as it achieved a higher ROC score (ROC = 0.864) and cross-validated ROC score (ROCcv = 0.828) for the training set compounds (**Appendix Table T8**). Additionally, for the test set molecules, Decision Tree-1 achieved a solid ROC score of 0.819 (**Appendix Table T9**). Other statistical parameters for the Recursive Partitioning model, Decision Tree-1, are provided in **Table 5.2**.

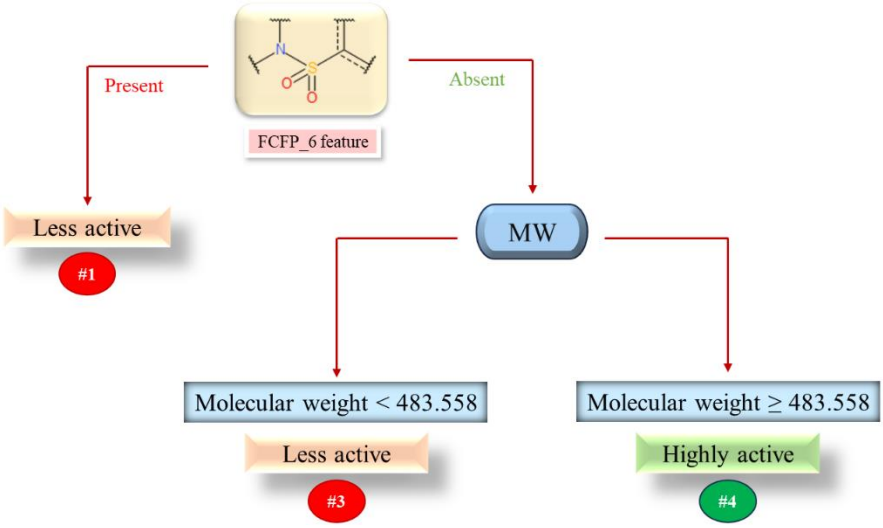

Figure 5.5. Recursive partitioning study generated decision tree 1

Decision Tree-1 distinguished less potent ADAM17 inhibitors from more potent ones based on the FCFP_6 fragment, specifically the sulfonamide group (**Figure 5.5**). The optimal tree (Tree 1) was structured with three leaves: Leaf ID-1 indicated the presence of the FCFP_6 fragment, which corresponded to less active molecules, while the absence of this fingerprint was associated with higher activity in compounds. Additionally, Decision Tree-1 highlights the significance of molecular weight (MW) in determining the activity of these molecules. It was observed that compounds with an MW < 483.558 (Leaf ID-3), such as compounds 9, 28-30, 32, 40-43, 54, and 66, tend to be less active. In contrast, a greater number of compounds with an MW ≥ 483.558 (Leaf ID-4), including compounds 33, 35-39, 46, 52, 58, 60, 62-65, 67, 69-70, 72-82, 84-86, and 89-90, were found to be highly active ADAM17 inhibitors.

5.4. SARpy analysis

The SARpy analysis was conducted to identify significant substructural features in the dataset molecules that are crucial for ADAM17 inhibition. This analysis produced three structural alerts, known as Active Ruleset, are provided below:

I. ***S(=O)(=O)CC2(CNCCC2)***
II. ***C2(CCN)CN(C2)C***
III. ***S(=O)(=O)C(C)***

For the training set molecules, the model yielded the following performance metrics: Sensitivity (Se) of 0.962, Specificity (Sp) of 0.763, Precision (Pr) of 0.743, Accuracy (Acc) of 0.846, and (MCC) of 0.717. For the test set compounds, the analysis provided a Se of 0.929, Sp of 0.867, Pr of 0.867, Acc of 0.897, and MCC of 0.795 (**Table 5.2**).

The analysis revealed that the first structural alert, *S(=O)(=O)CC2(CNCCC2)*, with an infinite (∞) LR value, indicates the positive influence of the 3-sulfonylmethyl piperidine moiety on the activity of the molecules. Additionally, the second structural alert, *C2(CCN)CN(C2)C*, with an LR value of 7.04, highlighted the presence of the 2-(1-methylazetidin-3-yl) ethanamine group in molecules as a positive indicator for enhanced inhibitory activity. The third structural alert, *S(=O)(=O)C(C)* [LR value = 3.69], indicated that the sulfonyl ethyl group has a significant impact on ADAM17 inhibition.

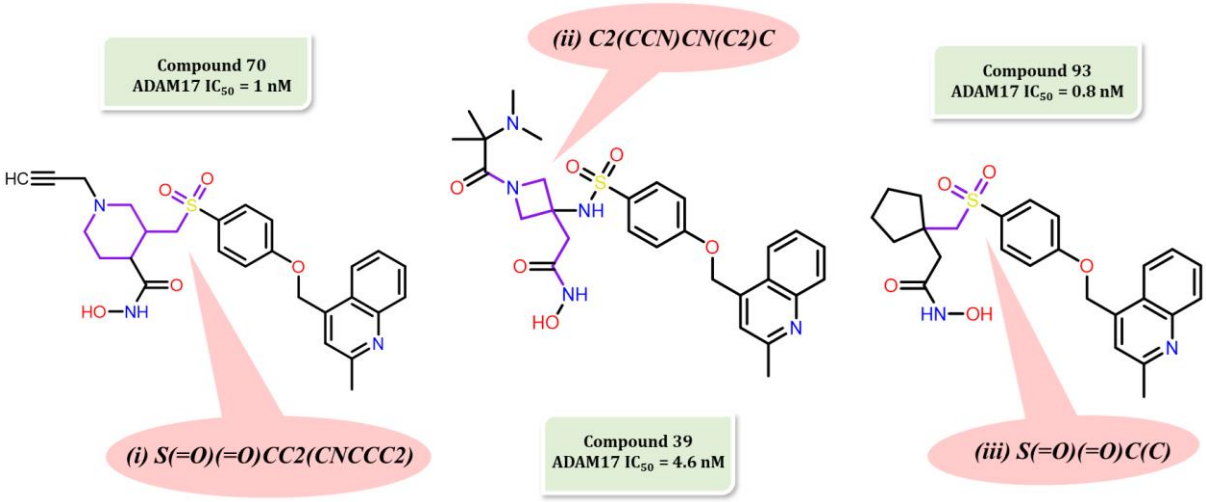

Figure 5.6. Structural alerts from the SARpy analysis along with the structure of compounds possessing respective structural features

Upon further assessment of all the structural alerts in relation to the dataset compounds, it was observed that highly active ADAM17 inhibitors (e.g., compounds 66-70 and 76-79) contained

the structural alert S(=O)(=O)CC2(CNCCC2) identified by the model. Compounds featuring the attribute C2(CCN)CN(C2)C were active ADAM17 inhibitors (e.g., compounds 34-39). Additionally, compounds with the S(=O)(=O)C(C) feature (e.g., compounds 65-73, 76-83, and 87-94) also demonstrated sturdy ADAM17 inhibitory activity (**Figure 5.6**).

5.5. Comprehensive analysis of the catalytic site of ADAM17

The earlier study on enzyme-ligand interactions was utilized to confirm the importance of the fragments identified through the classification-based models. To examine the detailed binding interactions, four structure-based topographic maps were generated for the catalytic site of ADAM17 (PDB ID: 2FV5). These maps included aromatic (**Figure 5.7A**), hydrogen bond (**Figure 5.7B**), ionizable (**Figure 5.7C**), and hydrophobic (**Figure 5.7D**) interactions, using the 'Display receptor surfaces' tool in DS 3.0 software [219]. The crystallographic data for ADAM17 (PDB IDs: 2FV5 and 2I47) were obtained from the RCSB Protein Data Bank (PDB) [228].

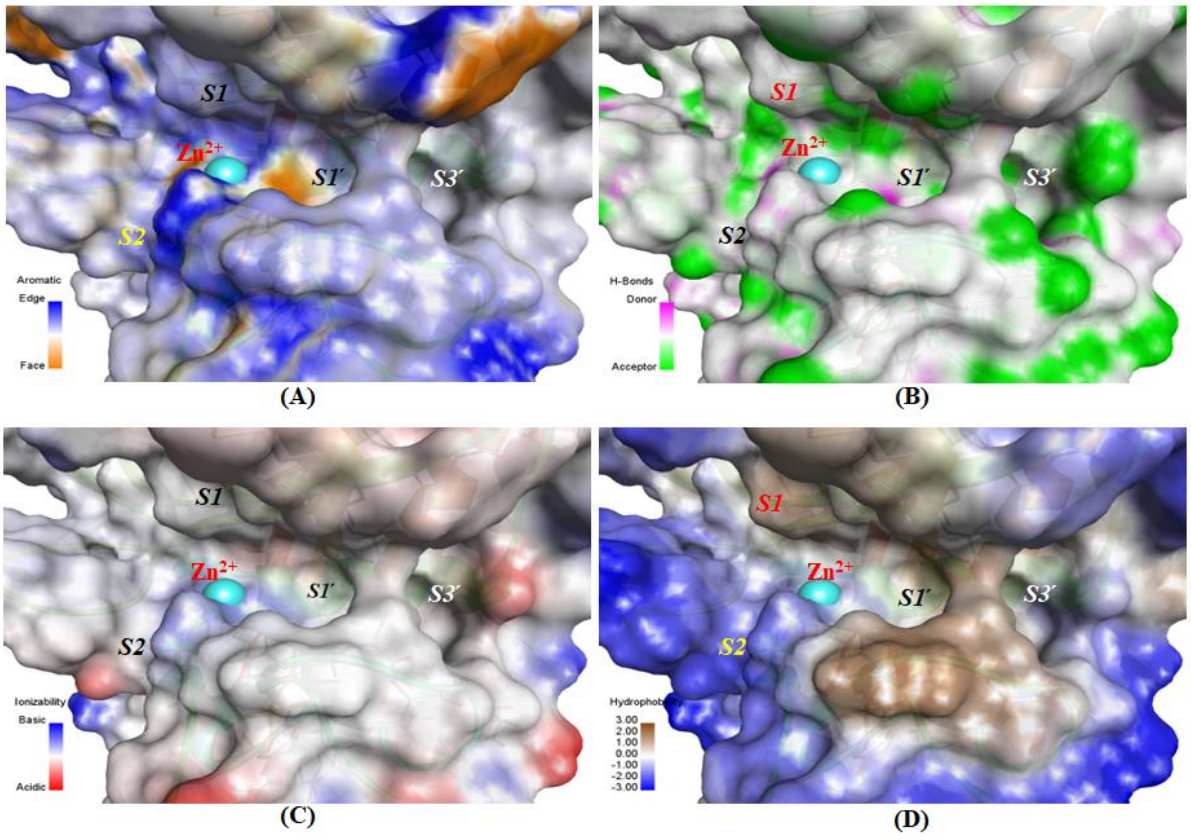

Figure 5.7. Structure-based surface maps for (**A**) aromatic, (**B**) H-bond, (**C**) ionizability, and (**D**) hydrophobicity

Analysing the surface topology of the ADAM17 catalytic site using the topographic maps suggests that the S1′ pocket is highly hydrophobic and is connected to a much hydrophobic S3′ pocket via a narrow tunnel. Additionally, the S1′ and S3′ sites may be conducive to aromatic substitution. **Figure 5.7.C** shows that a key area of the catalytic site exhibits notable basic ionizability, while the topographic map for hydrogen bonding suggests that certain regions within the S1′ and S3′ pockets may function as hydrogen bond acceptors. Consequently, these topographic maps are valuable for examining the precise binding interactions of compounds with the catalytic site of ADAM17.

The crystal structure analysis of the inbound ligands (IK682 and KGY, **Figure 5.8**) revealed that the hydroxamate group formed a complex with the catalytic Zn2+ ion at the active site. **Figure 5.8(A & C)** shows that the quinolinyl moiety entered through the S1′ pocket, while the quinoline moiety was positioned within the S3′ pocket. In addition to chelating Zn2+, the hydroxamate group also formed hydrogen bonds with the residues Gly349, His405, His409, His415, and Glu406. The Bayesian classification study (**Figure 5.3**) suggested that the presence of a substituted pyrrolidine/piperidine ring between the P1′ substituent and the hydroxamate zinc-binding group (ZBG) significantly contributes to ADAM17 inhibition. The oxo group of the phenyl pyrrolidinone moiety in IK682 interacted with the Gly349 and Leu348 residues and engaged in π-π interactions with the His405 residues at the binding site (**Figure 5.8(A & C)**). Notably, the heterocyclic nitrogen of the quinolinyl methoxy phenyl P1′ substituent formed hydrogen bonds with the Ser441 residue at the terminal end of the S3′ pocket, which is located within the specificity loop, thereby enhancing the stability of the molecule's binding in the S1′-S3′ pocket.

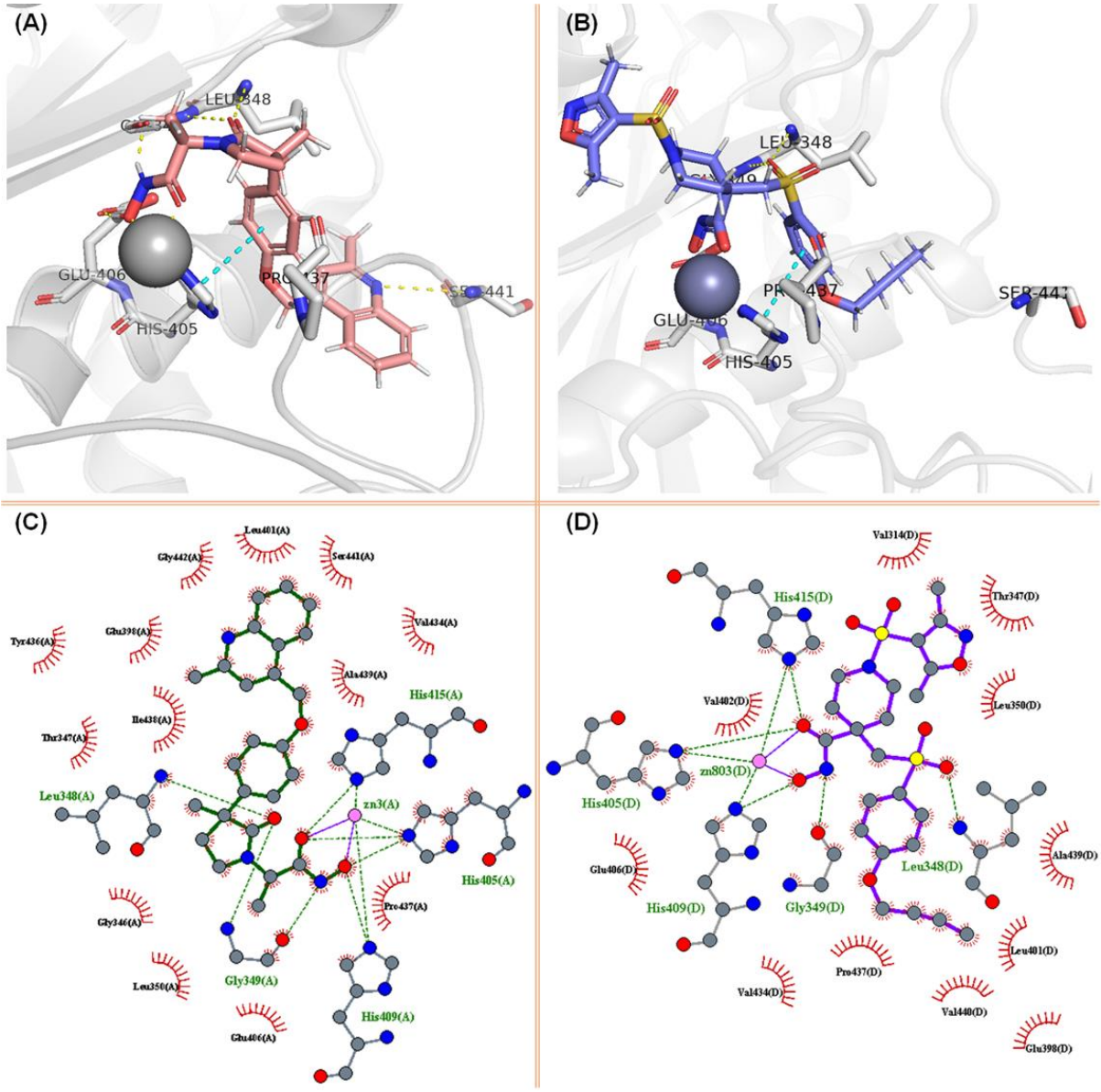

Figure 5.8. (A & C) Interactions between crystal-bound IK682 and key residues of ADAM17 catalytic site (PDB ID: 2FV5); **(B & D)** Interactions between crystal-bound KGY and key residues of ADAM17 catalytic site (PDB ID: 2I47)

In the crystal structure of the ADAM17-KGY complex (PDB ID: 2I47), the alkyl-substituted phenyl sulfonamido pyrrolidine was observed to form similar hydrogen bond interactions as those seen in the ADAM17-IK682 complex (**Figure 5.8(A & C)**). The Bayesian classification model identified valuable fragments such as G1, G2, G3, and G20, which are present in the structure of the bound KGY molecule (**Figure 5.8(B & D)**, PDB ID: 2I47). Additionally, the SARpy-mediated structural alert S(=O)(=O)CC2(CNCCC2) was present in the ADAM17 inhibitor KGY. The phenyl ring of the sulfonamido phenyl oxybutylene P1′ substituent in KGY was found to interact with key residues at the active site (**Figure 5.8(D)**). Specifically, one of

the two sulfonamido oxygen atoms formed a hydrogen bond with Leu348, while the phenyl ring engaged in π-π stacking with the heterocyclic ring of His405 (**Figure 5.8(B & D)**). Similar to the phenoxymethyl quinolinyl moiety in IK682, the compound KGY, bound to ADAM17, exhibited similar occupancy with its sulfonamido phenyl oxybutylene P1′ substituent in the S1′-S3′ pocket. However, unlike IK682, KGY lacks a heterocyclic nitrogen atom at the end of the P1′ substituent. While KGY still occupies the tunnel between the S1′ and S3′ pockets, it does not establish significant contacts at the terminal end of the S3′ pocket. The active site surfaces of ADAM17 (PDB ID: 2FV5, **Figure 5.7**) reveal that the terminal end of the S1′-S3′ pocket features a slightly acidic, less hydrophobic, and highly hydrogen-bonding region (**Figure 5.7**). This region is capable of interacting with the terminal groups of the P1′ substituents of ADAM17 inhibitors, as demonstrated by the interactions observed with the compound IK682.

5.6. Assessment of Binding Modes and Interactions for Dataset Compounds

For the binding mode and interaction analysis, molecular docking of both the most active and least active compounds from the dataset was performed at the active site of ADAM17 (PDB ID: 2FV5) using the GLIDE module in Schrodinger Maestro Software [227], following the same protocol described in our previous studies [230, 231], employing the OPLS_2005 force field and a ligand diameter midpoint box size of 15Å × 15Å × 15Å with the extra precision (XP) method. The crystal-structure-bound and redocked conformation of IK682 (GLIDE docking score = -12.4 kcal/mol), along with the docked poses of compound 93 (GLIDE docking score = -10.5 kcal/mol) and compound 9 (GLIDE docking score = -10.6 kcal/mol), are illustrated in **Figures 5.9A** and **5.9B**, respectively.

From the binding patterns observed in the most active compound (compound 93, **Figure 5.9C** and **5.9D**) and the least active compound (compound 9, **Figure 5.9E** and **5.9F**), it was evident that the quinolinyl methoxyphenyl sulfonyl P1′ substituent extended deep into the S1′ and S3′ pockets of ADAM17 (PDB ID: 2FV5, **Figure 5.9C** and **Figure 5.9E**). Both compounds 93 and 9, with their hydroxamate ZBG, interacted similarly with the active site amino acids Gly349, His405, His409, His415, Leu348, Ser441, and Glu406, as observed in the crystal structure (**Figure 5.9{C-F}** vs. **Figure 5.8**).

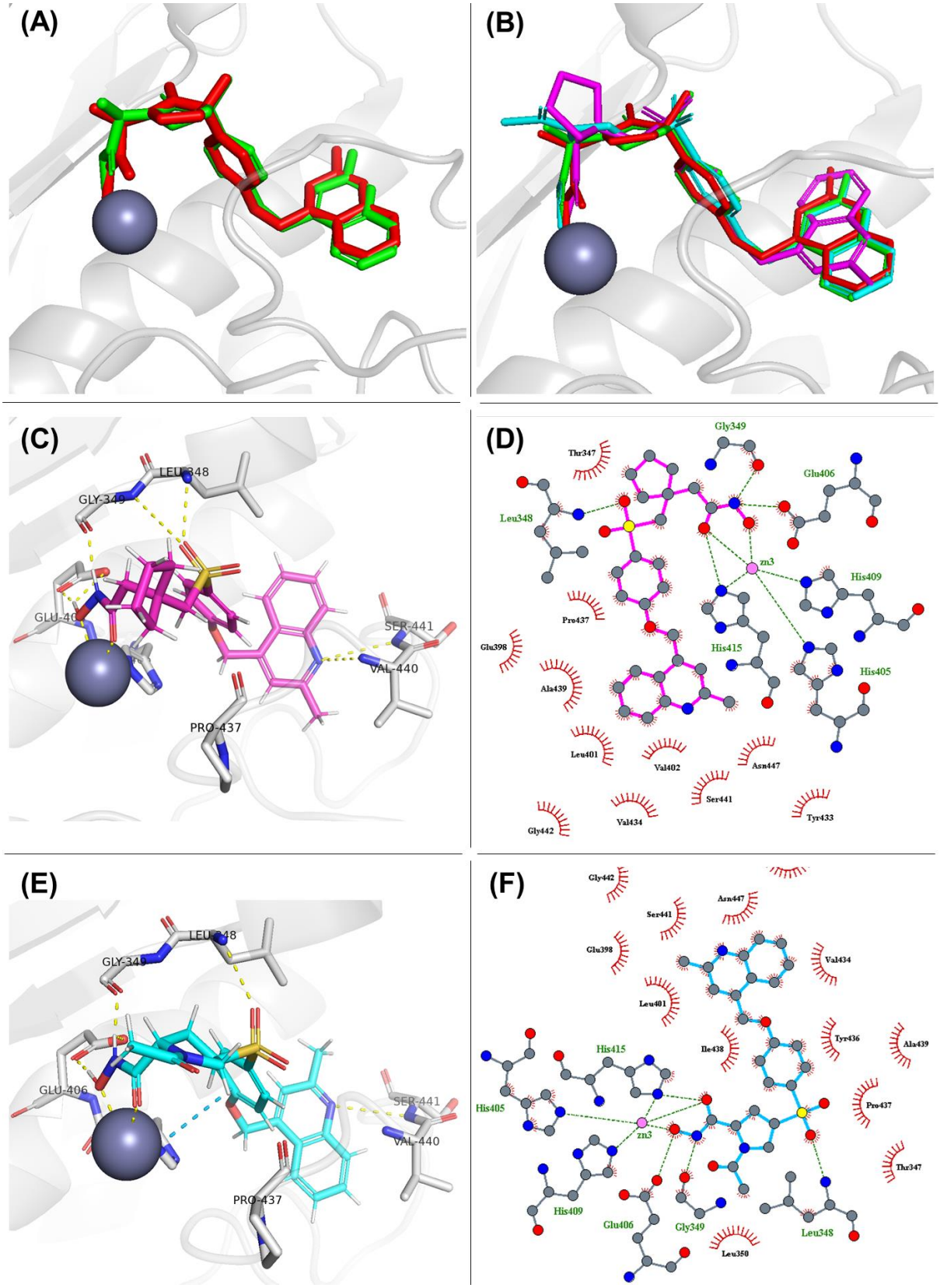

Figure 5.9. (A) Alignment of crystal structure (PDB ID: 2FV5)-bound ADAM17 inhibitor (IK682, red stick) and its redocked conformer (green stick); **(B)** Alignment of the crystal-bound ligand (red stick), redocked pose of the crystal-bound ligand (green stick), compound **93**

(magenta stick), and compound **9** (cyan stick) at the binding site of ADAM17 (PDB ID: 2FV5); **(C)** The 3D binding pattern and interactions of compound **93**; **(D)** The 2D interactions of compound **93**; **(E)** The 3D binding pattern and interactions of compound **9**, **(F)** The 2D interactions of compound **9** at the active site of ADAM17 (PDB ID: 2FV5)

Notably, while the least active compound 9 and the crystal-bound complexes only showed conventional interactions, the most active compound 93 displayed an additional interaction between the heterocyclic quinolinyl nitrogen atom and Val440, alongside Ser441, at the end of the S3′ pocket (**Figure 5.9C** vs. **Figure 5.9E**). This interaction between the quinolinyl group of the compound 93 and the terminal Val441 in the S3′ pocket may contribute to increased binding stability of the P1′ substituent, leading to more effective ADAM17 inhibition.

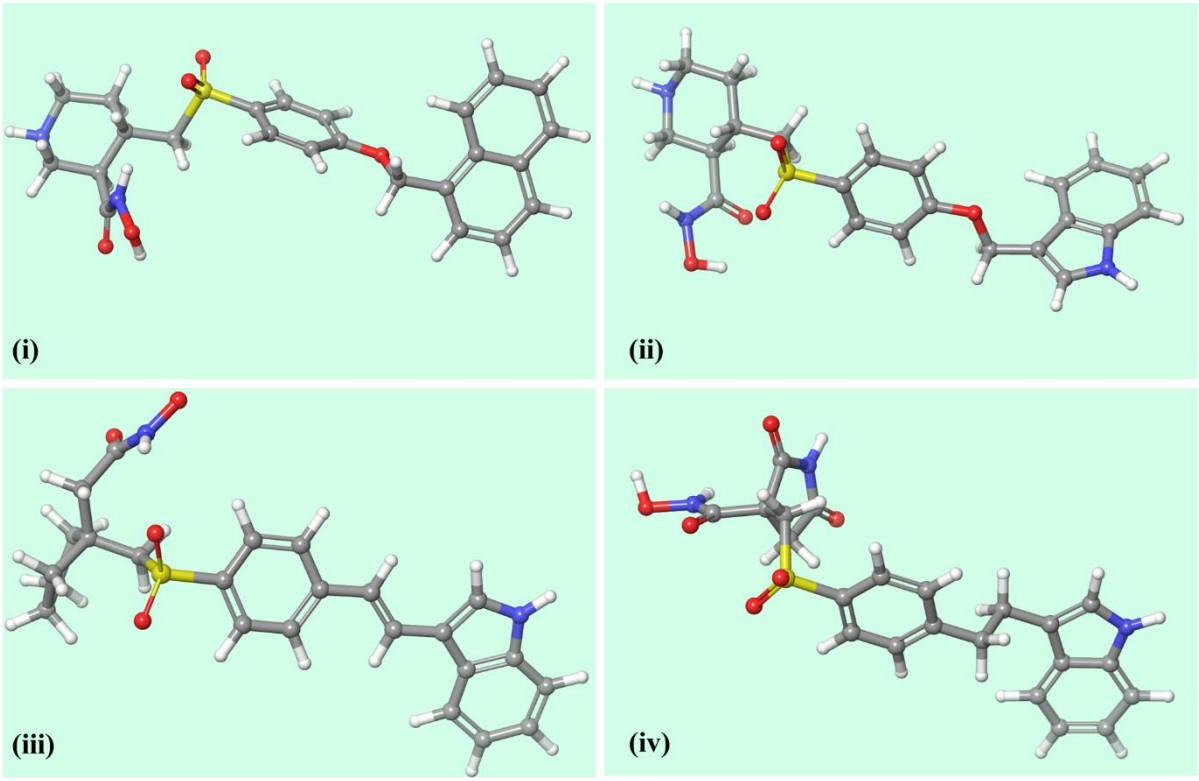

Figure 5.10. 3D representation of the designed compounds namely, (i) D1; (ii) D2; (iii) D3; (iv) D4

In addition to the dataset compounds, the molecular modelling study of the quinolinyl methoxyphenyl sulfonyl derivatives revealed various structural fragments and characteristics of these ADAM17 inhibitors. This information was used to design a smaller set of new hydroxamate derivatives (D1 to D4) (**Figure 5.10**). Furthermore, the SwissADME tool [232, 233] estimated the ADME properties, and the boiled egg plot for these probable ADAM17 inhibitors can be found in **Appendix Table T10** and **Appendix Figure F3**, respectively.

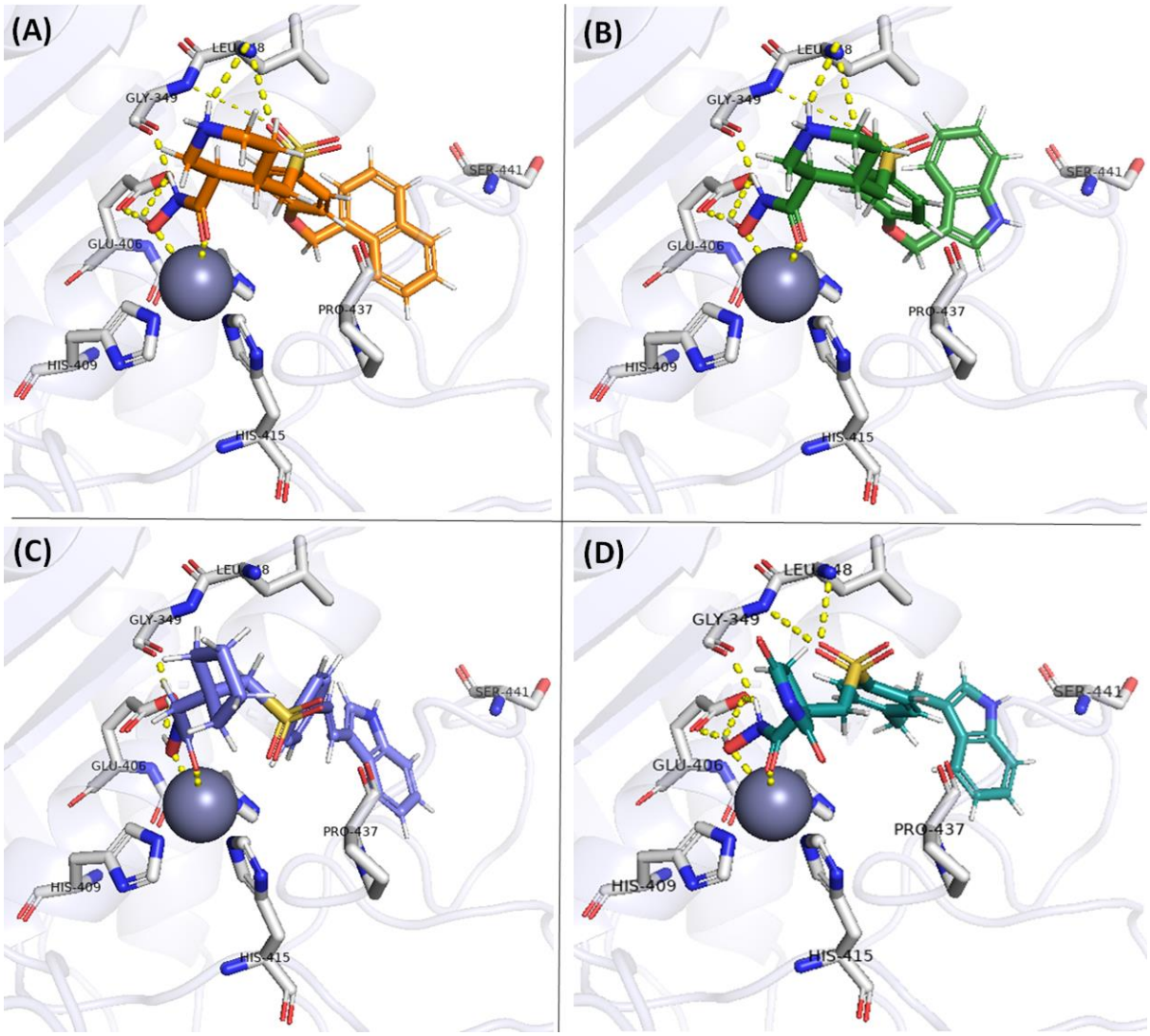

Figure 5.11. The 3D binding pattern of designed **(A)** compound **D1**, **(B)** compound **D2**, **(C)** compound **D3**, and **(D)** compound **D4** at ADAM17 (PDB ID: 2FV5) binding site

The molecular docking study of the newly designed derivatives revealed that the naphthyl methyloxy phenyl, indolyl methyloxy phenyl, 3-styryl-1H-indole, and 3-(phenoxymethyl)-1H-indole P1′ substituents similarly occupied the S1′-S3′ tunnel of the enzyme, comparable to the co-crystallized ligands and the docked dataset compounds (**Figure 5.11** vs. **Figures 5.8** and **5.9**). The 2D interaction analysis showed that these P1′ substituents extended their indolyl or naphthyl groups towards the Val440 and Ser441 residues at the end of the S3′ pocket while entering through the S1′ pocket. Additionally, the zinc-binding group (ZBG) of these compounds remained consistent, with the hydroxamate group maintaining typical bidentate

chelation with the catalytic zinc of ADAM17 and displaying similar hydrogen bonding interactions with Leu238, Gly239, Glu406, His409, and His415 residues (**Figure 5.12**).

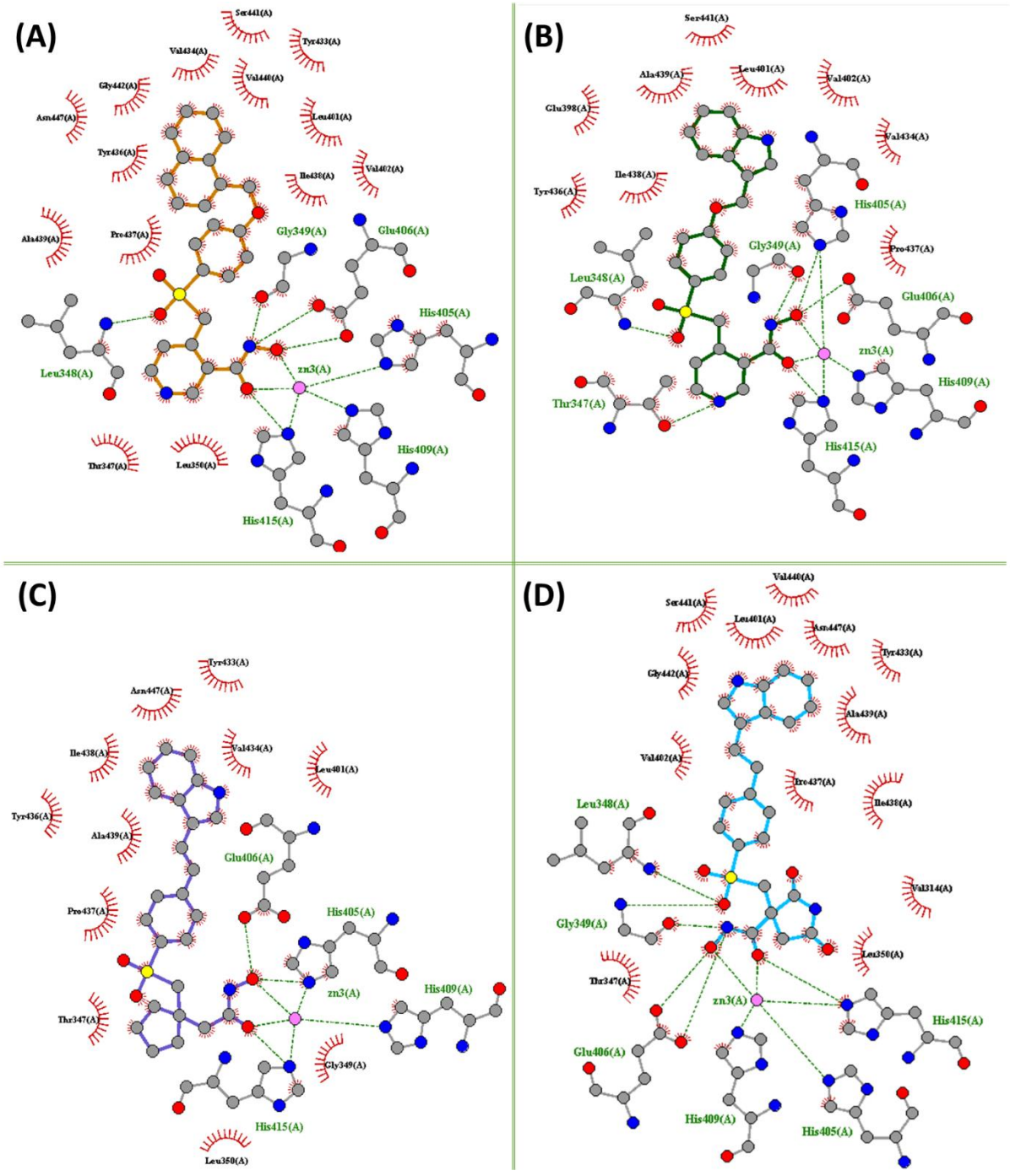

Figure 5.12. The 2D interactions of the designed **(A)** compound **D1**, **(B)** compound **D2**, **(C)** compound **D3**, and **(D)** compound **D4** at ADAM17 (PDB ID: 2FV5) binding site

An interesting observation was made regarding the modifications between the P1′ substituents and the ZBG in the designed compounds. Specifically, compounds D1 (GLIDE docking score = -10.5 kcal/mol) and D2 (GLIDE docking score = -9.8 kcal/mol), which include the piperidine

moiety, exhibited better interactions (**Figure 5.12A** and **Figure 5.12B**) compared to compound D3 with a c-pentane group (GLIDE docking score = -7.4 kcal/mol) and compound D4 with a pyrrolidine dione group (GLIDE docking score = -10.7 kcal/mol) (**Figure 5.12C** and **Figure 5.12D**). Due to its close proximity to the Thr347 residue, the heterocyclic nitrogen atom in the piperidine ring of compounds D1 and D2 may form an additional interaction with Thr347, enhancing the binding of these molecules at the ADAM17 active site (PDB ID: 2FV5), as observed for compound D2 (**Figure 5.12B**). In contrast, compound D3, which features a c-pentyl ring, did not interact with Thr347 despite its proximity to the residue. This lack of interaction may be attributed to the absence of a heterocyclic nitrogen in the c-pentyl ring of D3, unlike in D2 (**Figure 5.12C** vs. **Figure 5.12B**). Another notable observation was made when comparing the binding of compound D1 with compounds D2-D4 (**Figure 5.12**). It appears that the binding of the P1′ substituents of these new ADAM17 inhibitors (e.g., the naphthyl methyloxy phenyl group in D1 versus the 3-(phenoxymethyl)-1H-indole moiety in D2) can influence the interaction of other moieties within the compounds, potentially affecting their overall binding affinity and potency against ADAM17 (**Figure 5.12A** vs. **Figure 5.12B**). These observations suggest that altering the P1′ substituent and the group located between the P1′ substituent and the ZBG is a crucial pharmacophoric feature for ADAM17 inhibitors, alongside the ZBG itself. Additionally, fine-tuning the interactions between the P1′ substituent and the ZBG can help in designing novel and effective ADAM17 inhibitors.

Chapter 6: Conclusion and Future Outlook

In this study, various QSAR modeling techniques were applied to a set of hydroxamate-based ADAM17 inhibitors, all featuring a common sulfonylphenoxy-methylquinoline scaffold. These analyses successfully identified key structural features crucial for the significant biological activity of these small molecules. By evaluating the results from various classification-based QSAR methodologies (including LDA, Bayesian classification modeling, recursive partitioning, and SARpy analysis), similar substructural features were consistently identified as critical for ADAM17 inhibition across these different modeling approaches. Additionally, receptor-ligand interaction studies revealed that these structural fragments interact extensively with the catalytic site of ADAM17, contributing to enhanced inhibitory activity. Notably, compounds containing a methylsulfonyl-benzene moiety along with a substituted piperidine or azetidine ring demonstrated high activity, suggesting their utility in designing new inhibitors. This aligns with findings from our previous study on arylsulfonamide-derived ADAM17 inhibitors [234], The significance of the sulfonyl group was also noted, as the sulfonyl oxygen atoms were involved in hydrogen bond interactions with the active site residue Leu348. Additionally, previous pharmacophore mapping of aryl sulfonamide derivatives highlighted the sulfonyl phenyloxy butylene P1′ group as a key hydrophobic feature necessary for binding within the narrow hydrophobic S1′-S3′ tunnel of ADAM17, as shown in **Figure 5.8**. Similarly, the quinolinyl derivatives examined in this study exhibited a comparable hydrophobic function, effectively occupying the S1′-S3′ pocket of the enzyme and interacting with both the S1′ and S3′ terminals. This interaction contributes to enhanced potency.

Based on these findings, four new classes of compounds were designed: naphthyl methyloxy phenyl, indolyl methyloxy phenyl, 3-styryl-1H-indole, and 3-(phenoxymethyl)-1H-indole. Given the advancements in drug discovery facilitated by sophisticated software and computational methods, which have enhanced reproducibility and validation in recent years [235], the binding patterns and interactions of these newly designed ADAM17 inhibitors were further assessed by comparing them with the co-crystallized ligand bound to ADAM17. The similarities observed in interactions and binding patterns not only confirmed the results of this study but also underscored the importance of different substitutions for effective ADAM17 binding and inhibitor potency. Finally, yet importantly, it is crucial to recognize that small molecules need to possess specific structural features to achieve biological activity. This study can thus contribute to identifying effective and promising ADAM17 inhibitors, potentially offering new solutions for treating severe pathophysiological conditions such as cancer, inflammatory diseases, and Alzheimer’s disease in the future.

Chapter 7: Experimental Work

7.1. Relationship between glutamine & cancer

Even though glutamine (**Figure 7.1**) is classified as a non-essential amino acid, it plays a crucial and versatile role in the body. Among the 20 amino acids that make up proteins, glutamine is particularly significant due to its involvement in numerous physiological functions. Glutamine features a side chain with an amide group, which makes it a polar, uncharged amino acid. Its structure includes a backbone shared by all amino acids, comprising an amino group, a carboxyl group, and a central carbon, along with a side chain that has an amide group (–CONH2) bonded to the central carbon. Glutamine is classified as a conditionally essential amino acid and is present in the highest concentration in human blood compared to other amino acids. Typically, the body can synthesize sufficient amounts of glutamine on its own. However, during times of severe stress, trauma, or illness, the body's need for glutamine may surpass its production capacity, rendering it conditionally essential. Glutamine is a key component of proteins and is vital for muscle growth and repair. This is especially significant for athletes and individuals who are recovering from injuries or illnesses. It also acts as an essential energy source for immune cells, including lymphocytes and macrophages [236]. During periods of stress or illness, the need for glutamine rises to help support the immune system. Glutamine aids in the transport of nitrogen between tissues and helps regulate nitrogen levels in the body, which is essential for various metabolic processes. Additionally, it serves as a precursor to neurotransmitters like glutamate. Concisely, glutamine is a vital amino acid with numerous important functions in the body, from supporting protein synthesis and nitrogen balance to aiding in gut health and immune function. Its versatility makes it an essential element in both everyday physiology and clinical settings.

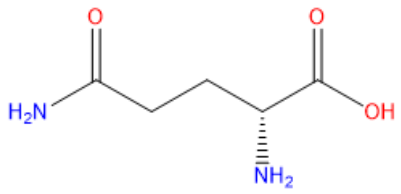

Figure 7.1. Structure of D-glutamine

The connection between glutamine and cancer is intricate and multifaceted. As an amino acid vital for numerous physiological processes, glutamine can affect cancer development and progression in multiple ways. Cancer cells frequently show changes in glutamate metabolism compared to normal cells. They often take up more glutamate and its derivatives to fuel their rapid growth and division. Researchers are exploring glutamate analogues to interfere with this

altered metabolic process, which could potentially slow or inhibit the growth of cancer cells. Glutamate, an essential neurotransmitter, can impact cancer cell behaviour by interacting with glutamate receptors. Some cancer cells have these receptors and use them to receive signals that promote growth and survival. Therefore, glutamate analogues can function as antagonists, blocking these receptors and consequently reducing cancer cell proliferation. Certain cancer cells depend on specific enzymes involved in glutamate metabolism for their survival. Glutamate analogues can inhibit these enzymes, decreasing the availability of glutamate and its derivatives. This reduction can either induce cancer cell death or impair their ability to proliferate. Glutamate analogues can trigger oxidative stress or other types of cellular stress in cancer cells. This stress can cause apoptosis (programmed cell death) or diminish the cancer cells' ability to manage their environment, making them more vulnerable to other treatments or to cell death. Studies have demonstrated that various human cancer cell lines, including those from small cell lung cancer, pancreatic cancer, acute myelogenous leukaemia, and glioblastoma multiforme, are particularly sensitive to glutamine deprivation. For these reasons, glutamate analogues have the potential to function as anti-cancer agents [237]. In a nutshell, glutamine is pivotal in cancer metabolism, impacting tumour growth, survival, and interactions with the immune system. Its role as both a supportive and potentially exploitable nutrient for cancer cells makes it a crucial area of ongoing research and therapeutic development.

7.2. Rationale behind synthesis of glutamine-based analogues as ADAM17 inhibitors

The development of glutamine analogues as inhibitors of ADAM17 (A Disintegrin and Metalloprotease 17), also known as TNF-alpha converting enzyme (TACE), is based on the biochemical and structural similarities between glutamate and the enzyme's active site. This approach aims to create specific inhibitors that can influence pathological processes associated with ADAM17 [238]. Glutamine is an amino acid with a carboxylate moiety, which resembles the functional groups involved in coordinating zinc ions in metalloproteinases. Researchers aim to design molecules that mimic glutamate's structure to fit into and interact with the enzyme's active site. Besides, Glutamine's amide group can engage in hydrogen bonding and other interactions that are crucial for binding to the enzyme's active site or substrate-binding site. ADAM17 targets substrates with peptide bonds that may interact with functional groups similar to those found in glutamine. By utilizing glutamine or its analogues, researchers aim to design molecules that can bind to the enzyme's active site or substrate-binding site, either mimicking or disrupting the natural interactions of substrates. Inhibitors like glutamine analogues face significant challenges related to specificity and selectivity. It is essential to

ensure that these analogues specifically target ADAM17 while minimizing off-target effects. The design process must carefully balance effective binding to ADAM17 with avoiding interactions with other metalloproteinases or similar enzymes.

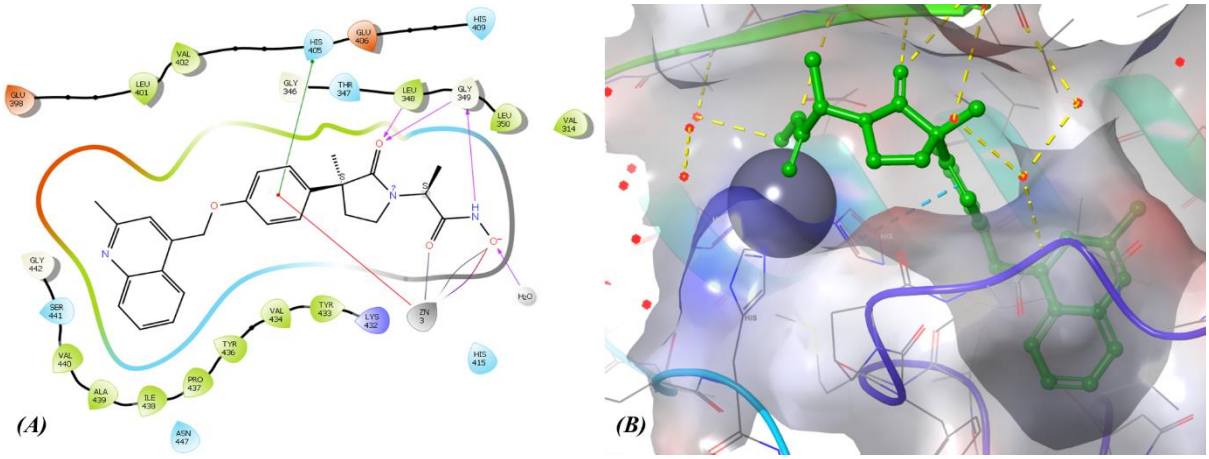

Figure 7.2. Molecular docking of the inbound ligand ***(A & B)*** IK682 (GLIDE docking score = -14.06 kcal/mol) (PDB ID: 2FV5)

Moreover, molecular docking studies of the designed glutamine analogues with the ADAM17 enzyme (PDB ID: 2FV5) revealed that the interactions observed were similar to those of the enzyme's in-bound ligand. The docking study revealed that more or less all the novel compounds, along with the bound ligand IK682, demonstrated π-π stacking interactions with His405, π-cation interactions with the Zn^{2+} ion, metal coordination, and salt bridge interactions with the co-factor Zn^{2+} (**Figure 7.2**). Additionally, these compounds formed hydrogen bonds with LEU348 and GLY349, and also engaged in water-mediated hydrogen bonding. Notably, the compound TBS-04 formed hydrogen bonds with Pro437 instead of GLY349, whereas the compound TBS-02 had an extra hydrogen bond with the THR347 amino acid and the compound TBS-10 not exhibited π-π stacking interactions with His405 but showed an additional hydrogen bonding with TYR436 (**Figure 7.3**).

This suggests that the newly developed glutamine analogues could potentially be effective in inhibiting the ADAM17 enzyme. In summary, the development of glutamine analogues as ADAM17 inhibitors is based on the concept that these analogues can either mimic or disrupt interactions with the enzyme's active site, potentially providing a targeted method for modulating ADAM17 activity.

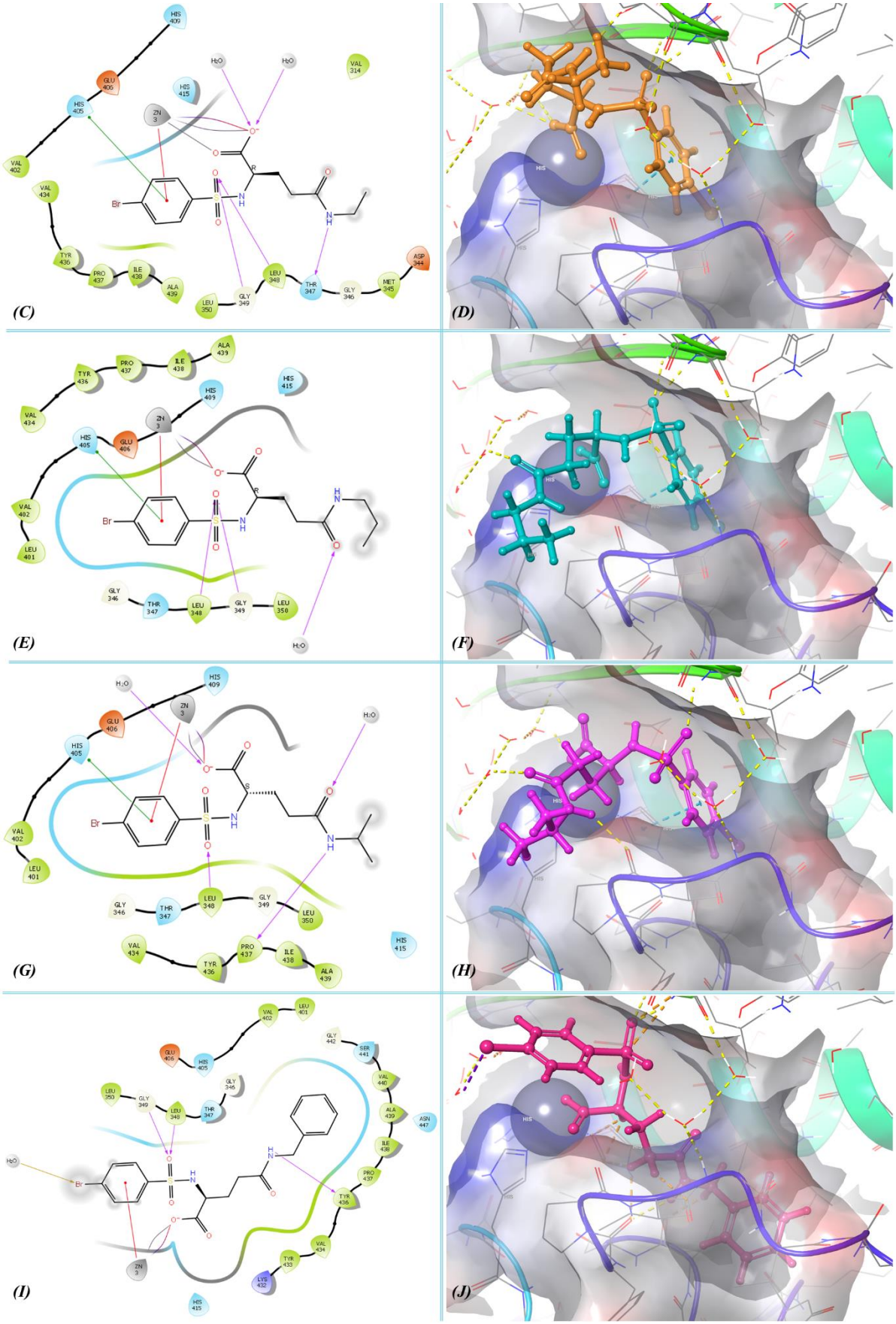

Figure 7.3. Molecular docking of the novel compounds, ***(C & D)*** TBS-02 (GLIDE docking

score = -7.66 kcal/mol), ***(E & F)*** TBS-03 (GLIDE docking score = -7.02 kcal/mol), ***(G & H)*** TBS-04 (GLIDE docking score = -6.9 kcal/mol), and (***I & J)*** TBS-10 (GLIDE docking score = -8.49 kcal/mol)

7.3. Synthesis of a few glutamine-based Aryl-sulfonamide derivatives as probable ADAM17 inhibitors

7.3.1. General synthetic scheme

For the synthesis of the glutamine analogues a general synthetic scheme (**Figure 7.4**) has been followed that is outlined below;

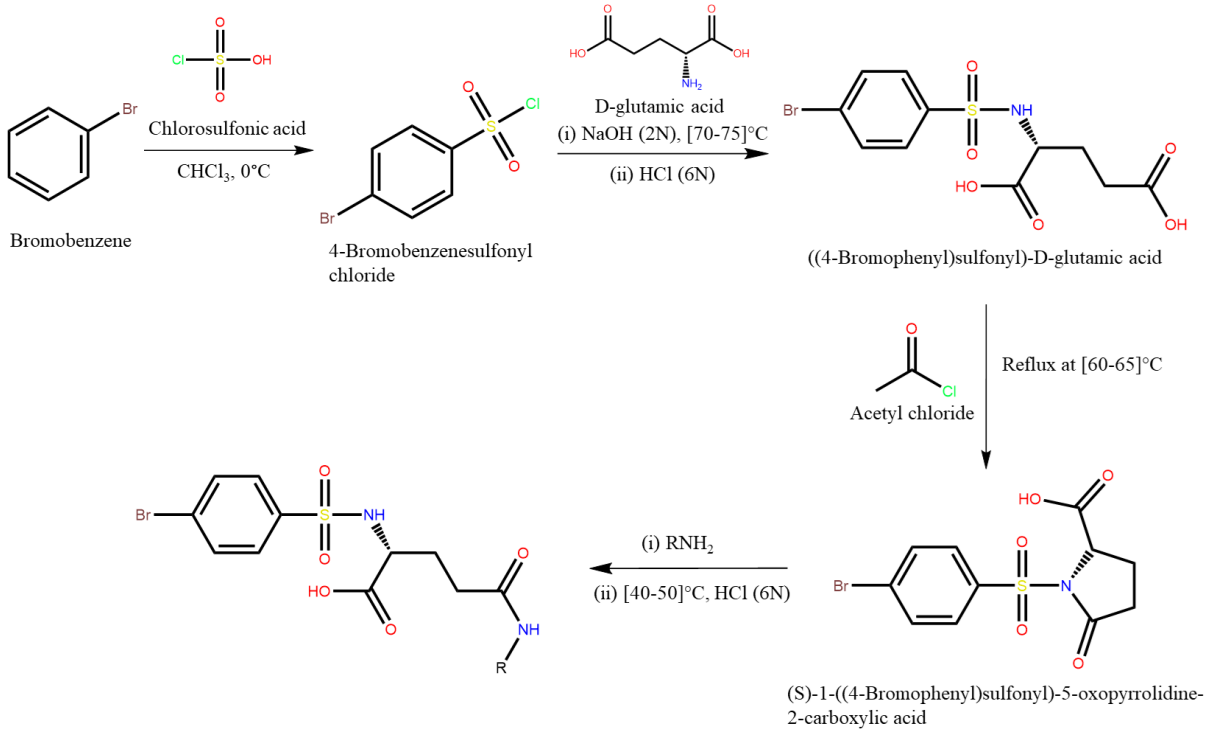

Figure 7.4. General synthetic route

A total of 11 compounds have been synthesized in our laboratory as D-glutamine analogues in our laboratory. The synthesis involves several steps to produce the final compounds, which are described in detail below.

7.3.2. First step: Synthesis of 4-bromobenzenesulfonyl chloride

Various grades of chemicals and reagents were utilized to synthesize 4-Bromobenzenesulfonyl chloride (**Figure 7.5**) that includes chlorobenzene, chloroform and chlorosulfonic acid.

Bromobenzene and chlorosulfonic acid were used in a 1:5 ratio. Initially, 1 gram of bromobenzene was dissolved in 5 ml of chloroform in a 250 ml flat-bottom flask. Chlorosulfonic acid (5 grams) was then added dropwise to the solution. The reaction was maintained in an ice bath at 0°C throughout the process. Once hydrogen chloride gas was released, the mixture was allowed to reach room temperature. After approximately 30 minutes, the contents of the flask were transferred to a beaker containing ice cubes. The chloroform layer was separated, washed with cold water, and the desired product was obtained after evaporating the solvent.

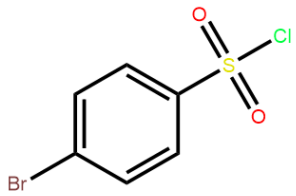

Figure 7.5. 4-bromobenzenesulfonyl chloride

Table 7.1. Physical data related to 4-bromobenzenesulfonyl chloride

Compound name	Molecular weight (g/mole)	Molecular formula	Percentage yield	Melting point
4-bromobenzenesulfonyl chloride	255.51	$C_6H_4BrClO_2S$	79.53%	57-63°C

7.3.3. Second step: Synthesis of (4-bromophenylsulfonyl)-D-glutamic acid (Diacid)

For the synthesis of diacid D-glutamic acid, 4-bromobenzenesulfonyl chloride (**Figure 7.6**), sodium 47 hydroxide solution (2N), P^H paper, hydrochloric acid (6N), ethyl acetate, anhydrous sodium sulphate etc.

D-glutamic acid and 4-bromobenzenesulfonyl chloride were taken in 1.1:1 ratio. The D-glutamic acid was placed in a 250 ml conical flask, and 2N sodium hydroxide (NaOH) solution was added until the mixture became alkaline, indicated by a pink colour (pH 8-9). The mixture was heated to 70-75°C, and 4-bromobenzenesulfonyl chloride was added gradually in small portions while stirring continuously. 2N sodium hydroxide (NaOH) solution was added intermittently to keep the reaction mixture alkaline. Once the reaction was complete, the mixture was allowed to cool to room temperature. The reaction mixture was then filtered

through a Buchner funnel under suction to remove any undissolved solids. The filtrate was acidified with a 6N hydrochloric acid (HCl) solution and was extracted three times with ethyl acetate and once with distilled water. The ethyl acetate layer was transferred to a round-bottom flask, and anhydrous sodium sulphate was added to absorb any excess water present in the layer. This mixture was left to stand overnight, and the next day, it was filtered through cotton using a funnel. After that, the ethyl acetate solvent was distilled off to obtain (4-bromophenylsulfonyl)-D-glutamic acid in solid form, which was then dried.

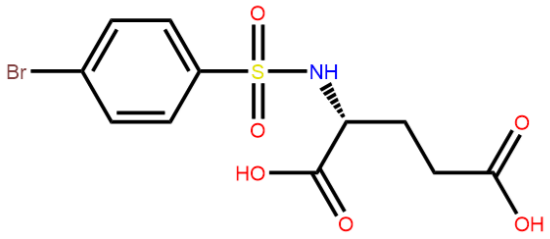

Figure 7.6. (4-bromophenylsulfonyl)-D-glutamic acid

Table 7.2. Physical data related to the Diacid

Compound name	Molecular weight (g/mole)	Molecular formula	Percentage yield	Melting point
(4-bromophenylsulfonyl)-D-glutamic acid	366.18	$C_{11}H_{12}BrNO_6S$	33.44%	83-90°C

7.3.4. Third step: Synthesis of (S)-1-(4-bromophenylsulfonyl)-5-oxopyrrolidine-2-carboxylic acid (Monoacid)

At first properly weighed (4-bromophenylsulfonyl)-D-glutamic acid was taken in a round bottom flask and acetyl chloride added as much as required (diacid: acetyl chloride at 1:3), to synthesize the monoacid (**Figure 7.7**). The reaction mixture was then refluxed at 60-65°C until hydrochloric acid (HCl) gas evolution stopped. Once the reaction was complete, the mixture was cooled to room temperature and poured onto crushed ice while stirring continuously. Finally, the precipitated product was extracted using chloroform and brine solution.

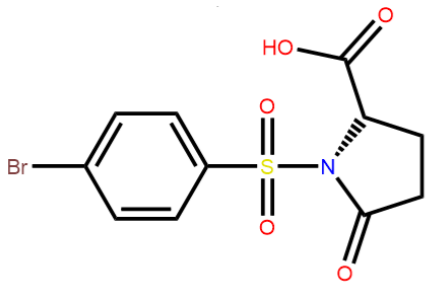

Figure 7.7. (S)-1-(4-bromophenylsulfonyl)-5-oxopyrrolidine-2-carboxylic acid

Table 7.3. Physical data related to the Monoacid

Compound name	Molecular weight (g/mole)	Molecular formula	Percentage yield
(S)-1-(4-bromophenylsulfonyl)-5-oxopyrrolidine-2-carboxylic acid	348.17	$C_{11}H_{10}BrNO_5S$	71.86%

7.3.5. Final step: synthesis of 5-N-substituted-2-(4-bromophenylsulfonyl)-D-glutamine compounds

To synthesize 5-N-substituted-2-(4-bromophenylsulfonyl)-D-glutamines, approximately 1 g of (S)-1-(4-bromophenylsulfonyl)-5-oxopyrrolidine-2-carboxylic acid (monoacid) was placed in a 100 ml conical flask. Ten additional conical flasks, each containing the same amount of monoacid, were prepared. Various amines were added to each flask to yield the desired compounds. The flasks were kept in a dark place for 12-13 hours to facilitate the reaction. Following this, the flasks were heated in a water bath at 40-50°C to remove excess unreacted amines. After cooling to room temperature, 6N HCl solution was added over ice bath. The resulting precipitate was filtered, washed sequentially with cold water and hexane, and then the residues were dried to obtain the solid products.

Table 7.4. Physical data related to the final compounds (TBS-01 to TBS-11)

Name of compound	IUPAC name	Molecular weight (g/mole)	Molecular formula	Percen-tage yield	Melting point
TBS-01	5-(methylamino)-2-(4-bromophenylsulfonamido)-5-oxopentanoic acid	379.23	$C_{12}H_{15}BrN_2O_5S$	43.15%	171-175°C

TBS-02	5-(ethylamino)-2-(4-bromophenylsulfonamido)-5-oxopentanoic acid	393.25	$C_{13}H_{17}BrN_2O_5S$	55%	195-198°C
TBS-03	5-(propylamino)-2-(4-bromophenylsulfonamido)-5-oxopentanoic acid	407.28	$C_{14}H_{19}BrN_2O_5S$	63.26%	207-211°C
TBS-04	5-(isopropylamino)-2-(4-bromophenylsulfonamido)-5-oxopentanoic acid	407.28	$C_{14}H_{19}BrN_2O_5S$	20.51%	199-203°C
TBS-05	5-(butylamino)-2-(4-bromophenylsulfonamido)-5-oxopentanoic acid	421.31	$C_{15}H_{21}BrN_2O_5S$	39%	205-207°C
TBS-06	5-(isobutylamino)-2-(4-bromophenylsulfonamido)-5-oxopentanoic acid	421.31	$C_{15}H_{21}BrN_2O_5S$	52.14%	208-211°C
TBS-07	5-(pentylamino)-2-(4-bromophenylsulfonamido)-5-oxopentanoic acid	435.33	$C_{15}H_{21}BrN_2O_5S$	58.38%	199-201°C
TBS-08	5-(*tert*-butylamino)-2-(4-bromophenylsulfonamido)-5-oxopentanoic acid	421.31	$C_{15}H_{21}BrN_2O_5S$	10.5%	200-203°C
TBS-09	5-(cyclohexylamino)-2-(4-bromophenylsulfonamido)-5-oxopentanoic acid	447.34	$C_{17}H_{23}BrN_2O_5S$	31.13%	218-223°C
TBS-10	5-(benzylamino)-2-(4-bromophenylsulfonamido)-5-oxopentanoic acid	455.32	$C_{18}H_{19}BrN_2O_5S$	38.23%	195-200°C
TBS-11	5-(phenylethylamino)-2-(4-bromophenylsulfonamido)-5-oxopentanoic acid	469.35	$C_{19}H_{21}BrN_2O_5S$	37.09%	201-205°C

7.3.6. Recrystallization of the synthesized compounds

Recrystallization is the most conventional technique used to purify the compounds. The dried solid product was placed in a conical flask, and a minimal amount of an alcoholic solution (ethanol: water = 3:2) was added. The flask was then heated to 50-60°C to fully dissolve the solid. Once boiling began, a small amount of charcoal was added and heated for 20-30 seconds. The mixture was then filtered hot using filter paper under suction. The resulting filtrate was transferred to a clean conical flask and cooled in the refrigerator to encourage crystal formation. The crystals were then separated from the solvent through vacuum filtration and washed with a small amount of cold solvent to remove any remaining impurities. Finally, the obtained product was dried.

7.3.7. Analysis of the synthesized compounds

Melting points of all synthesized compounds (**Table 7.4**) were measured with the help of *Mel-Temp*, a capillary tube melting point apparatus. To verify and confirm the identity and purity of the recrystallized compounds, spectrometric techniques are typically employed. However, due to time constraints, spectrophotometric analysis has not yet been performed. The process of characterizing the synthesized compounds is still in progress.

Chapter 8: Concluding Remarks

Despite ADAM17's involvement in various diseases such as cancer, Alzheimer's disease, and inflammatory conditions, no ADAM17 inhibitors are currently available as drug candidates on the market. Therefore, the primary objective of the study is to develop potential ADAM17 inhibitors. The rationale for synthesizing glutamine analogues as potential inhibitors of ADAM17 has already been discussed. Over the last few years, our laboratory has been investigating glutamine analogues with the goal of developing potent anti-cancer agents and these efforts have been documented in several publications.

All eleven glutamine-based Aryl-sulfonamide derivatives were synthesized through a straightforward method with the aim of developing them as novel ADAM17 inhibitors for anti-neoplastic applications. However, their characterization is still incomplete, and as a result, their biological evaluation has not been conducted. These compounds will soon be tested against the ADAM17 enzyme to evaluate their inhibitory activity. In the future, the synthesis of designed novel compounds (D1-D4), guided by classification-dependent molecular modelling approaches, can be carried out to evaluate their inhibitory activity against the ADAM17 enzyme.

References

1. Weinberg, R. A. (1996). How cancer arises. *Scientific American*, *275*(3), 62-70.
2. https://gco.iarc.fr/today/en.
3. Vargas-Camaño, M. E., Guido-Bayardo, R. L., Martínez-Aguilar, N. E., & Castrejón-Vázquez, M. I. (2016). El cáncer como inmunodeficiencia secundaria. Revisión. *Revista Alergia México*, *63*(2), 169-179.
4. Byrne, S., Boyle, T., Ahmed, M., Lee, S. H., Benyamin, B., & Hyppönen, E. (2023). Lifestyle, genetic risk and incidence of cancer: a prospective cohort study of 13 cancer types. *International Journal of Epidemiology*, *52*(3), 817-826.
5. Boutry, J., Tissot, S., Ujvari, B., Capp, J. P., Giraudeau, M., Nedelcu, A. M., & Thomas, F. (2022). The evolution and ecology of benign tumors. *Biochimica et Biophysica Acta (BBA)-Reviews on Cancer*, *1877*(1), 188643.
6. Hoadley, K. A., Yau, C., Hinoue, T., Wolf, D. M., Lazar, A. J., Drill, E., ... & Cope, L. (2018). Cell-of-origin patterns dominate the molecular classification of 10,000 tumors from 33 types of cancer. *Cell*, *173*(2), 291-304.
7. Cao, M., Li, H., Sun, D., He, S., Yan, X., Yang, F., ... & Chen, W. (2022). Current cancer burden in China: epidemiology, etiology, and prevention. *Cancer biology & medicine*, *19*(8), 1121.
8. De Visser, K. E., & Joyce, J. A. (2023). The evolving tumor microenvironment: From cancer initiation to metastatic outgrowth. *Cancer cell*, *41*(3), 374-403.
9. Kaur, R., Bhardwaj, A., & Gupta, S. (2023). Cancer treatment therapies: traditional to modern approaches to combat cancers. *Molecular biology reports*, *50*(11), 9663-9676.
10. Patrick, G. L. (2023). *An introduction to medicinal chemistry*. Oxford university press.
11. Nasir, A., Khan, A., Li, J., Naeem, M., Khalil, A. A., Khan, K., & Qasim, M. (2021). Nanotechnology, a tool for diagnostics and treatment of cancer. *Current topics in medicinal chemistry*, *21*(15), 1360-1376.
12. Jia, J., Wu, X., Long, G., Yu, J., He, W., Zhang, H., ... & Tian, J. (2023). Revolutionizing cancer treatment: Nanotechnology-enabled photodynamic therapy and immunotherapy with advanced photosensitizers. *Frontiers in Immunology*, *14*, 1219785.
13. Lee, A. M., & Diasio, R. B. (2010). ADAM-17: a target to increase chemotherapeutic efficacy in colorectal cancer?. *Clinical Cancer Research*, *16*(13), 3319-3321.
14. Calvete, J. J., Marcinkiewicz, C., & Sanz, L. (2007). KTS and RTS-disintegrins: anti-angiogenic viper venom peptides specifically targeting the α1β 1 integrin. *Current pharmaceutical design*, *13*(28), 2853-2859.

15. Edwards, D. R., Handsley, M. M., & Pennington, C. J. (2008). The ADAM metalloproteinases. *Molecular aspects of medicine*, *29*(5), 258-289.
16. Cho, C. (2012). Testicular and epididymal ADAMs: expression and function during fertilization. *Nature Reviews Urology*, *9*(10), 550-560.
17. Brocker, C. N., Vasiliou, V., & Nebert, D. W. (2009). Evolutionary divergence and functions of the ADAM and ADAMTS gene families. *Human genomics*, *4*, 1-13.
18. Kawai, T., Elliott, K. J., Scalia, R., & Eguchi, S. (2021). Contribution of ADAM17 and related ADAMs in cardiovascular diseases. *Cellular and Molecular Life Sciences*, *78*, 4161-4187.
19. Nagase, H., Visse, R., & Murphy, G. (2006). Structure and function of matrix metalloproteinases and TIMPs. *Cardiovascular research*, *69*(3), 562-573.
20. Black, R. A., & White, J. M. (1998). ADAMs: focus on the protease domain. *Current opinion in cell biology*, *10*(5), 654-659.
21. Milla, M. E., Gonzales, P. E., & Leonard, J. D. (2006). The TACE zymogen: re-examining the role of the cysteine switch. *Cell biochemistry and biophysics*, *44*, 342-348.
22. Fahrenholz, F., Gilbert, S., Kojro, E., Lammich, S., & Postina, R. (2000). α-Secretase activity of the disintegrin metalloprotease ADAM 10: influences of domain structure. *Annals of the New York Academy of Sciences*, *920*(1), 215-222.
23. Wang, Y., Herrera, A. H., Li, Y., Belani, K. K., & Walcheck, B. (2009). Regulation of mature ADAM17 by redox agents for L-selectin shedding. *The journal of immunology*, *182*(4), 2449-2457.
24. Caescu, C. I., Jeschke, G. R., & Turk, B. E. (2009). Active-site determinants of substrate recognition by the metalloproteinases TACE and ADAM10. *Biochemical Journal*, *424*(1), 79-88.
25. Niu, J., & Li, Z. (2017). The roles of integrin αvβ6 in cancer. *Cancer letters*, *403*, 128-137.
26. Huang, T. F., Holt, J. C., Lukasiewicz, H., & Niewiarowski, S. (1987). Trigramin. A low molecular weight peptide inhibiting fibrinogen interaction with platelet receptors expressed on glycoprotein IIb-IIIa complex. Journal of Biological Chemistry, 262(33), 16157-16163.
27. Trad, A., Riese, M., Shomali, M., Hedeman, N., Effenberger, T., Grötzinger, J., & Lorenzen, I. (2013). The disintegrin domain of ADAM17 antagonises

fibroblast-carcinoma cell interactions. *International journal of oncology*, *42*(5), 1793-1800.

28. Maney, S. K., McIlwain, D. R., Polz, R., Pandyra, A. A., Sundaram, B., Wolff, D., ... & Lang, P. A. (2015). Deletions in the cytoplasmic domain of iRhom1 and iRhom2 promote shedding of the TNF receptor by the protease ADAM17. *Science signaling*, *8*(401), ra109-ra109.
29. Blobel, C. P. (2005). ADAMs: key components in EGFR signalling and development. *Nature reviews Molecular cell biology*, *6*(1), 32-43.
30. Sommer, A., Kordowski, F., Büch, J., Maretzky, T., Evers, A., Andrä, J., ... & Reiss, K. (2016). Phosphatidylserine exposure is required for ADAM17 sheddase function. *Nature communications*, *7*(1), 11523.
31. Maskos, K., Fernandez-Catalan, C., Huber, R., Bourenkov, G. P., Bartunik, H., Ellestad, G. A., ... & Bode, W. (1998). Crystal structure of the catalytic domain of human tumor necrosis factor-α-converting enzyme. *Proceedings of the National Academy of Sciences*, *95*(7), 3408-3412.
32. Stöcker, W., Grams, F., Reinemer, P., Bode, W., Baumann, U., Gomis-Rüth, F. X., & Mckay, D. B. (1995). The metzincins—Topological and sequential relations between the astacins, adamalysins, serralysins, and matrixins (collagenases) define a super family of zinc-peptidases. *Protein science*, *4*(5), 823-840.
33. Zunke, F., & Rose-John, S. (2017). The shedding protease ADAM17: Physiology and pathophysiology. *Biochimica et Biophysica Acta (BBA)-Molecular Cell Research*, *1864*(11), 2059-2070.
34. Wang, Y., Kim, K. A., Kim, J. H., & Sul, H. S. (2006). Pref-1, a preadipocyte secreted factor that inhibits adipogenesis. *The Journal of nutrition*, *136*(12), 2953-2956.
35. Fiorentino, L., Vivanti, A., Cavalera, M., Marzano, V., Ronci, M., Fabrizi, M., ... & Federici, M. (2010). Increased tumor necrosis factor α–converting enzyme activity induces insulin resistance and hepatosteatosis in mice. *Hepatology*, *51*(1), 103-110.
36. Murthy, A., Defamie, V., Smookler, D. S., Di Grappa, M. A., Horiuchi, K., Federici, M., ... & Khokha, R. (2010). Ectodomain shedding of EGFR ligands and TNFR1 dictates hepatocyte apoptosis during fulminant hepatitis in mice. *The Journal of clinical investigation*, *120*(8), 2731-2744.
37. Garton, K. J., Gough, P. J., Philalay, J., Wille, P. T., Blobel, C. P., Whitehead, R. H., ... & Raines, E. W. (2003). Stimulated shedding of vascular cell adhesion molecule 1

(VCAM-1) is mediated by tumor necrosis factor-α-converting enzyme (ADAM 17). *Journal of Biological Chemistry*, *278*(39), 37459-37464.

38. Sahin, U., Weskamp, G., Kelly, K., Zhou, H. M., Higashiyama, S., Peschon, J., ... & Blobel, C. P. (2004). Distinct roles for ADAM10 and ADAM17 in ectodomain shedding of six EGFR ligands. *The Journal of cell biology*, *164*(5), 769-779.
39. Rovida, E., Paccagnini, A., Del Rosso, M., Peschon, J., & Dello Sbarba, P. (2001). TNF-α-converting enzyme cleaves the macrophage colony-stimulating factor receptor in macrophages undergoing activation. *The Journal of Immunology*, *166*(3), 1583-1589.
40. Lichtenthaler, S. F., & Steiner, H. (2007). Sheddases and intramembrane-cleaving proteases: RIPpers of the membrane: Symposium on Regulated Intramembrane Proteolysis. *EMBO reports*, *8*(6), 537-541.
41. Brou, C., Logeat, F., Gupta, N., Bessia, C., LeBail, O., Doedens, J. R., ... & Israël, A. (2000). A novel proteolytic cleavage involved in Notch signaling: the role of the disintegrin-metalloprotease TACE. *Molecular cell*, *5*(2), 207-216.
42. Masters, C. L., Simms, G., Weinman, N. A., Multhaup, G., McDonald, B. L., & Beyreuther, K. (1985). Amyloid plaque core protein in Alzheimer disease and Down syndrome. *Proceedings of the National Academy of Sciences*, *82*(12), 4245-4249.
43. Schwager, S. L., Chubb, A. J., Scholle, R. R., Brandt, W. F., Mentele, R., Riordan, J. F., ... & Ehlers, M. R. (1999). Modulation of juxtamembrane cleavage ("shedding") of angiotensin-converting enzyme by stalk glycosylation: evidence for an alternative shedding protease. *Biochemistry*, *38*(32), 10388-10397.
44. Leissring, M. A., Murphy, M. P., Mead, T. R., Akbari, Y., Sugarman, M. C., Jannatipour, M., ... & LaFerla, F. M. (2002). A physiologic signaling role for the γ-secretase-derived intracellular fragment of APP. *Proceedings of the National Academy of Sciences*, *99*(7), 4697-4702.
45. Anderson, J. P., Chen, Y. U., Kim, K. S., & Robakis, N. K. (1992). An alternative secretase cleavage produces soluble Alzheimer amyloid precursor protein containing a potentially amyloidogenic sequence. *Journal of neurochemistry*, *59*(6), 2328-2331.
46. Bao, J., Wolpowitz, D., Role, L. W., & Talmage, D. A. (2003). Back signaling by the Nrg-1 intracellular domain. *The Journal of cell biology*, *161*(6), 1133-1141.
47. Prenzel, N., Zwick, E., Daub, H., Leserer, M., Abraham, R., Wallasch, C., & Ullrich, A. (1999). EGF receptor transactivation by G-protein-coupled receptors requires metalloproteinase cleavage of proHB-EGF. *Nature*, *402*(6764), 884-888.

48. Zhang, Q., Thomas, S. M., Xi, S., Smithgall, T. E., Siegfried, J. M., Kamens, J., ... & Grandis, J. R. (2004). SRC family kinases mediate epidermal growth factor receptor ligand cleavage, proliferation, and invasion of head and neck cancer cells. *Cancer research*, *64*(17), 6166-6173.
49. Parekh, R. U., & Sriramula, S. (2020). Activation of kinin B1R upregulates ADAM17 and results in ACE2 shedding in neurons. *International Journal of Molecular Sciences*, *22*(1), 145.
50. Slack, B. E., Ma, L. K., & Seah, C. C. (2001). Constitutive shedding of the amyloid precursor protein ectodomain is up-regulated by tumour necrosis factor-α converting enzyme. *Biochemical Journal*, *357*(3), 787-794.
51. Yang, Y., Wang, Y., Zeng, X., Ma, X. J., Zhao, Y., Qiao, J., ... & Wang, Y. L. (2012). Self-control of HGF regulation on human trophoblast cell invasion via enhancing c-Met receptor shedding by ADAM10 and ADAM17. *The Journal of Clinical Endocrinology & Metabolism*, *97*(8), E1390-E1401.
52. Fan, D., Takawale, A., Shen, M., Samokhvalov, V., Basu, R., Patel, V., ... & Kassiri, Z. (2016). A Disintegrin and Metalloprotease-17 Regulates Pressure Overload–Induced Myocardial Hypertrophy and Dysfunction Through Proteolytic Processing of Integrin β1. *Hypertension*, *68*(4), 937-948.
53. Althoff, K., Reddy, P., Voltz, N., Rose-John, S., & Müllberg, J. (2000). Shedding of interleukin-6 receptor and tumor necrosis factor α: Contribution of the stalk sequence to the cleavage pattern of transmembrane proteins. *European journal of biochemistry*, *267*(9), 2624-2631.
54. Sammel, M., Peters, F., Lokau, J., Scharfenberg, F., Werny, L., Linder, S., ... & Becker-Pauly, C. (2019). Differences in Shedding of the Interleukin-11 Receptor by the Proteases ADAM9, ADAM10, ADAM17, Meprin α, Meprin β and MT1-MMP. *International journal of molecular sciences*, *20*(15), 3677.
55. Müller, M., Saunders, C., Senftleben, A., Heidbuechel, J. P., Halwachs, B., Bolik, J., ... & Schmidt-Arras, D. (2022). Tetraspanin 8 subfamily members regulate substrate-specificity of a disintegrin and metalloprotease 17. *Cells*, *11*(17), 2683.
56. Yashiro, M., Ohya, M., Mima, T., Nakashima, Y., Kawakami, K., Sonou, T., ... & Shigematsu, T. (2020). Excessive ADAM17 activation occurs in uremic patients and may contribute to their immunocompromised status. *Immunity, Inflammation and Disease*, *8*(2), 228-235.

57. Weskamp, G., Mendelson, K., Swendeman, S., Le Gall, S., Ma, Y., Lyman, S., ... & Blobel, C. P. (2010). Pathological neovascularization is reduced by inactivation of ADAM17 in endothelial cells but not in pericytes. *Circulation research*, *106*(5), 932-940.
58. Vidlickova, I., Dequiedt, F., Jelenska, L., Sedlakova, O., Pastorek, M., Stuchlik, S., ... & Pastorekova, S. (2016). Apoptosis-induced ectodomain shedding of hypoxia-regulated carbonic anhydrase IX from tumor cells: a double-edged response to chemotherapy. *BMC cancer*, *16*, 1-13.
59. Peng, M., Guo, S., Yin, N., Xue, J., Shen, L., Zhao, Q., & Zhang, W. (2010). Ectodomain shedding of Fcα receptor is mediated by ADAM10 and ADAM17. *Immunology*, *130*(1), 83-91.
60. Lattenist, L., Ochodnický, P., Ahdi, M., Claessen, N., Leemans, J. C., Satchell, S. C., ... & Roelofs, J. J. T. H. (2016). Renal endothelial protein C receptor expression and shedding during diabetic nephropathy. *Journal of Thrombosis and Haemostasis*, *14*(6), 1171-1182.
61. Bender, M., Hofmann, S., Stegner, D., Chalaris, A., Bösl, M., Braun, A., ... & Nieswandt, B. (2010). Differentially regulated GPVI ectodomain shedding by multiple platelet–expressed proteinases. *Blood, The Journal of the American Society of Hematology*, *116*(17), 3347-3355.
62. Schantl, J. A., Roza, M., Van Kerkhof, P., & Strous, G. J. (2004). The growth hormone receptor interacts with its sheddase, the tumour necrosis factor-alpha-converting enzyme (TACE). *Biochemical Journal*, *377*(2), 379-384.
63. Wei, G., Luo, Q., Wang, X., Wu, X., Xu, M., Ding, N., ... & Qiao, J. (2019). Increased GPIbα shedding from platelets treated with immune thrombocytopenia plasma. *International Immunopharmacology*, *66*, 91-98.
64. Brou, C., Logeat, F., Gupta, N., Bessia, C., LeBail, O., Doedens, J. R., ... & Israël, A. (2000). A novel proteolytic cleavage involved in Notch signaling: the role of the disintegrin-metalloprotease TACE. *Molecular cell*, *5*(2), 207-216.
65. Keisuke Miyake. (2018). *Activation of Transforming Growth Factor Beta 1 Signaling in Gastric Cancer-associated Fibroblasts Increases Their Motility, via Expression of Rhomboid 5 Homolog 2, and Ability to Induce Invasiveness of Gastric Cancer Cells* (Doctoral dissertation, Kumamoto University) .

66. Bolik, J., Krause, F., Stevanovic, M., Gandraß, M., Thomsen, I., Schacht, S. S., ... & Schmidt-Arras, D. (2021). Inhibition of ADAM17 impairs endothelial cell necroptosis and blocks metastasis. *Journal of experimental medicine*, *219*(1), e20201039.
67. Stoyanova, T., Goldstein, A. S., Cai, H., Drake, J. M., Huang, J., & Witte, O. N. (2012). Regulated proteolysis of Trop2 drives epithelial hyperplasia and stem cell self-renewal via β-catenin signaling. *Genes & development*, *26*(20), 2271-2285.
68. Jin, Y., Liu, Y., Lin, Q., Li, J., Druso, J. E., Antonyak, M. A., ... & Peng, X. (2013). Deletion of Cdc42 enhances ADAM17-mediated vascular endothelial growth factor receptor 2 shedding and impairs vascular endothelial cell survival and vasculogenesis. *Molecular and cellular biology*, *33*(21), 4181-4197.
69. Ma, X., Takahashi, Y., Wu, W., Liang, W., Chen, J., Chakraborty, D., ... & Ma, J. X. (2021). ADAM17 mediates ectodomain shedding of the soluble VLDL receptor fragment in the retinal epithelium. *Journal of Biological Chemistry*, *297*(4).
70. Liu, Q., Zhang, J., Tran, H., Verbeek, M. M., Reiss, K., Estus, S., & Bu, G. (2009). LRP1 shedding in human brain: roles of ADAM10 and ADAM17. *Molecular neurodegeneration*, *4*, 1-7.
71. Sommer, C., Lee, S., Gulseth, H. L., Jensen, J., Drevon, C. A., & Birkeland, K. I. (2018). Soluble leptin receptor predicts insulin sensitivity and correlates with upregulation of metabolic pathways in men. *The Journal of Clinical Endocrinology & Metabolism*, *103*(3), 1024-1032.
72. Tian, Y., Fopiano, K. A., Buncha, V., Lang, L., Rudic, R. D., Filosa, J. A., ... & Bagi, Z. (2022). Aging-induced impaired endothelial wall shear stress mechanosensing causes arterial remodeling via JAM-A/F11R shedding by ADAM17. *GeroScience*, 1-21.
73. Tüshaus, J., Müller, S. A., Shrouder, J., Arends, M., Simons, M., Plesnila, N., ... & Lichtenthaler, S. F. (2021). The pseudoprotease iRhom1 controls ectodomain shedding of membrane proteins in the nervous system. *FASEB journal: official publication of the Federation of American Societies for Experimental Biology*, *35*(11), e21962.
74. Zhang, Y., Wang, Y., Zhou, D., Zhang, L. S., Deng, F. X., Shu, S., ... & Yuan, Z. Y. (2019). Angiotensin II deteriorates advanced atherosclerosis by promoting MerTK cleavage and impairing efferocytosis through the AT1R/ROS/p38 MAPK/ADAM17 pathway. *American Journal of Physiology-Cell Physiology*, *317*(4), C776-C787.
75. Peschon, J. J., Slack, J. L., Reddy, P., Stocking, K. L., Sunnarborg, S. W., Lee, D. C., ... & Black, R. A. (1998). An essential role for ectodomain shedding in mammalian development. *Science*, *282*(5392), 1281-1284.

76. Kapp, K., Siemens, J., Häring, H. U., & Lammers, R. (2012). Proteolytic processing of the protein tyrosine phosphatase α extracellular domain is mediated by ADAM17/TACE. *European journal of cell biology*, *91*(9), 687-693.
77. Bell, J. H., Herrera, A. H., Li, Y., & Walcheck, B. (2007). Role of ADAM17 in the ectodomain shedding of TNF-α and its receptors by neutrophils and macrophages. *Journal of Leucocyte Biology*, *82*(1), 173-176.
78. Young, J., Yu, X., Wolslegel, K., Nguyen, A., Kung, C., Chiang, E., ... & Grogan, J. L. (2010). Lymphotoxin-αβ heterotrimers are cleaved by metalloproteinases and contribute to synovitis in rheumatoid arthritis. *Cytokine*, *51*(1), 78-86.
79. Arai, J., Goto, K., Tanoue, Y., Ito, S., Muroyama, R., Matsubara, Y., ... & Kato, N. (2018). Enzymatic inhibition of MICA sheddase ADAM17 by lomofungin in hepatocellular carcinoma cells. *International Journal of Cancer*, *143*(10), 2575-2583.
80. Boutet, P., Agüera-González, S., Atkinson, S., Pennington, C. J., Edwards, D. R., Murphy, G., ... & Valés-Gómez, M. (2009). Cutting edge: the metalloproteinase ADAM17/TNF-α-converting enzyme regulates proteolytic shedding of the MHC class I-related chain B protein. *The Journal of Immunology*, *182*(1), 49-53.
81. Kanzaki, H., Shinohara, F., Suzuki, M., Wada, S., Miyamoto, Y., Yamaguchi, Y., ... & Nakamura, Y. (2016). A-disintegrin and metalloproteinase (ADAM) 17 enzymatically degrades interferon-gamma. *Scientific reports*, *6*(1), 32259.
82. Tang, J., Frey, J. M., Wilson, C. L., Moncada-Pazos, A., Levet, C., Freeman, M., ... & Bornfeldt, K. E. (2018). Neutrophil and macrophage cell surface colony-stimulating factor 1 shed by ADAM17 drives mouse macrophage proliferation in acute and chronic inflammation. *Molecular and cellular biology*, *38*(17), e00103-18.
83. Garton, K. J., Gough, P. J., Blobel, C. P., Murphy, G., Greaves, D. R., Dempsey, P. J., & Raines, E. W. (2001). Tumor necrosis factor-α-converting enzyme (ADAM17) mediates the cleavage and shedding of fractalkine (CX3CL1). *Journal of Biological Chemistry*, *276*(41), 37993-38001.
84. Kawaguchi, N., Horiuchi, K., Becherer, J. D., Toyama, Y., Besmer, P., & Blobel, C. P. (2007). Different ADAMs have distinct influences on Kit ligand processing: phorbol-ester-stimulated ectodomain shedding of Kitl1 by ADAM17 is reduced by ADAM19. Journal of cell science, 120(6), 943-952.
85. Li, N., Wang, Y., Forbes, K., Vignali, K. M., Heale, B. S., Saftig, P., ... & Vignali, D. A. (2007). Metalloproteases regulate T-cell proliferation and effector function via LAG-3. *The EMBO journal*, *26*(2), 494-504.

86. Tsakadze, N. L., Sithu, S. D., Sen, U., English, W. R., Murphy, G., & D'Souza, S. E. (2006). Tumor necrosis factor-α-converting enzyme (TACE/ADAM-17) mediates the ectodomain cleavage of intercellular adhesion molecule-1 (ICAM-1). *Journal of Biological Chemistry*, *281*(6), 3157-3164.
87. Maretzky, T., Schulte, M., Ludwig, A., Rose-John, S., Blobel, C., Hartmann, D., ... & Reiss, K. (2005). L1 is sequentially processed by two differently activated metalloproteases and presenilin/γ-secretase and regulates neural cell adhesion, cell migration, and neurite outgrowth. *Molecular and cellular biology*, *25*(20), 9040-9053.
88. Kalus, I., Bormann, U., Mzoughi, M., Schachner, M., & Kleene, R. (2006). Proteolytic cleavage of the neural cell adhesion molecule by ADAM17/TACE is involved in neurite outgrowth. *Journal of neurochemistry*, *98*(1), 78-88.
89. Garton, K. J., Gough, P. J., Philalay, J., Wille, P. T., Blobel, C. P., Whitehead, R. H., ... & Raines, E. W. (2003). Stimulated shedding of vascular cell adhesion molecule 1 (VCAM-1) is mediated by tumor necrosis factor-α-converting enzyme (ADAM 17). *Journal of Biological Chemistry*, *278*(39), 37459-37464.
90. Maetzel, D., Denzel, S., Mack, B., Canis, M., Went, P., Benk, M., ... & Gires, O. (2009). Nuclear signalling by tumour-associated antigen EpCAM. *Nature cell biology*, *11*(2), 162-171.
91. Iwagishi, R., Tanaka, R., Seto, M., Takagi, T., Norioka, N., Ueyama, T., ... & Shirakabe, K. (2020). Negatively charged amino acids in the stalk region of membrane proteins reduce ectodomain shedding. *Journal of Biological Chemistry*, *295*(35), 12343-12352.
92. Ma, Z., Gao, Y., Liu, W., Zheng, L., Jin, B., Duan, B., ... & Li, L. (2020). CD82 Suppresses ADAM17-Dependent E-Cadherin Cleavage and Cell Migration in Prostate Cancer. *Disease Markers*, *2020*(1), 8899924.
93. Li, Y., Brazzell, J., Herrera, A., & Walcheck, B. (2006). ADAM17 deficiency by mature neutrophils has differential effects on L-selectin shedding. *Blood*, *108*(7), 2275-2279.
94. Nanba, D., Toki, F., Asakawa, K., Matsumura, H., Shiraishi, K., Sayama, K., ... & Nishimura, E. K. (2021). EGFR-mediated epidermal stem cell motility drives skin regeneration through COL17A1 proteolysis. *Journal of Cell Biology*, *220*(11), e202012073.
95. Bech-Serra, J. J., Santiago-Josefat, B., Esselens, C., Saftig, P., Baselga, J., Arribas, J., & Canals, F. (2006). Proteomic identification of desmoglein 2 and activated leukocyte cell adhesion molecule as substrates of ADAM17 and ADAM10 by difference gel electrophoresis. *Molecular and cellular biology*.

96. Gnosa, S. P., Blasco, L. P., Piotrowski, K. B., Freiberg, M. L., Savickas, S., Madsen, D. H., ... & Kveiborg, M. (2022). ADAM17-mediated EGFR ligand shedding directs macrophage-promoted cancer cell invasion. *JCI insight*, *7*(18).
97. Sahin, U., & Blobel, C. P. (2007). Ectodomain shedding of the EGF-receptor ligand epigen is mediated by ADAM17. *FEBS letters*, *581*(1), 41-44.
98. Sahin, U., Weskamp, G., Kelly, K., Zhou, H. M., Higashiyama, S., Peschon, J., ... & Blobel, C. P. (2004). Distinct roles for ADAM10 and ADAM17 in ectodomain shedding of six EGFR ligands. *The Journal of cell biology*, *164*(5), 769-779.
99. Peschon, J. J., Slack, J. L., Reddy, P., Stocking, K. L., Sunnarborg, S. W., Lee, D. C., ... & Black, R. A. (1998). An essential role for ectodomain shedding in mammalian development. *Science*, *282*(5392), 1281-1284.
100. Shin, D. H., Kim, S. H., Choi, M., Bae, Y. K., Han, C., Choi, B. K., ... & Han, J. Y. (2022). Oncogenic KRAS promotes growth of lung cancer cells expressing SLC3A2-NRG1 fusion via ADAM17-mediated shedding of NRG1. *Oncogene*, *41*(2), 280-292.
101. Murthy, A., Defamie, V., Smookler, D. S., Di Grappa, M. A., Horiuchi, K., Federici, M., ... & Khokha, R. (2010). Ectodomain shedding of EGFR ligands and TNFR1 dictates hepatocyte apoptosis during fulminant hepatitis in mice. *The Journal of clinical investigation*, *120*(8), 2731-2744.
102. Elahi, A., Ajidahun, A., Hendrick, L., Getun, I., Humphries, L. A., Hernandez, J., & Shibata, D. (2020). Hpp1 ectodomain shedding is mediated by Adam17 and is necessary for tumor suppression in colon cancer. *Journal of Surgical Research*, *254*, 183-190.
103. Rhee, M., Kim, J. W., Lee, M. W., Yoon, K. H., & Lee, S. H. (2019). Preadipocyte factor 1 regulates adipose tissue browning via TNF-α-converting enzyme-mediated cleavage. *Metabolism*, *101*, 153977.
104. Chen, C. D., Podvin, S., Gillespie, E., Leeman, S. E., & Abraham, C. R. (2007). Insulin stimulates the cleavage and release of the extracellular domain of Klotho by ADAM10 and ADAM17. *Proceedings of the National Academy of Sciences*, *104*(50), 19796-19801.
105. Hosur, V., Farley, M. L., Burzenski, L. M., Shultz, L. D., & Wiles, M. V. (2018). ADAM17 is essential for ectodomain shedding of the EGF-receptor ligand amphiregulin. *FEBS Open Bio*, *8*(4), 702-710.

106. Zou, Z., Li, L., Li, Q., Zhao, P., Zhang, K., Liu, C., ... & Huang, Q. (2022). The role of S100B/RAGE-enhanced ADAM17 activation in endothelial glycocalyx shedding after traumatic brain injury. *Journal of neuroinflammation*, *19*(1), 46.

107. Motani, K., & Kosako, H. (2018). Activation of stimulator of interferon genes (STING) induces ADAM17-mediated shedding of the immune semaphorin SEMA4D. *Journal of Biological Chemistry*, *293*(20), 7717-7726.

108. Malapeira, J., Esselens, C., Bech-Serra, J. J., Canals, F., & Arribas, J. (2011). ADAM17 (TACE) regulates TGFβ signaling through the cleavage of vasorin. *Oncogene*, *30*(16), 1912-1922.

109. Maretzky, T., Evers, A., Zhou, W., Swendeman, S. L., Wong, P. M., Rafii, S., ... & Blobel, C. P. (2011). Migration of growth factor-stimulated epithelial and endothelial cells depends on EGFR transactivation by ADAM17. *Nature communications*, *2*(1), 229.

110. Blackhall, F., Ranson, M., & Thatcher, N. (2006). Where next for gefitinib in patients with lung cancer?. *The lancet oncology*, *7*(6), 499-507. Blackhall, F., Ranson, M., & Thatcher, N. (2006). Where next for gefitinib in patients with lung cancer?. *The lancet oncology*, *7*(6), 499-507.

111. Saad, M. I., Alhayyani, S., McLeod, L., Yu, L., Alanazi, M., Deswaerte, V., ... & Jenkins, B. J. (2019). ADAM 17 selectively activates the IL-6 trans-signaling/ERK MAPK axis in KRAS-addicted lung cancer. *EMBO molecular medicine*, *11*(4), e9976.

112. Ni, S. S., Zhang, J., Zhao, W. L., Dong, X. C., & Wang, J. L. (2013). ADAM17 is overexpressed in non-small cell lung cancer and its expression correlates with poor patient survival. *Tumor Biology*, *34*, 1813-1818.

113. Gatzemeier U, Groth G, Butts C, Van Zandwijk N, Shepherd F, Ardizzoni A, Barton C, Ghahramani P, Hirsh V. Randomized phase II trial of gemcitabine-cisplatin with or without trastuzumab in HER2-positive non-small-cell lung cancer. Ann Oncol. 2004 Jan;15(1):19-27. doi: 10.1093/annonc/mdh031. PMID: 14679114

114. Kim, K., Chie, E. K., Han, W., Noh, D. Y., Oh, D. Y., Im, S. A., ... & Ha, S. W. (2010). Prognostic factors affecting the outcome of salvage radiotherapy for isolated locoregional recurrence after mastectomy. *American journal of clinical oncology*, *33*(1), 23-27.

115. Kenny, P. A. (2007). TACE: a new target in epidermal growth factor receptor dependent tumors. *Differentiation*, *75*(9), 800-808.

116. Curry, J. M., Eubank, T. D., Roberts, R. D., Wang, Y., Pore, N., Maity, A., & Marsh, C. B. (2008). M-CSF signals through the MAPK/ERK pathway via Sp1 to induce VEGF production and induces angiogenesis in vivo. *PloS one*, *3*(10), e3405.

117. McGowan, P. M., Ryan, B. M., Hill, A. D., McDermott, E., O'Higgins, N., & Duffy, M. J. (2007). ADAM-17 expression in breast cancer correlates with variables of tumor progression. *Clinical cancer research*, *13*(8), 2335-2343.

118. Ni, P., Yu, M., Zhang, R., He, M., Wang, H., Chen, S., & Duan, G. (2020). Prognostic significance of ADAM17 for gastric cancer survival: a meta-analysis. *Medicina*, *56*(7), 322.

119. Xu, M., Zhou, H., Zhang, C., He, J., Wei, H., Zhou, M., ... & Gong, A. (2016). ADAM17 promotes epithelial-mesenchymal transition via TGF-β/Smad pathway in gastric carcinoma cells. *International journal of oncology*, *49*(6), 2520-2528.

120. Fabbi, M., Costa, D., Russo, D., Arenare, L., Gaggero, G., Signoriello, S., ... & Pignata, S. (2022). Analysis of a disintegrin and metalloprotease 17 (Adam17) expression as a prognostic marker in ovarian cancer patients undergoing first-line treatment plus bevacizumab. *Diagnostics*, *12*(9), 2118.

121. Hedemann, N., Rogmans, C., Sebens, S., Wesch, D., Reichert, M., Schmidt-Arras, D., ... & Bauerschlag, D. O. (2018). ADAM17 inhibition enhances platinum efficiency in ovarian cancer. *Oncotarget*, *9*(22), 16043.

122. Saha, S. K., Choi, H. Y., Yang, G. M., Biswas, P. K., Kim, K., Kang, G. H., ... & Cho, S. G. (2020). GPR50 promotes hepatocellular carcinoma progression via the notch signaling pathway through direct interaction with ADAM17. *Molecular Therapy-Oncolytics*, *17*, 332-349.

123. Fridman, J. S., Caulder, E., Hansbury, M., Liu, X., Yang, G., Wang, Q., ... & Vaddi, K. (2007). Selective inhibition of ADAM metalloproteases as a novel approach for modulating ErbB pathways in cancer. *Clinical cancer research*, *13*(6), 1892-1902.

124. Abdel-Nasser, A. M., Rasker, J. J., & Vaikenburg, H. A. (1997, October). Epidemiological and clinical aspects relating to the variability of rheumatoid arthritis. In *Seminars in arthritis and rheumatism* (Vol. 27, No. 2, pp. 123-140). WB Saunders.

125. Majithia, V., & Geraci, S. A. (2007). Rheumatoid arthritis: diagnosis and management. *The American journal of medicine*, *120*(11), 936-939.

126. Firestein, G. S. (2003). Evolving concepts of rheumatoid arthritis. *Nature*, *423*(6937), 356-361.

127. Patel, I. R., Attur, M. G., Patel, R. N., Stuchin, S. A., Abagyan, R. A., Abramson, S. B., & Amin, A. R. (1998). TNF-α convertase enzyme from human arthritis-affected cartilage: isolation of cDNA by differential display, expression of the active enzyme, and regulation of TNF-α. *The Journal of Immunology*, *160*(9), 4570-4579.

128. Qian, M., Bai, S. A., Brogdon, B., Wu, J. T., Covington, M. B., Vaddi, K., ... & Christ, D. D. (2007). Pharmacokinetics and pharmacodynamics of DPC 333, a potent and selective inhibitor of tumor necrosis factor-α converting enzyme in rodents, dogs, chimpanzees and humans. *Drug Metabolism and Disposition*.

129. Yang, C. Y., Chanalaris, A., & Troeberg, L. (2017). ADAMTS and ADAM metalloproteinases in osteoarthritis–looking beyond the 'usual suspects'. *Osteoarthritis and cartilage*, *25*(7), 1000-1009.

130. Saklatvala, J. (1986). Tumour necrosis factor α stimulates resorption and inhibits synthesis of proteoglycan in cartilage. *Nature*, *322*(6079), 547-549.

131. Reboul, P., Pelletier, J. P., Tardif, G., Cloutier, J. M., & Martel-Pelletier, J. (1996). The new collagenase, collagenase-3, is expressed and synthesized by human chondrocytes but not by synoviocytes. A role in osteoarthritis. *The Journal of clinical investigation*, *97*(9), 2011-2019.

132. Philp, A. M., Davis, E. T., & Jones, S. W. (2017). Developing anti-inflammatory therapeutics for patients with osteoarthritis. *Rheumatology*, *56*(6), 869-881.

133. Mohd Nor, N. S., Al-Khateeb, A. M., Chua, Y. A., Mohd Kasim, N. A., & Mohd Nawawi, H. (2019). Heterozygous familial hypercholesterolaemia in a pair of identical twins: a case report and updated review. *BMC pediatrics*, *19*, 1-8.

134. Rizza, S., Copetti, M., Cardellini, M., Menghini, R., Pecchioli, C., Luzi, A., ... & Federici, M. (2015). A score including ADAM17 substrates correlates to recurring cardiovascular event in subjects with atherosclerosis. *Atherosclerosis*, *239*(2), 459-464.

135. Ruparelia, N., & Choudhury, R. (2020). Inflammation and atherosclerosis: what is on the horizon?. *Heart*, *106*(1), 80-85.

136. Liao, J., An, X., Yang, X., Lin, Q. Y., Liu, S., Xie, Y., ... & Li, H. H. (2020). Deficiency of LMP10 attenuates diet-induced atherosclerosis by inhibiting macrophage polarization and inflammation in apolipoprotein E deficient mice. *Frontiers in cell and developmental biology*, *8*, 592048.

137. Rosen, M. J., Dhawan, A., & Saeed, S. A. (2015). Inflammatory bowel disease in children and adolescents. *JAMA pediatrics*, *169*(11), 1053-1060.

138. Bzowska, M., Jura, N., Lassak, A., Black, R. A., & Bereta, J. (2004). Tumour necrosis factor-α stimulates expression of TNF-α converting enzyme in endothelial cells. *European Journal of Biochemistry*, *271*(13), 2808-2820.

139. Kolios, G., Valatas, V., & Ward, S. G. (2004). Nitric oxide in inflammatory bowel disease: a universal messenger in an unsolved puzzle. *Immunology*, *113*(4), 427-437.

140. Colon, A. L., Menchen, L. A., Hurtado, O., De Cristobal, J., Lizasoain, I., Leza, J. C., ... & Moro, M. A. (2001). Implication of TNF-α convertase (TACE/ADAM17) in inducible nitric oxide synthase expression and inflammation in an experimental model of colitis. *Cytokine*, *16*(6), 220-226.

141. Stelzma, RA, Schnitzlein, HN, & Murllagh, FR (1995). An English translation of Alzheimer's 1907 Paper, on a peculiar description of the cerebral cortex. *Clinical anatomy*, *8*, 429-431.

142. Rubio-Perez, J. M., & Morillas-Ruiz, J. M. (2012). A review: inflammatory process in Alzheimer′ s disease, role of cytokines. *The Scientific World Journal*, *2012*(1), 756357.

143. Ballard, C., Gauthier, S., Corbett, A., Brayne, C., Aarsland, D., & Jones, E. (2011). Alzheimer's disease. *the Lancet*, *377*(9770), 1019-1031.

144. Vassar, R., Bennett, B. D., Babu-Khan, S., Kahn, S., Mendiaz, E. A., Denis, P., ... & Citron, M. (1999). β-Secretase cleavage of Alzheimer's amyloid precursor protein by the transmembrane aspartic protease BACE. *science*, *286*(5440), 735-741.

145. Colombo, A., Wang, H., Kuhn, P. H., Page, R., Kremmer, E., Dempsey, P. J., ... & Lichtenthaler, S. F. (2013). Constitutive α-and β-secretase cleavages of the amyloid precursor protein are partially coupled in neurons, but not in frequently used cell lines. *Neurobiology of disease*, *49*, 137-147.

146. Kuhn, P. H., Wang, H., Dislich, B., Colombo, A., Zeitschel, U., Ellwart, J. W., ... & Lichtenthaler, S. F. (2010). ADAM10 is the physiologically relevant, constitutive α-secretase of the amyloid precursor protein in primary neurons. *The EMBO journal*, *29*(17), 3020-3032.

147. Buxbaum, J. D., Liu, K. N., Luo, Y., Slack, J. L., Stocking, K. L., Peschon, J. J., ... & Black, R. A. (1998). Evidence that tumor necrosis factor α converting enzyme is involved in regulated α-secretase cleavage of the Alzheimer amyloid protein precursor. *Journal of Biological Chemistry*, *273*(43), 27765-27767.

148. Akiyama, H., Barger, S., Barnum, S., Bradt, B., Bauer, J., Cole, G. M., ... & Wyss–Coray, T. (2000). Inflammation and Alzheimer's disease. *Neurobiology of aging*, *21*(3), 383-421.

149. Kemp, S. V., Polkey, M. I., & Shah, P. L. (2009). The epidemiology, etiology, clinical features, and natural history of emphysema. *Thoracic surgery clinics*, *19*(2), 149-158.

150. Olin, J. T., & Wechsler, M. E. (2014). Asthma: pathogenesis and novel drugs for treatment. *Bmj*, *349*.

151. Stolarczyk, M., Amatngalim, G. D., Yu, X., Veltman, M., Hiemstra, P. S., & Scholte, B. J. (2016). ADAM 17 and EGFR regulate IL-6 receptor and amphiregulin mRNA expression and release in cigarette smoke-exposed primary bronchial epithelial cells from patients with chronic obstructive pulmonary disease (COPD). *Physiological reports*, *4*(16), e12878.

152. Gómez, M. I., Sokol, S. H., Muir, A. B., Soong, G., Bastien, J., & Prince, A. S. (2005). Bacterial induction of TNF-α converting enzyme expression and IL-6 receptor α shedding regulates airway inflammatory signaling. *The Journal of Immunology*, *175*(3), 1930-1936.

153. Lemjabbar-Alaoui, H., Sidhu, S. S., Mengistab, A., Gallup, M., & Basbaum, C. (2011). TACE/ADAM-17 phosphorylation by PKC-epsilon mediates premalignant changes in tobacco smoke-exposed lung cells. *PloS one*, *6*(3), e17489.

154. Brightling, C., Berry, M., & Amrani, Y. (2008). Targeting TNF-α: a novel therapeutic approach for asthma. *Journal of Allergy and Clinical Immunology*, *121*(1), 5-10.

155. Shi, W., Chen, H., Sun, J., Buckley, S., Zhao, J., Anderson, K. D., ... & Warburton, D. (2003). TACE is required for fetal murine cardiac development and modeling. *Developmental biology*, *261*(2), 371-380.

156. Shimoda, Y., Satoh, M., Nakamura, M., Akatsu, T., & Hiramori, K. (2005). Activated tumour necrosis factor-α shedding process is associated with in-hospital complication in patients with acute myocardial infarction. *Clinical science*, *108*(4), 339-347.

157. Takayanagi, T., Kawai, T., Forrester, S. J., Obama, T., Tsuji, T., Fukuda, Y., ... & Eguchi, S. (2015). Role of epidermal growth factor receptor and endoplasmic reticulum stress in vascular remodeling induced by angiotensin II. *Hypertension*, *65*(6), 1349-1355.

158. Pérez-Vizcaíno, F. (2020). Lung ACE2 and ADAM17 in pulmonary arterial hypertension: Implications for COVID-19?. *The Journal of Heart and Lung Transplantation*, *39*(10), 1167-1169.

159. Spin, J. M., Hsu, M., Azuma, J., Tedesco, M. M., Deng, A., Dyer, J. S., ... & Tsao, P. S. (2011). Transcriptional profiling and network analysis of the murine angiotensin II-induced abdominal aortic aneurysm. *Physiological genomics*, *43*(17), 993-1003.

160. Kaneko, H., Anzai, T., Horiuchi, K., Kohno, T., Nagai, T., Anzai, A., ... & Fukuda, K. (2011). Tumor necrosis factor-α converting enzyme is a key mediator of abdominal aortic aneurysm development. *Atherosclerosis*, *218*(2), 470-478.

161. Lautrette, A., Li, S., Alili, R., Sunnarborg, S. W., Burtin, M., Lee, D. C., ... & Terzi, F. (2005). Angiotensin II and EGF receptor cross-talk in chronic kidney diseases: a new therapeutic approach. *Nature medicine*, *11*(8), 867-874.

162. Shah, B. H., & Catt, K. J. (2006). TACE-dependent EGF receptor activation in angiotensin-II-induced kidney disease. *Trends in pharmacological sciences*, *27*(5), 235-237.

163. Voros, G., Maquoi, E., Collen, D., & Lijnen, H. R. (2003). Differential expression of plasminogen activator inhibitor-1, tumor necrosis factor-α, TNF-α converting enzyme and ADAMTS family members in murine fat territories. *Biochimica et Biophysica Acta (BBA)-Gene Structure and Expression*, *1625*(1), 36-42.

164. Kaneko, H., Anzai, T., Horiuchi, K., Morimoto, K., Anzai, A., Nagai, T., ... & Fukuda, K. (2011). Tumor necrosis factor-α converting enzyme inactivation ameliorates high-fat diet-induced insulin resistance and altered energy homeostasis. *Circulation Journal*, *75*(10), 2482-2490.

165. Moriyama, H., Tsukida, T., Inoue, Y., Yokota, K., Yoshino, K., Kondo, H., ... & Nishimura, S. I. (2004). Azasugar-based MMP/ADAM inhibitors as antipsoriatic agents. *Journal of medicinal chemistry*, *47*(8), 1930-1938.

166. Kieseier, B. C., Pischel, H., Neuen-Jacob, E., Tourtellotte, W. W., & Hartung, H. P. (2003). ADAM-10 and ADAM-17 in the inflamed human CNS. *Glia*, *42*(4), 398-405.

167. Teles, R. M., Antunes, S. L., Jardim, M. R., Oliveira, A. L., Nery, J. A., Sales, A. M., ... & Sarno, E. N. (2007). Expression of metalloproteinases (MMP-2, MMP-9, and TACE) and TNF-α in the nerves of leprosy patients. *Journal of the Peripheral Nervous System*, *12*(3), 195-204.

168. Nuti, E., Casalini, F., Santamaria, S., Fabbi, M., Carbotti, G., Ferrini, S., ... & Rossello, A. (2013). Selective arylsulfonamide inhibitors of ADAM-17: hit optimization and activity in ovarian cancer cell models. *Journal of medicinal chemistry*, *56*(20), 8089-8103.

169. Cuffaro, D., Camodeca, C., Tuccinardi, T., Ciccone, L., Bartsch, J. W., Kellermann, T., ... & Rossello, A. (2021). Discovery of Dimeric Arylsulfonamides as Potent ADAM8 Inhibitors. *ACS Medicinal Chemistry Letters*, *12*(11), 1787-1793.

170. Rosner, K. E., Guo, Z., Orth, P., Shipps Jr, G. W., Belanger, D. B., Chan, T. Y., ... & Strickland, C. O. (2010). The discovery of novel tartrate-based TNF-α converting enzyme (TACE) inhibitors. *Bioorganic & medicinal chemistry letters*, *20*(3), 1189-1193.

171. Yu, W., Guo, Z., Orth, P., Madison, V., Chen, L., Dai, C., ... & Zhou, G. (2010). Discovery and SAR of hydantoin TACE inhibitors. Bioorganic & Medicinal Chemistry Letters, 20(6), 1877-1880.

172. Yu, W., Tong, L., Kim, S. H., Wong, M. K., Chen, L., Yang, D. Y., ... & Kozlowski, J. A. (2010). Biaryl substituted hydantoin compounds as TACE inhibitors. *Bioorganic & medicinal chemistry letters*, *20*(17), 5286-5289.

173. Pu, Y., Cao, D., Xie, C., Pei, H., Li, D., Tang, M., & Chen, L. (2015). Anti-arthritis effect of a novel quinazoline derivative through inhibiting production of TNF-α mediated by TNF-α converting enzyme in murine collagen-induced arthritis model. *Biochemical and Biophysical Research Communications*, *462*(4), 288-293.

174. Bandarage, U. K., Wang, T., Come, J. H., Perola, E., Wei, Y., & Rao, B. G. (2008). Novel thiol-based TACE inhibitors. Part 2: Rational design, synthesis, and SAR of thiol-containing aryl sulfones. *Bioorganic & medicinal chemistry letters*, *18*(1), 44-48.

175. Zhang, C., Lovering, F., Behnke, M., Zask, A., Sandanayaka, V., Sun, L., ... & Levin, J. I. (2009). Synthesis and activity of quinolinylmethyl P1′ α-sulfone piperidine hydroxamate inhibitors of TACE. *Bioorganic & medicinal chemistry letters*, *19*(13), 3445-3448.

176. Nelson, F. C., Santos, E. D., Levin, J. I., Chen, J. M., Skotnicki, J. S., DiJoseph, J. F., ... & Albright, J. D. (2002). Benzodiazepine inhibitors of the MMPs and TACE. *Bioorganic & medicinal chemistry letters*, *12*(20), 2867-2870.

177. Zask, A., Kaplan, J., Du, X., MacEwan, G., Sandanayaka, V., Eudy, N., ... & Skotnicki, J. (2005). Synthesis and SAR of diazepine and thiazepine TACE and MMP inhibitors. *Bioorganic & medicinal chemistry letters*, *15*(6), 1641-1645.

178. Lombart, H. G., Feyfant, E., Joseph-McCarthy, D., Huang, A., Lovering, F., Sun, L., ... & Levin, J. (2007). Design and synthesis of 3, 3-piperidine hydroxamate analogs as selective TACE inhibitors. *Bioorganic & medicinal chemistry letters*, *17*(15), 4333-4337.

179. Guo, Z., Orth, P., Wong, S. C., Lavey, B. J., Shih, N. Y., Niu, X., ... & Kozlowski, J. A. (2009). Discovery of novel spirocyclopropyl hydroxamate and carboxylate

compounds as TACE inhibitors. *Bioorganic & Medicinal Chemistry Letters*, *19*(1), 54-57.

180. Park, K., Aplasca, A., Du, M. T., Sun, L., Zhu, Y., Zhang, Y., & Levin, J. I. (2006). Design and synthesis of butynyloxyphenyl β-sulfone piperidine hydroxamates as TACE inhibitors. *Bioorganic & medicinal chemistry letters*, *16*(15), 3927-3931.
181. Pfizer limited. TACE inhibitors. EP 1104412; 2005
182. Pfizer Products. Selective inhibitors of aggrecanase in osteoarthritis treatment. EP 01081137; 2001
183. Wyeth Holding Corporation. Allenic aryl sulphonamide hydroxamic acid as MMP and TACE inhibitors. US7282496; 2007
184. Wyeth Holding Corporation. Preparation and use of acetylenic ortho-sulfonamido and phosphinic acid amido bicyclic heteroaryl hydroxamic acids as TACE Inhibitors. US6946473; 2005
185. Wyeth. Preparation and use of ortho-sulfonamido aryl hydoxamic acids as marix metalloproteinase inhibitors. US6465508; 2002
186. American Home Products Corporation. N-Hydroxy-2-(alkyl, aryl, or heteroaryl sufanyl, sulfinyl or sulfonyl)-3-substituted alkyl, aryl or heteroarylamides as matrix metalloproteinase inhibitors. US6331563; 2001
187. American Cynamid Company. Preparation and use of ortho-sulfonamido bicyclic heteroaryl hydroxamic acids as matrix metalloproteinase and TACE inhibitors. US6498167; 2002
188. American Cynamid Company. Acetylenic beta-sulfonamido and phosphinic acid amide hydroxamic acid TACE inhibitors. US6326516; 2001
189. Bristol-Myers Squibb Company. Barbituric acid derivatives as inhibitors of TNF-alpha converting enzyme (TACE) and/or matrix metalloproteinases. US7294624; 2007
190. Duan, J. J. W., Chen, L., Lu, Z., Jiang, B., Asakawa, N., Sheppeck II, J. E., ... & Decicco, C. P. (2007). Discovery of low nanomolar non-hydroxamate inhibitors of tumor necrosis factor-α converting enzyme (TACE). *Bioorganic & Medicinal Chemistry Letters*, *17*(1), 266-271.
191. Bristol-Myers Squibb Company. Hydantoins and related heterocycles as inhibitors of matrix metalloproteinases and/or TNF-alpha converting enzyme (TACE). US6906053; 2005
192. Sheppeck II, J. E., Gilmore, J. L., Yang, A., Chen, X. T., Xue, C. B., Roderick, J., ... & Duan, J. J. W. (2007). Discovery of novel hydantoins as selective non-hydroxamate

inhibitors of tumor necrosis factor-α converting enzyme (TACE). *Bioorganic & medicinal chemistry letters*, *17*(5), 1413-1417.

193. Bristol-Myers Squibb Pharma. Spiro-cyclic beta-amino acid derivatives as inhibitors of matrix metalloproteinases and/or TNF-alpha converting enzyme (TACE). US6720329; 2004
194. Darwin Discovery Ltd. Hydroxamic and carboxylic acid derivatives having MMP and TNF inhibitory activity. WO00187844; 2001
195. Glaxo Wellcome, Inc. Formamides as therapeutic agents. US6172064; 2001
196. Glaxo Wellcome, Inc. Formamide compounds as therapeutic agents. US6191150; 2001
197. Vertex Pharmaceuticals, Inc. Inhibitors of TACE. US7485664; 2009
198. Kaken Pharmaceutical Co., LtdReverse hydroxamic acid derivatives. US751114; 2009
199. Yang, J. S., Chun, K., Park, J. E., Cho, M., Seo, J., Song, D., ... & Han, G. (2010). Structure based optimization of chromen-based TNF-α converting enzyme (TACE) inhibitors on S1′ pocket and their quantitative structure–activity relationship (QSAR) study. *Bioorganic & medicinal chemistry*, *18*(24), 8618-8629.
200. Bahia, M. S., Gunda, S. K., Gade, S. R., Mahmood, S., Muttineni, R., & Silakari, O. (2011). Anthranilate derivatives as TACE inhibitors: docking based CoMFA and CoMSIA analyses. *Journal of molecular modeling*, *17*, 9-19.
201. National library of medicine; *www.clinicaltrials.gov.*
202. Drag, M., & Salvesen, G. S. (2010). Emerging principles in protease-based drug discovery. *Nature reviews Drug discovery*, *9*(9), 690-701.
203. López-Otín, C., & Bond, J. S. (2008). Proteases: multifunctional enzymes in life and disease. *Journal of Biological Chemistry*, *283*(45), 30433-30437.
204. Wolfsberg, T. G., Straight, P. D., Gerena, R. L., Huovila, A. P. J., Primakoff, P., Myles, D. G., & White, J. M. (1995). ADAM, a Widely Distributed and Developmentally Regulated Gene Family Encoding Membrane Proteins with A Disintegrin A nd M etalloprotease Domain. *Developmental biology*, *169*(1), 378-383.
205. Turk, B., Turk, D., & Turk, V. (2012). Protease signalling: the cutting edge. *The EMBO journal*, *31*(7), 1630-1643.
206. Edwards, D. R., Handsley, M. M., & Pennington, C. J. (2008). The ADAM metalloproteinases. *Molecular aspects of medicine*, *29*(5), 258-289.

207. López-Otín, C., & Bond, J. S. (2008). Proteases: multifunctional enzymes in life and disease. *Journal of Biological Chemistry*, *283*(45), 30433-30437.

208. Black, R. A., & White, J. M. (1998). ADAMs: focus on the protease domain. *Current opinion in cell biology*, *10*(5), 654-659.

209. Blobel, C. P. (2005). ADAMs: key components in EGFR signalling and development. *Nature reviews Molecular cell biology*, *6*(1), 32-43.

210. Gooz, M. (2010). ADAM-17: the enzyme that does it all. *Critical reviews in biochemistry and molecular biology*, *45*(2), 146-169.

211. Moss, M. L., & Minond, D. (2017). Recent advances in ADAM17 research: a promising target for cancer and inflammation. *Mediators of inflammation*, *2017*(1), 9673537.

212. Nuti, E., Casalini, F., Avramova, S. I., Santamaria, S., Fabbi, M., Ferrini, S., ... & Rossello, A. (2010). Potent arylsulfonamide inhibitors of tumor necrosis factor-α converting enzyme able to reduce activated leukocyte cell adhesion molecule shedding in cancer cell models. *Journal of medicinal chemistry*, *53*(6), 2622-2635.

213. Zhang, C., Lovering, F., Behnke, M., Zask, A., Sandanayaka, V., Sun, L., ... & Levin, J. I. (2009). Synthesis and activity of quinolinylmethyl P1′ α-sulfone piperidine hydroxamate inhibitors of TACE. *Bioorganic & medicinal chemistry letters*, *19*(13), 3445-3448.

214. Boiteau, J. G., Ouvry, G., Arlabosse, J. M., Astri, S., Beillard, A., Bhurruth-Alcor, Y., ... & Hennequin, L. F. (2018). Discovery and process development of a novel TACE inhibitor for the topical treatment of psoriasis. *Bioorganic & Medicinal Chemistry*, *26*(4), 945-956.

215. Ouvry, G., Berton, Y., Bhurruth-Alcor, Y., Bonnary, L., Bouix-Peter, C., Bouquet, K., ... & Hennequin, L. F. (2017). Identification of novel TACE inhibitors compatible with topical application. *Bioorganic & Medicinal Chemistry Letters*, *27*(8), 1848-1853.

216. Xue, C. B., Chen, X. T., He, X., Roderick, J., Corbett, R. L., Ghavimi, B., ... & Decicco, C. P. (2004). Synthesis and structure–activity relationship of a novel sulfone series of TNF-α converting enzyme inhibitors. *Bioorganic & medicinal chemistry letters*, *14*(17), 4453-4459.

217. Yap, C. W. (2011). PaDEL-descriptor: An open-source software to calculate molecular descriptors and fingerprints. *Journal of computational chemistry*, *32*(7), 1466-1474.

218. The simple, user-friendly and reliable online standalone tools freely available at http://teqip. jdvu.ac.in/QSAR_Tools/.

219. Discovery Studio 3.0 (DS 3.0). Accelrys Inc., CA, USA, 2015; software available at http://www.accelrys.com.

220. Statistica 7, StatSoft Inc. 2300 East 14th Street Tulsa, OK 74104, United States

221. Gettys, C. F., & Willke, T. A. (1969). The application of Bayes's theorem when the true data state is uncertain. *Organizational Behavior and Human Performance*, *4*(2), 125-141.

222. Banerjee, S., Amin, S. A., Adhikari, N., & Jha, T. (2020). Essential elements regulating HDAC8 inhibition: A classification based structural analysis and enzyme-inhibitor interaction study of hydroxamate based HDAC8 inhibitors. *Journal of Biomolecular Structure and Dynamics*, *38*(18), 5513-5525.

223. Strobl, C., Malley, J., & Tutz, G. (2009). An introduction to recursive partitioning: rationale, application, and characteristics of classification and regression trees, bagging, and random forests. *Psychological methods*, *14*(4), 323.

224. Yang, H., Li, J., Wu, Z., Li, W., Liu, G., & Tang, Y. (2017). Evaluation of different methods for identification of structural alerts using chemical ames mutagenicity data set as a benchmark. *Chemical Research in Toxicology*, *30*(6), 1355-1364.

225. Adhikari, N., Banerjee, S., Baidya, S. K., Ghosh, B., & Jha, T. (2021). Robust classification-based molecular modelling of diverse chemical entities as potential SARS-CoV-2 3CLpro inhibitors: Theoretical justification in light of experimental evidences. *SAR and QSAR in Environmental Research*, *32*(6), 473-493.

226. Campestre, C., Agamennone, M., Tortorella, P., Preziuso, S., Biasone, A., Gavuzzo, E., ... & Gallina, C. (2006). N-Hydroxyurea as zinc binding group in matrix metalloproteinase inhibition: mode of binding in a complex with MMP-8. *Bioorganic & medicinal chemistry letters*, *16*(1), 20-24.

227. Schrodinger Suite, Schrodinger LLC, New York, USA, 2019; software available at https://www.schrodinger.com

228. RCSB Protein Data Bank. https://www.rcsb.org/ as accessed in August 2023.

229. Todeschini, R., & Consonni, V. (2009). *Molecular descriptors for chemoinformatics: volume I: alphabetical listing/volume II: appendices, references*. John Wiley & Sons.

230. Banerjee, S., Baidya, S. K., Ghosh, B., Adhikari, N., & Jha, T. (2022). The first report on predictive comparative ligand-based multi-QSAR modeling analysis of 4-pyrimidinone and 2-pyridinone based APJ inhibitors. *New Journal of Chemistry*, *46*(24), 11591-11607.

231. Banerjee, S., Baidya, S. K., Ghosh, B., Nandi, S., Mandal, M., Jha, T., & Adhikari, N. (2023). Quantitative structural assessments of potential meprin β inhibitors by non-linear QSAR approaches and validation by binding mode of interaction analysis. *New Journal of Chemistry*, *47*(15), 7051-7069.

232. SwissADME Webtool available at http://www.swissadme.ch/.

233. Daina, A., Michielin, O., & Zoete, V. (2017). SwissADME: a free web tool to evaluate pharmacokinetics, drug-likeness and medicinal chemistry friendliness of small molecules. *Scientific reports*, *7*(1), 42717.

234. Baidya, S. K., Amin, S. A., Banerjee, S., Adhikari, N., & Jha, T. (2019). Structural exploration of arylsulfonamide-based ADAM17 inhibitors through validated comparative multi-QSAR modelling studies. *Journal of Molecular Structure*, *1185*, 128-142.

235. Gentile, F., Oprea, T. I., Tropsha, A., & Cherkasov, A. (2023). Surely you are joking, Mr Docking!. *Chemical Society Reviews*, *52*(3), 872-878.

236. Cruzat, V., Macedo Rogero, M., Noel Keane, K., Curi, R., & Newsholme, P. (2018). Glutamine: metabolism and immune function, supplementation and clinical translation. *Nutrients*, *10*(11), 1564.

237. Li, T., Copeland, C., & Le, A. (2021). Glutamine metabolism in cancer. In *The Heterogeneity of Cancer Metabolism* (pp. 17-38). Cham: Springer International Publishing.

238. Jin, J., Byun, J. K., Choi, Y. K., & Park, K. G. (2023). Targeting glutamine metabolism as a therapeutic strategy for cancer. *Experimental & Molecular Medicine*, *55*(4), 706-715.

Appendix

Appendix Table T1. Dataset molecules (*N* = 94) with their respective ADAM17 inhibitory activity

Cpd. No.	*Structure (SMILES)*	*ADAM17 IC_{50} (nM)*	*pIC_{50}*
1	c1(COc2ccc(cc2)S(=O)(=O)N2CC(CC2)C(=O)NO)cc(nc2c1cccc2)C	*210*	6.678
2	c1(COc2ccc(cc2)S(=O)(=O)N2CC(CCC2)C(=O)NO)cc(nc2c1cccc2)C	*60*	*7.222*
3	c1(COc2ccc(cc2)S(=O)(=O)N2CC(c3c(C2)cccc3)C(=O)NO)cc(nc2c1cccc2)C	*84*	*7.076*
4	c1(COc2ccc(cc2)S(=O)(=O)N2CC(OCC2)C(=O)NO)cc(nc2c1cccc2)C	*180*	*6.745*
5	c1(COc2ccc(cc2)S(=O)(=O)N2CC(OCCC2)C(=O)NO)cc(nc2c1cccc2)C	*71*	7.149
6	c1(COc2ccc(cc2)S(=O)(=O)N2CC(N(CC2)C(=O)C)C(=O)NO)cc(nc2c1cccc2)C	*14*	*7.854*
7	c1(COc2ccc(cc2)S(=O)(=O)N2CC(N(CCC2)C(=O)C)C(=O)NO)cc(nc2c1cccc2)C	*200*	*6.699*
8	c1(COc2ccc(cc2)S(=O)(=O)[C@H]2C[C@H](N(C2)C(=O)C)C(=O)NO)cc(nc2c1cccc2)C	*350*	*6.456*
9	c1(COc2ccc(cc2)S(=O)(=O)[C@@H]2C[C@H](N(C2)C(=O)C)C(=O)NO)cc(nc2c1cccc2)C	*3600*	*5.444*
10	c1(COc2ccc(cc2)S(=O)(=O)[C@@H]2C[C@H](N(C2)C(=O)C)C(=O)NO)cc(nc2c1cccc2)C	*35*	*7.456*
11	c1(COc2ccc(cc2)S(=O)(=O)N2CC(CC2)(C(=O)NO)CC)cc(nc2c1cccc2)C	*16*	*7.796*
12	c1(COc2ccc(cc2)S(=O)(=O)N2CC(CC2)(C(=O)NO)C(C)(C)C)cc(nc2c1cccc2)C	*35*	7.456
13	c1(COc2ccc(cc2)S(=O)(=O)N2CC(CC2)(C(=O)NO)Cc2ccccc2)cc(nc2c1cccc2)C	*42*	7.377
14	c1(COc2ccc(cc2)S(=O)(=O)N2CC(CCC2)(C(=O)NO)C)cc(nc2c1cccc2)C	*40*	7.398
15	c1(COc2ccc(cc2)S(=O)(=O)N2CC(N(CC2)C(=O)C)(C(=O)NO)C)cc(nc2c1cccc2)C	*30*	*7.523*
16	c1(COc2ccc(cc2)S(=O)(=O)N2CC(N(CC2)C(=O)CC)C(=O)NO)cc(nc2c1cccc2)C	*23*	*7.638*
17	c1(COc2ccc(cc2)S(=O)(=O)N2CC(N(CC2)C(=O)C(C)C)C(=O)NO)cc(nc2c1cccc2)C	*26*	*7.585*
18	c1(COc2ccc(cc2)S(=O)(=O)N2CC(N(CC2)C(=O)C2CC2)C(=O)NO)cc(nc2c1cccc2)C	*13*	7.886
19	c1(COc2ccc(cc2)S(=O)(=O)N2CC(N(CC2)C(=O)C2CCC2)C(=O)NO)cc(nc2c1cccc2)C	*19*	7.721
20	c1(COc2ccc(cc2)S(=O)(=O)N2CC(N(CC2)C(=O)CC(C)C)C(=O)NO)cc(nc2c1cccc2)C	*23*	*7.638*
21	c1(COc2ccc(cc2)S(=O)(=O)N2CC(N(CC2)C(=O)c2ccccc2)C(=O)NO)cc(nc2c1cccc2)C	*16*	7.796
22	c1(COc2ccc(cc2)S(=O)(=O)N2CC(N(CC2)C(=O)C(C)(C)C)C(=O)NO)cc(nc2c1cccc2)C	*12*	*7.921*
23	c1(COc2ccc(cc2)S(=O)(=O)N2CC(N(CC2)C(=O)OC)C(=O)NO)cc(nc2c1cccc2)C	*40*	7.398
24	c1(COc2ccc(cc2)S(=O)(=O)N2CC(N(CC2)S(=O)(=O)C)C(=O)NO)cc(nc2c1cccc2)C	*29*	7.538

25	c1(COc2ccc(cc2)S(=O)(=O)N2CC(NCC2)C(=O)NO)cc(nc2c1cccc2)C	*110*	*6.959*
26	c1(COc2ccc(cc2)S(=O)(=O)N2CC(N(CC2)C)C(=O)NO)cc(nc2c1cccc2)C	*160*	6.796
27	c1(COc2ccc(cc2)S(=O)(=O)N2CC(N(CC2)C2CCC2)C(=O)NO)cc(nc2c1cccc2)C	*150*	*6.824*
28	c1(COc2ccc(cc2)S(=O)(=O)NCCC(=O)NO)cc(nc2c1cccc2)C	*2300*	5.638
29	c1(COc2ccc(cc2)S(=O)(=O)NC(CC(=O)NO)(C)C)cc(nc2c1cccc2)C	*43*	*7.367*
30	c1(COc2ccc(cc2)S(=O)(=O)NC(CC(=O)NO)(C)C)cc(nc2c1cccc2)C	*84*	*7.076*
31	c1(COc2ccc(cc2)S(=O)(=O)NC2(CC(=O)NO)CCC2)cc(nc2c1cccc2)C	*13*	*7.886*
32	c1(COc2ccc(cc2)S(=O)(=O)NC2(CC(=O)NO)COC2)cc(nc2c1cccc2)C	*10*	*8.000*
33	c1(COc2ccc(cc2)S(=O)(=O)NC2(CC(=O)NO)CC3(C2)CN(C3)C(=O)C)cc(nc2c1cccc2)C	*4*	*8.398*
34	c1(COc2ccc(cc2)S(=O)(=O)NC2(CC(=O)NO)CN(C2)C(=O)CC(C)C)cc(nc2c1cccc2)C	*6*	*8.222*
35	c1(COc2ccc(cc2)S(=O)(=O)NC2(CC(=O)NO)CN(C2)CCCC)cc(nc2c1cccc2)C	*12*	*7.921*
36	c1(COc2ccc(cc2)S(=O)(=O)NC2(CC(=O)NO)CN(C2)CCC(F)(F)F)cc(nc2c1CCC=C2)C	*10*	*8.000*
37	c1(COc2ccc(cc2)S(=O)(=O)NC2(CC(=O)NO)CN(C2)C(=O)OC(C)C)cc(nc2c1cccc2)C	*6*	*8.222*
38	c1(COc2ccc(cc2)S(=O)(=O)NC2(CC(=O)NO)CN(C2)C(=O)N2CCCCC2)cc(nc2c1cccc2)C	*5*	*8.301*
39	c1(COc2ccc(cc2)S(=O)(=O)NC2(CC(=O)NO)CN(C2)C(=O)C(N(C)C)(C)C)cc(nc2c1cccc2)C	*4.6*	*8.337*
40	c1(COc2ccc(cc2)S(=O)(=O)NCC(=O)NO)cc(nc2c1cccc2)C	*82*	*7.086*
41	c1(COc2ccc(cc2)S(=O)(=O)NC(C(=O)NO)(C)C)cc(nc2c1ccc2)C	*140*	*6.854*
42	c1(COc2ccc(cc2)S(=O)(=O)NC2(C(=O)NO)CC2)cc(nc2c1cccc2)C	*210*	*6.678*
43	c1(COc2ccc(cc2)S(=O)(=O)NC2(C(=O)NO)CCC2)cc(nc2c1cccc2)C	*30*	*7.523*
44	c1(COc2ccc(cc2)S(=O)(=O)NC2(C(=O)NO)CCCC2)cc(nc2c1cccc2)C	*68*	*7.167*
45	c1(COc2ccc(cc2)S(=O)(=O)NC2(C(=O)NO)CCCCC2)cc(nc2c1cccc2)C	*100*	*7.000*
46	c1(COc2ccc(cc2)S(=O)(=O)NC2(C(=O)NO)CCN(CC2)C(=O)C)cc(nc2c1cccc2)C	*61*	*7.215*
47	c1(COc2ccc(cc2)S(=O)(=O)NC2(C(=O)NO)CN(C2)C(=O)C(C)C)cc(nc2c1cccc2)C	*16*	*7.796*
48	c1(COc2ccc(cc2)S(=O)(=O)N(C2(C(=O)NO)CN(C2)C(=O)C(C)C)C)cc(nc2c1cccc2)C	*9*	*8.046*
49	c1(COc2ccc(cc2)S(=O)(=O)N(C2(C(=O)NO)CN(C2)C(=O)C(C)C)CC)cc(nc2c1cccc2)C	*37*	*7.432*
50	c1(COc2ccc(cc2)S(=O)(=O)N(C2(C(=O)NO)CN(C2)C(=O)C(C)C)CCOC)cc(nc2c1cccc2)C	*31*	*7.509*
51	c1(COc2ccc(cc2)S(=O)(=O)N(C2(C(=O)NO)CN(C2)C(=O)C(C)C)C(C)C)cc(nc2c1cccc2)C	*790*	*6.102*

52	c1(COc2ccc(cc2)S(=O)(=O)NC2(C(=O)NO)CN(C2)C(=O)C(C)(C)C)cc(nc2c1cccc2)C	*33*	*7.481*
53	c1(COc2ccc(cc2)S(=O)(=O)N(C2(C(=O)NO)CN(C2)C(=O)C(C)(C)C)C)cc(nc2c1cccc2)C	*33*	*7.481*
54	c1(COc2ccc(cc2)S(=O)(=O)C2(C(=O)NO)CCNCC2)cc(nc2c1cccc2)C	*33*	*7.481*
55	c1(COc2ccc(cc2)S(=O)(=O)C2(C(=O)NO)CCN(CC2)C=O)cc(nc2c1cccc2)C	*2*	*8.699*
56	c1(COc2ccc(cc2)S(=O)(=O)C2(C(=O)NO)CCN(CC2)C(=O)C)cc(nc2c1cccc2)C	*1*	*9.000*
57	c1(COc2ccc(cc2)S(=O)(=O)C2(C(=O)NO)CCN(CC2)C(=O)C(C)C)cc(nc2c1cccc2)C	*2*	*8.699*
58	c1(COc2ccc(cc2)S(=O)(=O)C2(C(=O)NO)CCN(CC2)C(=O)c2ccccc2)cc(nc2c1cccc2)C	*1*	*9.000*
59	c1(COc2ccc(cc2)S(=O)(=O)C2(C(=O)NO)CCN(CC2)C(=O)NCC)cc(nc2c1cccc2)C	*2*	*8.699*
60	c1(COc2ccc(cc2)S(=O)(=O)C2(C(=O)NO)CCN(CC2)C(=O)N(CC)CC)cc(nc2c1cccc2)C	*3*	*8.523*
61	c1(COc2ccc(cc2)S(=O)(=O)C2(C(=O)NO)CCN(CC2)C)cc(nc2c1cccc2)C	*11*	*7.959*
62	c1(COc2ccc(cc2)S(=O)(=O)C2(C(=O)NO)CCN(CC2)CC2=C[Cl]=[Cl]C=C2)cc(nc2c1cccc2)C	*65*	*7.187*
63	c1(COc2ccc(cc2)S(=O)(=O)C2(C(=O)NO)CCN(CC2)S(=O)(=O)C)cc(nc2c1cccc2)C	*1.2*	*8.921*
64	c1(COc2ccc(cc2)S(=O)(=O)C2(C(=O)NO)CCN(CC2)S(=O)(=O)C(C)C)cc(nc2c1cccc2)C	*10*	*8.000*
65	c1(COc2ccc(cc2)S(=O)(=O)CC2N(CCCC2C(=O)NO)C)cc(nc2c1cccc2)C	*1.1*	*8.959*
66	c1(COc2ccc(cc2)S(=O)(=O)CC2CNCCC2C(=O)NO)cc(nc2c1cccc2)C	*1*	*9.000*
67	c1(COc2ccc(cc2)S(=O)(=O)CC2CN(CCC2C(=O)NO)C)cc(nc2c1cccc2)C	*1.9*	*8.721*
68	c1(COc2ccc(cc2)S(=O)(=O)CC2CN(CCC2C(=O)NO)C(C)C)cc(nc2c1cccc2)C	*1.5*	*8.824*
69	c1(COc2ccc(cc2)S(=O)(=O)CC2CN(CCC2C(=O)NO)CC=C)cc(nc2c1cccc2)C	*1.8*	*8.745*
70	c1(COc2ccc(cc2)S(=O)(=O)CC2CN(CCC2C(=O)NO)CC#C)cc(nc2c1cccc2)C	*1*	*9.000*
71	c1(COc2ccc(cc2)S(=O)(=O)CC2CCNCC2C(=O)NO)cc(nc2c1cccc2)C	*1.5*	*8.824*
72	c1(COc2ccc(cc2)S(=O)(=O)CC2CCN(CC2C(=O)NO)C)cc(nc2c1cccc2)C	*6.5*	*8.187*
73	c1(COc2ccc(cc2)S(=O)(=O)CC2CCN(CC2C(=O)NO)C(C)C)cc(nc2c1cccc2)C	*11*	*7.959*
74	c1(COc2ccc(cc2)S(=O)(=O)CC2(N(CCCC2)C)CC(=O)NO)cc(nc2c1cccc2)C	*5.1*	*8.292*
75	c1(COc2ccc(cc2)S(=O)(=O)CC2(N(CCCC2)C(C)(C)C)CC(=O)NO)cc(nc2c1cccc2)C	*48*	*7.319*
76	c1(COc2ccc(cc2)S(=O)(=O)CC2(CNCCC2)CC(=O)NO)cc(nc2c1cccc2)C	*2.8*	*8.553*
77	c1(COc2ccc(cc2)S(=O)(=O)CC2(CN(CCC2)C)CC(=O)NO)cc(nc2c1cccc2)C	*3.6*	*8.444*
78	c1(COc2ccc(cc2)S(=O)(=O)CC2(CN(CCC2)C(C)C)CC(=O)NO)cc(nc2c1cccc2)C	*2.7*	*8.569*

79	c1(COc2ccc(cc2)S(=O)(=O)CC2(CN(CCC2)C(C)(C)C)CC(=O)NO)cc(nc2c1cccc2)C	*3.3*	*8.481*
80	c1(COc2ccc(cc2)S(=O)(=O)CC2(CCNCC2)CC(=O)NO)cc(nc2c1cccc2)C	*14*	*7.854*
81	c1(COc2ccc(cc2)S(=O)(=O)CC2(CCN(CC2)C)CC(=O)NO)cc(nc2c1cccc2)C	*2*	*8.699*
82	c1(COc2ccc(cc2)S(=O)(=O)CC2(CCOCC2)CC(=O)NO)cc(nc2c1cccc2)C	*1*	*9.000*
83	c1(COc2ccc(cc2)S(=O)(=O)CC2(CC(=O)NO)CCCN2)cc(nc2c1cccc2)C	*1*	*9.000*
84	c1(COc2ccc(cc2)S(=O)(=O)CC2(CC(=O)NO)CCCN2C)cc(nc2c1cccc2)C	*2.9*	*8.538*
85	c1(COc2ccc(cc2)S(=O)(=O)CC2(CC(=O)NO)CCCN2C(C)(C)C)cc(nc2c1cccc2)C	*20*	*7.699*
86	c1(COc2ccc(cc2)S(=O)(=O)CC2(CC(=O)NO)CCCN2C(=O)C)cc(nc2c1cccc2)C	*660*	*6.180*
87	c1(COc2ccc(cc2)S(=O)(=O)CC2(CC(=O)NO)CCCO2)cc(nc2c1cccc2)C	*1*	*9.000*
88	c1(COc2ccc(cc2)S(=O)(=O)CC2(CC(=O)NO)CCNC2)cc(nc2c1cccc2)C	*1.5*	*8.824*
89	c1(COc2ccc(cc2)S(=O)(=O)CC2(CC(=O)NO)CCN(C2)C)cc(nc2c1cccc2)C	*3.2*	*8.495*
90	c1(COc2ccc(cc2)S(=O)(=O)CC2(CC(=O)NO)CCN(C2)C(C)C)cc(nc2c1cccc2)C	*1.6*	*8.796*
91	c1(COc2ccc(cc2)S(=O)(=O)CC2(CC(=O)NO)CCN(C2)C(C)(C)C)cc(nc2c1cccc2)C	*2.6*	*8.585*
92	c1(COc2ccc(cc2)S(=O)(=O)CC2(CC(=O)NO)CCN(C2)CC(C)(C)C)cc(nc2c1cccc2)C	*3.4*	*8.469*
93	c1(COc2ccc(cc2)S(=O)(=O)CC2(CC(=O)NO)CCCC2)cc(nc2c1cccc2)C	*0.8*	*9.097*
94	c1(COc2ccc(cc2)S(=O)(=O)CC2(CC(=O)NO)COC2)cc(nc2c1cccc2)C	*1*	*9.000*

Appendix Table T2. Descriptors used to construct the LDA model for training and test sets

Training set ($N_{Training}$ = 65)								
Cpd No.	***GATS5i***	***GATS3v***	***GATS2m***	***MATS6c***	***AATSC1m***	***GATS8v***	***GATS3c***	***Binary***
2	0.984675	1.071035	0.821108	0.125108	8.407111	1.009915	0.932561	0
3	1.075736	1.092566	0.813311	0.13068	7.566151	1.052289	0.941954	0
4	0.9498	1.04529	0.836166	0.121745	8.381081	1.0032	0.958042	0
5	0.990988	1.015946	0.844518	0.089052	8.292626	0.999278	0.974276	0
6	0.970999	1.02681	0.788754	0.072127	7.833068	0.982052	1.003842	0
7	1.010394	1.001895	0.799438	0.038753	7.740756	0.981148	1.001708	0
9	1.053801	1.059105	0.863043	0.179256	7.156409	1.10842	0.947513	0
11	0.886673	1.118001	0.784515	0.159792	8.277101	1.096087	0.941692	0
13	1.044805	1.160228	0.821379	0.135422	7.420837	0.956545	0.944003	0
14	1.023878	1.163128	0.784515	0.117856	8.277101	1.031611	0.9351	0
15	1.028403	1.053971	0.75003	0.068848	7.740756	1.005812	1.05008	0
16	1.006908	0.995494	0.799438	0.092524	7.740756	1.001501	0.991133	0
17	1.040946	1.050772	0.788393	0.111808	7.636209	1.018468	0.98845	0

21	0.959309	1.038179	0.825793	0.087495	7.055629	0.951206	0.96778	0
24	0.926922	1.035614	0.90705	0.064656	13.206	0.988433	0.992728	0
25	0.950167	1.048506	0.830845	0.115713	8.161959	1.005177	0.924847	0
26	0.850598	1.091453	0.818486	0.125447	8.422835	1.065698	0.953295	0
28	0.94981	1.024271	0.869187	0.176063	8.396262	1.07312	0.974203	0
29	0.855253	1.135329	0.796893	0.11868	8.156552	0.992866	1.103727	0
30	0.874692	1.037826	0.850416	0.130771	8.135705	1.014785	1.071296	0
32	0.864156	1.115058	0.875362	0.157159	8.002426	1.022858	0.914501	1
33	0.910185	1.206135	0.820025	0.036337	7.260846	1.066013	1.031029	1
35	0.87122	1.074282	0.875894	0.146957	7.707791	1.041329	0.987971	0
36	0.793835	1.135564	0.788801	0.063171	6.691641	1.020287	0.942069	1
37	0.859577	1.09378	0.815899	-0.1122	7.265996	1.057846	1.121213	1
38	0.907258	1.086427	0.865705	-0.08314	7.22575	0.976352	1.020144	1
39	0.784881	1.185387	0.795187	0.040928	7.162436	1.017155	1.056626	1
40	0.963228	1.054884	0.86302	0.245986	8.472742	1.10146	0.866945	0
41	0.820031	1.110972	0.784254	0.246653	8.287265	1.007348	0.995315	0
42	0.843778	1.005226	0.842168	0.247411	8.204503	1.034077	0.949587	0
43	0.87695	1.00854	0.841649	0.214328	8.135705	1.044226	0.941444	0
46	0.858027	1.031672	0.81594	0.184107	7.412965	1.03402	1.015702	0
49	1.012478	1.017749	0.765796	0.104468	7.523184	1.081045	1.035542	0
50	0.981859	1.060449	0.81103	0.159388	7.371462	1.041708	0.965082	0
51	1.08747	1.022647	0.754213	0.081754	7.404523	1.043698	1.068493	0
52	1.05071	1.236026	0.772987	0.143764	7.322466	1.047336	0.98787	0
53	0.987101	1.2297	0.727216	0.132758	7.523184	1.207609	1.011807	0
54	0.908144	1.03909	0.851967	-0.00821	7.374115	0.963588	1.04553	0
58	0.902275	1.056168	0.844495	-0.07808	6.404185	0.916238	1.07466	1
60	0.858021	0.993883	0.828322	-0.10818	6.877973	0.881664	1.172311	1
62	0.900113	1.094859	0.843994	0.037712	15.43742	0.964543	1.077927	0
63	0.824661	1.062824	0.918117	-0.08677	12.56222	0.987276	1.081891	1
64	0.92833	1.116493	0.841834	-0.08478	12.25081	1.073091	1.068102	1
65	1.047993	1.054899	0.952024	0.020457	7.530157	1.102661	1.023257	1
66	0.918051	1.041647	0.971693	0.103968	7.293294	1.103193	0.879983	1
67	0.911565	1.107385	0.956151	0.177452	7.530157	1.1325	0.888068	1
69	0.941388	1.068991	0.977843	0.13322	7.203644	1.078661	0.912098	1
70	0.931831	1.092675	0.976689	0.116311	7.10524	1.079679	0.873512	1
72	0.971208	1.107385	0.956151	0.080082	7.530157	1.029392	0.919555	1
73	0.941461	1.045413	0.940528	0.119065	7.282735	0.978516	1.054611	0
74	0.990565	1.051322	0.932754	0.015382	7.409343	1.047595	1.092048	1
75	1.14278	1.076501	0.886628	0.112985	7.021287	1.120216	1.286526	0
76	0.928406	1.109823	0.954022	0.088168	7.1974	1.040981	0.87124	1
77	0.97699	1.169679	0.940685	0.154784	7.409343	1.072354	0.879416	1
78	0.918124	1.105265	0.928065	0.10526	7.152776	1.043587	1.015797	1
79	0.895206	1.177745	0.893757	0.082661	7.021287	1.032833	1.090628	1
80	0.94756	1.091948	0.954022	0.181724	7.1974	1.020272	0.875032	0
81	0.894558	1.152506	0.940685	0.153553	7.409343	1.008422	0.881863	1
82	0.931328	1.105321	0.961019	0.146644	7.422922	1.012405	0.884702	1

84	0.95746	1.072075	0.925151	-0.01634	7.530157	1.028383	1.09632	1
85	1.146526	1.094686	0.876366	0.106677	7.152776	1.110051	1.292286	0
86	1.046616	1.015263	0.892693	0.118181	7.012191	1.076252	1.10659	0
89	0.939994	1.199196	0.933404	0.131847	7.530157	1.054782	0.873911	1
90	0.897481	1.126609	0.919474	0.088514	7.282735	1.026693	1.012103	1
92	1.065139	1.315179	0.900885	0.096325	7.021287	0.940608	0.916314	1
Test set (N_{Test} = 29)								
Cpd No.	***GATS5i***	***GATS3v***	***GATS2m***	***MATS6c***	***AATSC1m***	***GATS8v***	***GATS3c***	***Binary***
1	0.941481	1.100174	0.810368	0.168451	8.521003	1.016481	0.941077	0
8	1.053801	1.059105	0.863043	0.179256	7.156409	1.10842	0.947513	0
10	0.947764	1.197432	0.771426	0.160182	8.407111	1.040234	0.942766	0
12	0.806506	1.224031	0.744392	0.161808	7.989311	1.191998	0.975508	0
18	1.010382	0.981829	0.832133	0.106323	7.646893	1.003511	0.979359	0
19	0.990542	0.998797	0.83446	0.099375	7.565873	0.939093	0.967371	0
20	0.933588	1.062704	0.799826	0.069767	7.523184	0.825912	0.998597	0
22	1.073246	1.177752	0.758056	0.130175	7.523184	1.033458	0.993831	0
23	0.923712	1.06841	0.806241	0.082976	7.736884	1.032414	0.966097	0
27	1.038026	0.98633	0.855896	0.099397	8.086389	0.983007	1.015231	0
31	0.923309	1.038282	0.850908	0.10643	8.041078	1.008372	1.040311	0
34	0.841127	1.130002	0.827529	-0.01524	7.222335	1.050785	1.030136	1
44	0.905883	1.04515	0.8347	0.185332	8.041078	1.052434	0.917245	0
45	0.895839	1.021582	0.844969	0.187777	7.928498	1.067881	0.904814	0
47	0.982581	1.100459	0.806707	0.14363	7.412965	1.039361	0.985114	0
48	0.92573	1.099153	0.7569	0.132035	7.636209	1.12729	1.008904	1
55	0.849769	1.092936	0.848547	-0.05883	7.156409	0.990949	0.975861	1
56	0.860905	1.049138	0.809313	-0.0679	7.092088	0.98045	1.106855	1
57	0.967525	1.068523	0.808881	-0.06811	6.921117	1.070984	1.093434	1
59	0.859908	1.015581	0.830656	-0.10887	6.750783	0.923827	1.116641	1
61	0.841797	1.108508	0.839953	0.061964	7.641897	1.01397	1.058957	0
68	0.890638	1.045413	0.940528	0.132078	7.282735	1.089116	1.024344	1
71	0.954945	1.041647	0.971693	0.106782	7.293294	1.078044	0.907296	1
83	0.98495	1.06186	0.939348	0.014701	7.293294	1.034505	1.092716	1
87	1.000989	1.041599	0.938883	0.004327	7.517393	1.045622	1.193636	1
88	0.921333	1.136613	0.947959	0.057943	7.293294	1.018282	0.864863	1
91	0.88163	1.202181	0.883738	0.068194	7.152776	1.016422	1.087853	1
93	0.969921	1.113557	0.934335	0.080498	7.486437	1.01181	0.865118	1
94	0.895917	1.174991	0.969462	0.159023	7.594691	1.034396	0.816973	1

Appendix Table T3. Summary of the descriptors of the LDA model

Discriminant Function Analysis Summary (ADAM17_LDA_csv) Step 7, N of vars in model: 7; Grouping: Binary (2 groups) Wilks' Lambda: .17546 approx. F (7,57) =38.267 p<0.0000						
N=65	***Wilks' λ***	***Partial Lambda***	***F-remove (1,57)***	***P-level***	***Toler.***	***1-Toler.***
GATS2m	0.391882	0.447725	70.31034	0.000000	0.598609	0.401391
MATS2m	0.410972	0.426929	76.51180	0.000000	0.318993	0.681007
GATS3v	0.263038	0.667034	28.45286	0.000002	0.714219	0.285781
GATS5i	0.246754	0.711054	23.16268	0.000011	0.688864	0.311136
AATSC1m	0.226214	0.775618	16.48979	0.000151	0.739823	0.260177
GATS8v	0.194202	0.903467	6.09028	0.016618	0.691871	0.308129
GATS3c	0.192497	0.911471	5.53624	0.022101	0.569050	0.430950

Appendix Table T4. Values of metrics for assessing the quality and goodness of fit of the LDA model

Eigen-value	***Caconical R***	***Wilks' λ***	***Chi-square***	***df***	***P level***
4.699451	0.908044	0.175455	103.5520	7	0.00

Appendix Table T5. Classification functions summary of LDA model

Classification Functions; grouping: Binary		
Variable	***G_1:0***	***G_2:1***
GATS2m	530.067	614.794
MATS2m	-212.409	-299.924
GATS3v	460.826	514.564
GATS5i	-38.461	-79.254
AATSC1m	0.944	-0.796
GATS8v	342.077	374.678
GATS3c	153.490	132.867
Constant	-691.805	-776.988

Appendix Table T6. Raw coefficients for canonical variables of LDA model

Raw Coefficients for Canonical Variables	
Variable	***Root 1***
GATS2m	19.5634
MATS2m	-20.2074
GATS3v	12.4080
GATS5i	-9.4191
AATSC1m	-0.4017
GATS8v	7.5275
GATS3c	-4.7618
Constant	-19.3023
Eigen-value	4.6995
Cum.Prop	1.0000

Appendix Table T7. Squared Mahalanobis distances and Posterior probabilities of the constructed LDA model

Cpd.no.	*Observed classification*	*Squared Mahalanobis distances*		*Posterior probabilities*	
		G_1:0 (Inactives)	***G_2:1(Actives)***	***G_1:0 (Inactives)***	***G_2:1(Actives)***
2	*0*	*1.40599*	*21.62204*	*0.999959*	*0.000041*
3	*0*	*3.53845*	*25.86489*	*0.999986*	*0.000014*
4	*0*	*0.77584*	*19.17150*	*0.999899*	*0.000101*
5	*0*	*1.85331*	*20.24313*	*0.999898*	*0.000102*
6	*0*	*2.25186*	*25.07400*	*0.999989*	*0.000011*
7	*0*	*4.31775*	*25.02946*	*0.999968*	*0.000032*
9	*0*	*3.36145*	*22.71348*	*0.999937*	*0.000063*
11	*0*	*4.94773*	*18.69773*	*0.998968*	*0.001032*
13	*0*	*7.38687*	*25.20227*	*0.999865*	*0.000135*
14	*0*	*4.61510*	*21.30103*	*0.999762*	*0.000238*
15	*0*	*4.34082*	*34.95179*	*1.000000*	*0.000000*
16	*0*	*3.84245*	*32.60602*	*0.999999*	*0.000001*
17	*0*	*3.18541*	*32.45152*	*1.000000*	*0.000000*
21	*0*	*3.70643*	*18.58523*	*0.999413*	*0.000587*
24	*0*	*13.48343*	*28.22881*	*0.999372*	*0.000628*
25	*0*	*1.66755*	*17.33297*	*0.999604*	*0.000396*
26	*0*	*5.74894*	*10.60811*	*0.919056*	*0.080944*
28	*0*	*1.87650*	*22.60416*	*0.999968*	*0.000032*
29	*0*	*7.40622*	*20.43123*	*0.998517*	*0.001483*
30	*0*	*3.56798*	*18.86550*	*0.999524*	*0.000476*
32	*1*	*7.23121*	*6.30279*	*0.385988*	*0.614012*
33	*1*	*23.81480*	*4.49500*	*0.000064*	*0.999936*
35	*0*	*5.21725*	*8.17266*	*0.814226*	*0.185774*
36	*1*	*21.38061*	*7.47265*	*0.000954*	*0.999046*
37	*1*	*44.06815*	*11.66528*	*0.000000*	*1.000000*
38	*1*	*35.68334*	*5.61294*	*0.000000*	*1.000000*
39	*1*	*26.85152*	*8.44999*	*0.000101*	*0.999899*
40	*0*	*4.89927*	*30.70979*	*0.999998*	*0.000002*
41	*0*	*11.42639*	*43.77542*	*1.000000*	*0.000000*
42	*0*	*8.48980*	*40.54353*	*1.000000*	*0.000000*
43	*0*	*4.63190*	*32.09638*	*0.999999*	*0.000001*
46	*0*	*4.45286*	*28.16797*	*0.999993*	*0.000007*
49	*0*	*5.15230*	*35.65805*	*1.000000*	*0.000000*
50	*0*	*0.98965*	*25.48659*	*0.999995*	*0.000005*
51	*0*	*8.38572*	*45.85190*	*1.000000*	*0.000000*
52	*0*	*8.78368*	*24.14205*	*0.999538*	*0.000462*
53	*0*	*21.51381*	*29.42791*	*0.981239*	*0.018761*
54	*0*	*11.85540*	*4.78297*	*0.028299*	*0.971701*
58	*1*	*27.12504*	*7.68923*	*0.000060*	*0.999940*
60	*1*	*25.79846*	*14.84862*	*0.004173*	*0.995827*
62	*0*	*25.87021*	*50.86505*	*0.999996*	*0.000004*
63	*1*	*36.08711*	*12.69879*	*0.000008*	*0.999992*
64	*1*	*29.64555*	*14.97383*	*0.000651*	*0.999349*
65	*1*	*24.96487*	*6.22206*	*0.000085*	*0.999915*
66	*1*	*29.54877*	*6.14472*	*0.000008*	*0.999992*
67	*1*	*21.53824*	*5.28217*	*0.000295*	*0.999705*
69	*1*	*21.02191*	*3.27305*	*0.000140*	*0.999860*
70	*1*	*29.61318*	*3.77489*	*0.000002*	*0.999998*
72	*1*	*22.21633*	*1.80491*	*0.000037*	*0.999963*
73	*0*	*9.93229*	*11.25193*	*0.659220*	*0.340780*
74	*1*	*18.01702*	*3.35770*	*0.000655*	*0.999345*

75	*0*	*18.56088*	*40.45037*	*0.999982*	*0.000018*
76	*1*	*29.00368*	*2.70810*	*0.000002*	*0.999998*
77	*1*	*19.12095*	*3.30507*	*0.000368*	*0.999632*
78	*1*	*15.38241*	*1.76540*	*0.001103*	*0.998897*
79	*1*	*23.11230*	*5.02371*	*0.000118*	*0.999882*
80	*0*	*11.38243*	*6.45268*	*0.078358*	*0.921642*
81	*1*	*19.96826*	*3.32662*	*0.000243*	*0.999757*
82	*1*	*16.79291*	*3.47210*	*0.001279*	*0.998721*
84	*1*	*24.41723*	*2.41225*	*0.000017*	*0.999983*
85	*0*	*18.61604*	*40.84949*	*0.999985*	*0.000015*
86	*0*	*4.90581*	*20.82625*	*0.999651*	*0.000349*
89	*1*	*26.82949*	*3.38096*	*0.000008*	*0.999992*
90	*1*	*18.87448*	*1.20528*	*0.000146*	*0.999854*
92	*1*	*40.97405*	*21.98611*	*0.000075*	*0.999925*
1	*0*	*1.44627*	*24.73229*	*0.999991*	*0.000009*
8	*0*	*3.36145*	*22.71348*	*0.999937*	*0.000063*
10	*0*	*5.39633*	*22.01815*	*0.999754*	*0.000246*
12	*0*	*29.03371*	*26.13945*	*0.190444*	*0.809556*
18	*0*	*3.69579*	*30.14331*	*0.999998*	*0.000002*
19	*0*	*5.38569*	*30.20417*	*0.999996*	*0.000004*
20	*0*	*16.06316*	*38.57205*	*0.999987*	*0.000013*
22	*0*	*6.59409*	*32.05496*	*0.999997*	*0.000003*
23	*0*	*3.01442*	*11.26804*	*0.984122*	*0.015878*
27	*0*	*4.48881*	*31.81457*	*0.999999*	*0.000001*
31	*0*	*1.34699*	*15.02903*	*0.998932*	*0.001068*
34	*1*	*31.30279*	*5.05362*	*0.000002*	*0.999998*
44	*0*	*1.98689*	*22.11685*	*0.999957*	*0.000043*
45	*0*	*3.46410*	*22.08384*	*0.999909*	*0.000091*
47	*0*	*0.59968*	*19.95346*	*0.999937*	*0.000063*
48	*1*	*6.56655*	*23.85779*	*0.999824*	*0.000176*
55	*1*	*37.94291*	*6.62543*	*0.000000*	*1.000000*
56	*1*	*21.18755*	*6.41012*	*0.000618*	*0.999382*
57	*1*	*23.31409*	*8.13715*	*0.000506*	*0.999494*
59	*1*	*28.89943*	*9.76856*	*0.000070*	*0.999930*
61	*0*	*11.97910*	*4.55189*	*0.023809*	*0.976191*
68	*1*	*14.91842*	*5.90967*	*0.010939*	*0.989061*
71	*1*	*21.31193*	*4.17670*	*0.000190*	*0.999810*
83	*1*	*20.04033*	*3.03124*	*0.000203*	*0.999797*
87	*1*	*19.52015*	*8.47764*	*0.003985*	*0.996015*
88	*1*	*37.03229*	*4.56813*	*0.000000*	*1.000000*
91	*1*	*27.28996*	*6.04616*	*0.000024*	*0.999976*
93	*1*	*21.86652*	*3.20527*	*0.000089*	*0.999911*
94	*1*	*31.89972*	*5.30834*	*0.000002*	*0.999998*

Appendix Table T8. Tree report for training set in Recursive Partitioning model

Model Information	***Y property***	***Confusion Matrix***	***ROC-score***	***ROC-score (cross-validated)***
Tree 1: 3 leaves Error Rate (training data): 10.105 Min alpha: 0	Binary	**Actual\Pred.** 1 0 1 25 2 0 9 29	0.864	0.828

Tree 2: 2 leaves Error Rate (training data): 15.395 Min alpha: 8.938	Binary	**Actual\Pred.** / 1 / 0 1 / 27 / 0 0 / 18 / 20	0.763	0.764

Appendix Table T9. Tree report for test set in RP model

Confusion Matrix	***Tree ID***	***Y property***	***ROC-score***	***ROC Rating***
Actual\Pred. / 1 / 0 1 / 6 / 8 0 / 1 / 14	1	Binary	0.81905	Quality 0.819; Good
Actual\Pred. / 1 / 0 1 / 13 / 1 0 / 6 / 9	2	Binary	0.76429	Quality 0.764; Fair

Appendix Table T10. The SwissADME predicted ADME properties of designed inhibitors

Cpd.	*Canonical smiles*	*GI absor-ption*	*BBB perme-ation*	*inhibitor*				*Lipinski violations*	*Veber violations*
				CYP3A4	*CYP2C19*	*CYP2C9*	*CYP1A2*		
D1	*ONC(=O)C1CNCC[C@@H]1CS(=O)(=O)c1ccc(cc1)OCc1c2c(ccc1)cccc2*	*High*	*No*	*Yes*	*No*	*Yes*	*No*	*0*	*0*
D2	*ONC(=O)C1CNCC[C@@H]1CS(=O)(=O)c1ccc(cc1)OCc1c[nH]c2c1cccc2*	*High*	*No*	*Yes*	*No*	*No*	*No*	*0*	*0*
D3	*ONC(=O)CC1(CCCC1)CS(=O)(=O)c1ccc(cc1)/C=C/c1c[nH]c2c1cccc2*	*Low*	*No*	*Yes*	*Yes*	*Yes*	*Yes*	*0*	*0*
D4	*ONC(=O)[C@]1(CC(=O)NC1=O)CS(=O)(=O)c1ccc(cc1)CCc1c[nH]c2c1cccc2*	*Low*	*No*	*No*	*No*	*No*	*No*	*0*	*1*

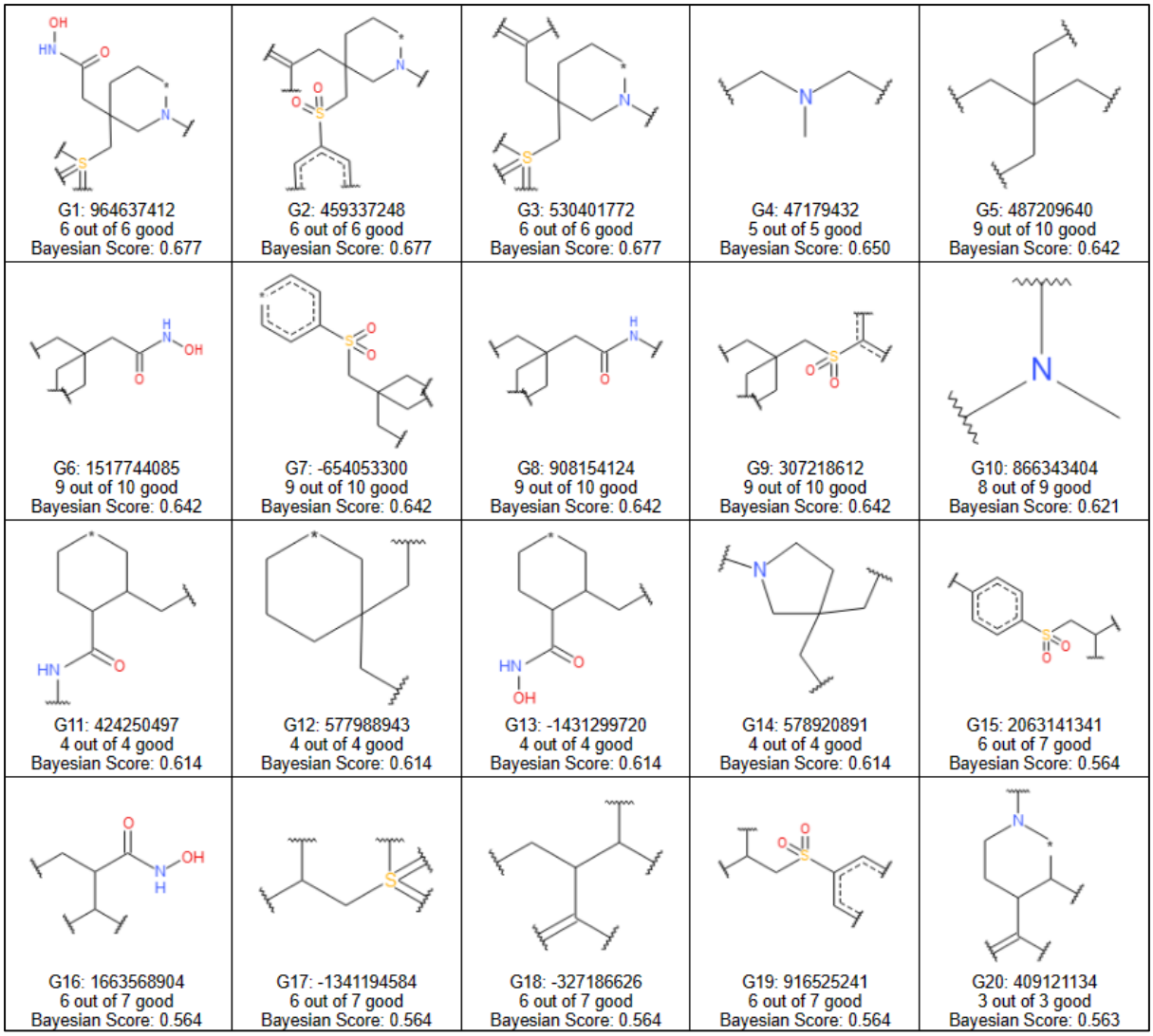

Appendix Figure F1. Good sub-structural features generated in Bayesian classification model

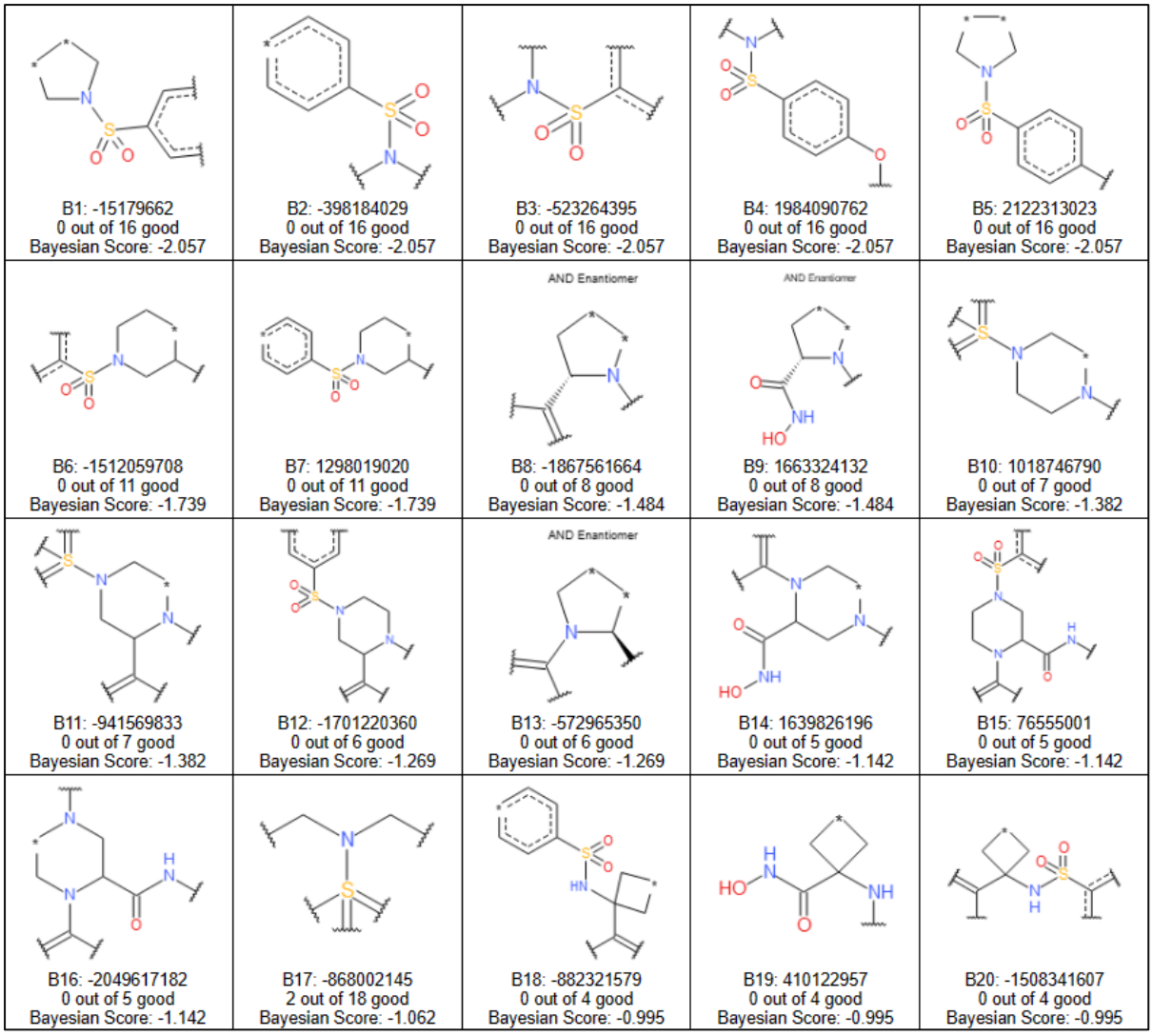

Appendix Figure F2. Bad sub-structural features generated in Bayesian classification model

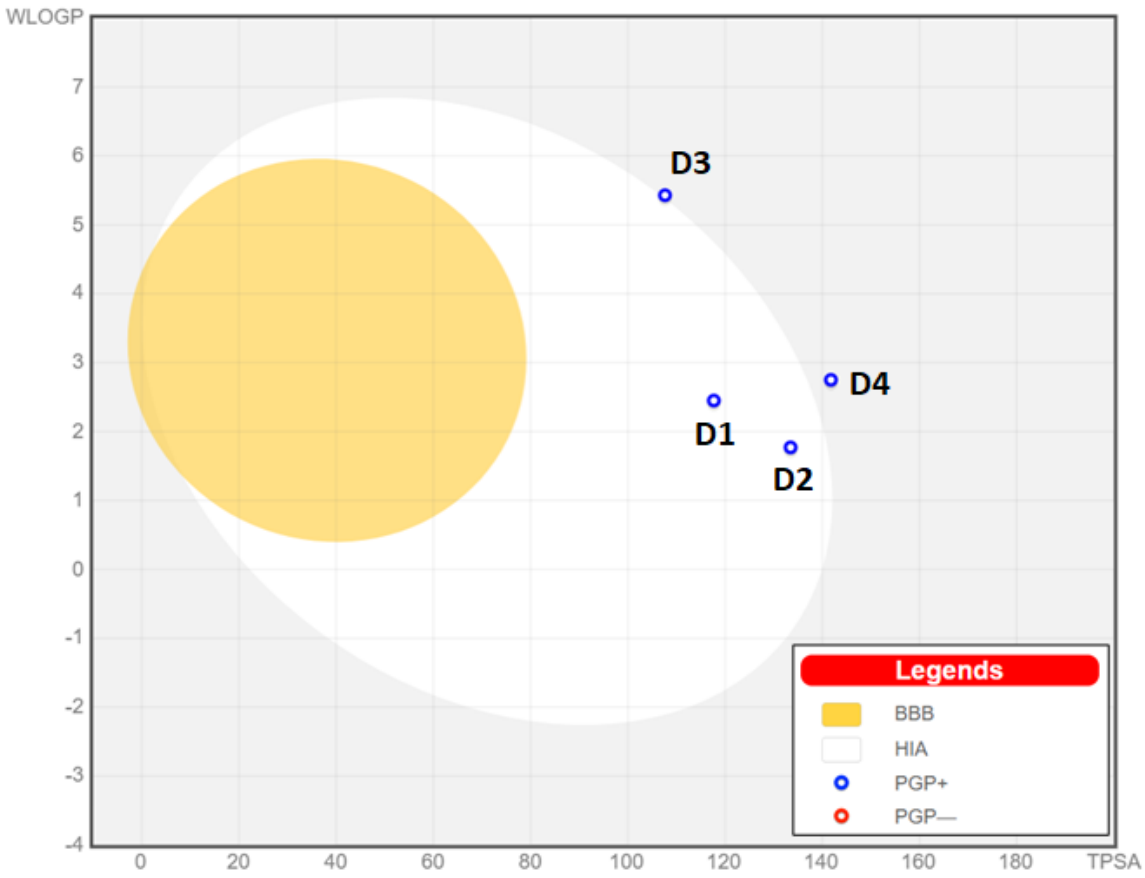

Appendix Figure F3. SwissADME generated the boiled egg plot (TPSA vs WLogP) for the designed compounds

Preprint

SAR AND QSAR IN ENVIRONMENTAL RESEARCH
2024, VOL. 35, NO. 2, 157–179
https://doi.org/10.1080/1062936X.2024.2311689

Taylor & Francis
Taylor & Francis Group

Exploring crucial structural attributes of quinolinyl methoxyphenyl sulphonyl-based hydroxamate derivatives as ADAM17 inhibitors through classification-dependent molecular modelling approaches

T.B. Samoi[a*], S. Banerjee[a*], B. Ghosh[b], T. Jha[a] and N. Adhikari[a]

[a]Natural Science Laboratory, Division of Medicinal and Pharmaceutical Chemistry, Department of Pharmaceutical Technology, Jadavpur University, Kolkata, India; [b]Epigenetic Research Laboratory, Department of Pharmacy, Birla Institute of Technology and Science-Pilani, Hyderabad, India

ABSTRACT

A Disintegrin and Metalloproteinase 17 (ADAM17), a Zn^{2+}-dependent metalloenzyme of the adamalysin family of the metzincin superfamily, is associated with various pathophysiological conditions including rheumatoid arthritis and cancer. However, no specific inhibitors have been marketed yet for ADAM17-related disorders. In this study, 94 quinolinyl methoxyphenyl sulphonyl-based hydroxamates as ADAM17 inhibitors were subjected to classification-based molecular modelling and binding pattern analysis to identify the significant structural attributes contributing to ADAM17 inhibition. The statistically validated classification-based models identified the importance of the P1' substituents such as the quinolinyl methoxyphenyl sulphonyl group of these compounds for occupying the S1' - S3' pocket of the enzyme. The quinolinyl function of these compounds was found to explore stable binding of the P1' substituents at the S1' – S3' pocket whereas the importance of the sulphonyl and the orientation of the P1' moiety also revealed stable binding. Based on the outcomes of the current study, four novel compounds of different classes were designed as promising ADAM17 inhibitors. These findings regarding the crucial structural aspects and binding patterns of ADAM17 inhibitors will aid the design and discovery of novel and effective ADAM17 inhibitors for therapeutic advancements of related diseases.

ARTICLE HISTORY
Received 13 November 2023
Accepted 23 January 2024

KEYWORDS
ADAM17; TACE; molecular modelling; classification QSAR; binding mode analysis

Introduction

A Disintegrin and Metalloproteinases (ADAMs) are Zn^{2+}-dependent transmembrane glycoproteins that belong to the adamalysin protease family [1]. ADAMs being a member of the protease family, catalyse the mechanisms of proteolytic cleavage of peptide bonds, yielding either the degradation of proteins or the release of active peptides [2]. ADAMs are associated with a divergent number of cellular processes including proliferation and differentiation of cells, morphogenesis, tissue remodelling, haemostasis, inflammation, angiogenesis,

CONTACT N. Adhikari nilanjan_juphar@rediffmail.com
*Authors have contributed equally.
Supplemental data for this article can be accessed at: https://doi.org/10.1080/1062936X.2024.2311689.